THE JOURNAL
OF
CHEMICAL PHYSICS

VOLUME 10 APRIL, 1942 NUMBER 4

The Diffraction of X-Rays by Liquid Benzene-Cyclohexane Mixtures

A. EISENSTEIN AND N. S. GINGRICH
University of Missouri, Columbia, Missouri

(Received February 2, 1942)

The x-ray diffraction pattern of a liquid mixture of benzene and cyclohexane is investigated, using both the photographic method and the Geiger-Mueller tube counter method. The fine structure on the main peak, and a secondary peak as reported by Bell and Davey, cannot be obtained. It is concluded that these features do not exist in this pattern.

INTRODUCTION

IN a recent article, Bell and Davey[1] reported that they found some very unusual fine structure in the main diffraction peak from benzene-cyclohexane mixtures. A repetition of this work is highly desirable for three reasons: first, no liquid x-ray diffraction pattern has heretofore shown fine structure of this type; second, this particular mixture has been worked upon by Ward,[2] by Murray and Warren,[3] and by Bell and Davey,[1] and all three reports of these workers are in disagreement; third, the extent of succeeding arguments based on the results of Bell and Davey is so great that it is desirable to examine critically the experimental basis for these arguments. The present authors have made an experimental study of the diffraction of x-rays by benzene, by cyclohexane, and by one mixture of these liquids, using both the photographic and the Geiger-Mueller counter methods of detection of the x-rays. Particular attention was given to the controversial matter of fine structure in the main peaks of the mixture.

[1] P. H. Bell and W. P. Davey, J. Chem. Phys. **9**, 441 (1941).
[2] H. K. Ward, J. Chem. Phys. **2**, 153 (1934).
[3] G. E. Murray and B. E. Warren, J. Chem. Phys. **7**, 141 (1939).

EXPERIMENTAL

Benzene and cyclohexane of high purity were purchased, and no further purification of the liquids was attempted. The index of refraction of the benzene used here was measured and found to be 1.5008 at 20°C while that used by Bell and Davey was given as 1.5009. The index of refraction of the cyclohexane used here was measured and found to be 1.4263 at 20°C, and that used by Bell and Davey was given as 1.4263. The mixture studied was approximately 50 percent benzene—50 percent cyclohexane by volume, and its index of refraction was 1.4597. The cell holder consisted of a brass cylinder 1.1 cm long and 1.9 cm diameter with thin Cellophane windows clamped on the ends. After the various liquids were contained in the cell for several days, tests on the index of refraction were made. In the cases of benzene and of cyclohexane alone, no difference in the index of refraction was ever obtained. In the case of the mixture, no difference greater than 0.0001 was obtained when adequate care in rinsing the cell was taken and when precautions were taken against evaporation through the filling tube.

Two cameras were used in the photographic studies here reported, a small camera of 9.20-cm

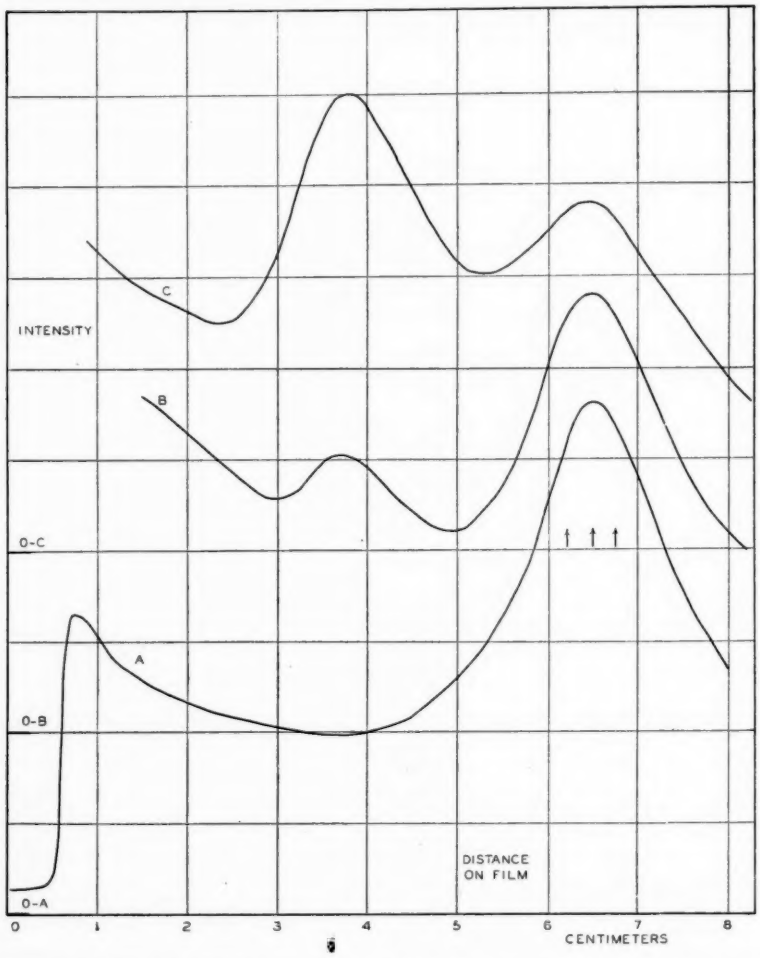

FIG. 1. X-ray diffraction patterns of a 50–50 mixture of liquid benzene and cyclohexane, showing intensity as a function of distance on the films in cm. One cm corresponds to about 1° 16′. Curve *A* taken with Mo $K\alpha$ radiation; curve *B* with Mo radiation filtered through 0.08 mm Zr equivalent; curve *C* with Mo radiation filtered through the above Zr and 0.132 cm Al.

radius and a large camera of approximately 44.6-cm radius. Using the small camera, no indication of fine structure on the main peak could be obtained with either pure liquid or with the mixture, but it was observed that in pictures taken with filtered radiation a weak peak appeared at nearly half the angle for the main peak whereas with crystal reflected Mo $K\alpha$ radiation, no secondary peak could be observed. Further work on the mixture was done using the large camera and three different types of radiation, first, crystal reflected Mo $K\alpha$, second Zr filtered Mo radiation, and third, Zr and Al filtered Mo radiation. Intensity curves obtained from microphotometering typical films are shown in Fig. 1. The intensity, computed in the usual manner, is plotted as a function of distance on the film from the center of the film. In the lower curve, taken with Mo $K\alpha$ crystal reflected radiation, it is to be noted, first, that no fine structure appears on the main peak, and second that no secondary peak at roughly half the distance (or angle) of the main peak can be detected. This is in contradiction to the results of Bell and Davey who state that in all cases a small intensity peak was observed at about 4°, and which had an intensity approximately one-eighth of the high intensity peaks.

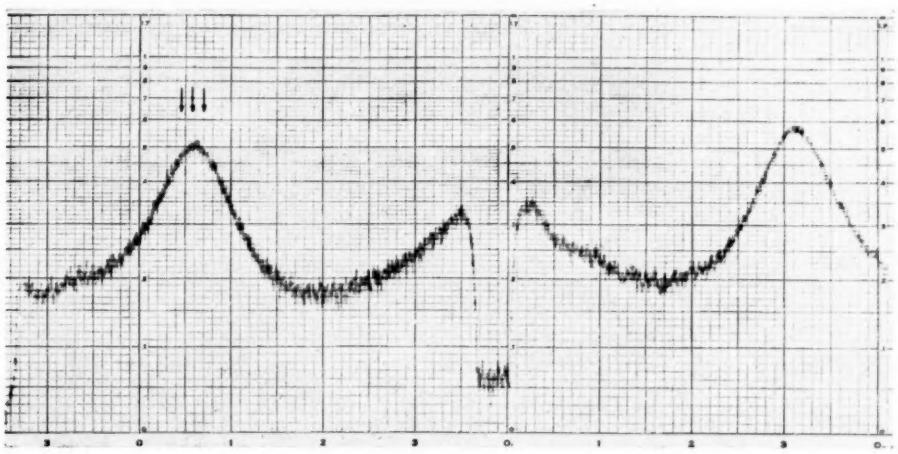

FIG. 2. A microphotometer trace for the benzene-cyclohexane mixture, using Mo $K\alpha$ radiation, showing the main diffraction peak on each side of the direct x-ray beam. The three arrows indicate the approximate position of the three fine structure peaks as reported by Bell and Davey.

The total horizontal angular divergence of the incident beam was measured photographically to be slightly less than 7 minutes, a value which compares favorably with that of Bell and Davey. The density of the film at the peak was of such value that the fine structure as reported could easily have been detected. Furthermore the region of the film over which the fine structure should have appeared is more than half a centimeter, the general location of the three peaks being indicated by the three spurs in Fig. 1. Both the film and the microphotometer are easily capable of showing up structure of this type. Figure 2 shows a portion of a microphotometer trace typical of the one from which the lower intensity curve of Fig. 1 was obtained. The gradual increase of intensity at small angles is due to air scattering, and the cut-off at still smaller angles is due to a lead strip to suppress the direct beam.

In an attempt to find a possible explanation for the secondary peak at about half the angle of the main peak, two other patterns were obtained. These are shown in Fig. 1, the middle curve being taken with Mo radiation filtered with ZrO_2 of 0.08 mm Zr equivalent thickness, the upper curve with Mo radiation filtered with the same Zr filter and 0.132 cm of Al. In both cases, the total horizontal angular divergence of the incident beam was measured photographically to be 10 minutes, and the same camera was used for all three curves of Fig. 1. The origin of the extra peak at nearly half the angle of the main peak is unquestionably that which is given in detail elsewhere.[4] Residual continuous radiation forming the spurious peak in the Zr filtered pattern is greatly enhanced in the Zr+Al filtered pattern due to the greater absorption of 0.710A as compared to that of the continuous radiation at about 0.4A. This rough effective wave-length is that obtained with the x-ray tube operated at about 40 kv peak, whereas Bell and Davey, operating their tube at 59 kv peak, obtained the secondary peak at an angle smaller than that obtained in the present work. This is qualitatively in accord with the above possible explanation of the origin of their secondary peak. In the use of the balanced filter method, extreme care must be taken to be sure that a perfect balance is obtained over the entire region studied, especially when compounds of the balancing elements are used.

Using a Geiger-Mueller tube counter, an amplifier, a scale of sixteen and a Cenco counter, a further study was made of the diffraction of x-rays by the same liquid benzene-cyclohexane mixture as was used above. Rocksalt reflected Mo $K\alpha$ radiation was passed through two slits as shown in Fig. 3. The total horizontal angular divergence of the incident beam, determined

[4] R. O. Gregg and N. S. Gingrich, Rev. Sci. Inst. **11**, 305 (1940).

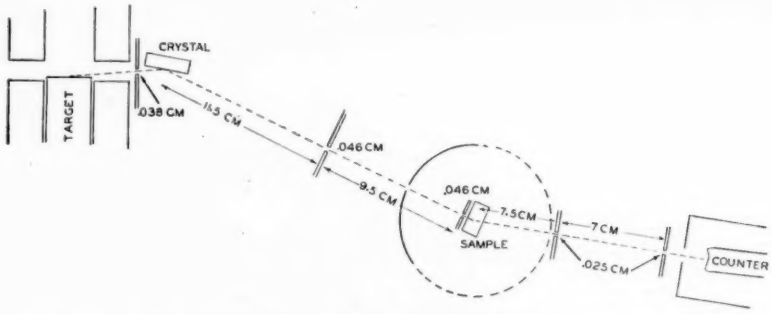

FIG. 3. Geometrical arrangement using the Geiger-Mueller counter method.

largely by the crystal, was measured photographically and found to be 10 minutes. The maximum possible divergence of the diffracted beam through the last two slits is 26 minutes or about the same as that of Bell and Davey's Soller slit system. Many runs were taken, particularly over the top of the main peak and the average of these runs is shown in Fig. 4, together with a reproduction of one of Bell and Davey's curves at roughly the same temperature and mixture. The maximum counting rates in the two cases are roughly 120 per minute in the previous work, and 470 per minute in the present work. The total number of counts per point in the present work is from 12,000 to 16,000. The probable error in the determination of each point was calculated according to the expression

$$\text{p.e.} = \pm 0.67N/(NT)^{\frac{1}{2}}$$

where N is the rate of counting, and NT the total counts. This probable error is indicated on the lower curve of Fig. 4. It is seen that though the points do not fall on a perfectly smooth curve, the curve drawn does pass through some portion of the limits of the probable errors. In no case could the results here obtained show a fine structure anywhere near as large as that reported by Bell and Davey. In preliminary runs in which only a few hundred counts per point were taken, irregularities were obtained which, if no further work was done, might conceivably have been interpreted as fine structure, though never, in the present work, as great as that in question. Furthermore, these irregularities appeared quite at random. It was found, for example, that reliable curves could be taken only after midnight and before 7 A.M., during which time the line voltage was most steady. Even assuming ideal experimental conditions, however, the results, using a Geiger counter, can only be statistical in nature, and fluctuations always appear more prominent on a flat or nearly flat portion of the curve.

CONCLUSIONS

In a photographic method of recording the x-ray diffraction pattern of a liquid benzene-cyclohexane mixture, especially designed to show any possible fine structure, no significant trace of fine structure could be observed such as

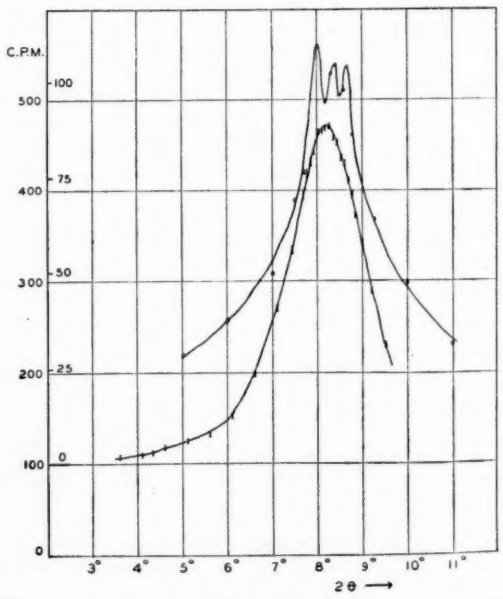

FIG. 4. Lower curve shows counts per minute as a function of scattering angle, 2θ, as determined in the present work. The probable error is indicated by vertical arrows. Upper curve is one reproduced from Bell and Davey's work.

was reported by Bell and Davey. Further studies were made, demonstrating the fact that impure radiation can give rise to a secondary peak at small angles. It is suggested that it may be possible that this is the origin of Bell and Davey's secondary peak, caused by a slight unbalance of their balanced filters.

Using the Geiger-Mueller counter method, as Bell and Davey did, but with pure radiation and with geometrical conditions at least as good as in their work, no fine structure could be obtained. Slight fluctuations of the observed points about a smooth curve are not large enough to establish fine structure, and these fluctuations are considered to be wholly statistical.

It is concluded, further, that the extensive deductions made by Bell and Davey are without experimental foundation.

ACKNOWLEDGMENTS

It is a pleasure to acknowledge that this work was supported in part by grants from the Rumford Fund of the American Academy of Arts and Science, the American Association for the Advancement of Science, and the Elizabeth Thompson Science Fund.

APRIL, 1942 JOURNAL OF CHEMICAL PHYSICS VOLUME 10

The Infra-Red Absorption of Silver Cyanide

W. DAVID STALLCUP AND DUDLEY WILLIAMS
University of Florida, Gainesville, Florida

(Received January 17, 1942)

The spectrum of powdered AgCN has been studied in the region 2500–1800 cm^{-1}. Intense absorption at 2178 cm^{-1} is attributed to an oscillation involving the CN group. The CN frequency for AgCN is almost 100 cm^{-1} higher than the CN frequencies of NaCN and KCN.

INVESTIGATIONS of the infra-red and Raman spectra of the organic cyanides have revealed the existence of a vibrational frequency of approximately 2245 cm^{-1} which is characteristic of the CN groups, while similar studies of the organic isocyanides indicate that the NC group has a characteristic frequency of 2146–2161 cm^{-1}. The simpler inorganic cyanides, NaCN and KCN, have CN frequencies of approximately 2080 cm^{-1}, while in the complex cyanides such as $KAg(CN)_2$ and $K_3Fe(CN)_6 \cdot 3H_2O$ the characteristic frequencies are in the neighborhood of 2150 cm^{-1}.[1,2] It has been suggested by several workers[3] that in inorganic cyanides the CN frequency increases when there is an increase in the homopolar nature of the M-CN binding.

It seemed desirable to test this hypothesis by determining the CN frequency for a simple cyanide in which the M−CN bond possesses some homopolar properties. As the existing data provide only comparisons of NaCN and KCN with double cyanides and with complex cyanides of the type mentioned above, the study of the infra-red spectrum of AgCN for comparison with NaCN immediately suggested itself, since the homopolar properties of the silver salts are well known.[4]

The silver cyanide used in the present work was prepared by adding an equimolecular amount of potassium cyanide solution to an approximately 0.1*M* solution of silver nitrate with constant and vigorous stirring. After precipitation was complete, the supernatant liquid was decanted and the precipitate was placed in a two

[1] Summary of the Raman data: K. W. F. Kohlrausch, *Der Smekal-Raman Effekt* (J. Springer, Berlin, 1931), p. 320; J. H. Hibben, *The Raman Effect and Its Chemical Applications* (Reinhold, New York, 1939), p. 452.

[2] Infra-red data: W. Gordy and D. Williams, J. Chem. Phys. **3**, 664 (1935); **4**, 85 (1936); F. K. Bell, J. Am. Chem. Soc. **57**, 1023 (1935).

[3] P. Krishnamurti, Ind. J. Phys. **5**, 651 (1930); R. Samuel and M. J. Khan, Zeits. f. Physik **84**, 87 (1933); Volkenshtein, Acta Physicochim. (U. S. S. R.) **7**, 315 (1937).

[4] L. Pauling, *The Nature of the Chemical Bond* (Cornell University Press, 1940), p. 73.

and a half foot large glass test tube. A fine jet of water was then directed into the precipitate. In this manner the precipitate was continuously washed for two days. The precipitated silver cyanide was then collected and dried.

The spectrometer used was a rocksalt prism instrument of the Littrow type. The samples used in making the absorption measurements consisted of layers of powder deposited on fluorite plates. The thickness of the absorbing layers varied from 0.02 to 0.05 mm in different samples. As the mean diameter of the particles was approximately three microns, considerable scattering took place in the spectral region studied. In order to minimize this scattering the powder was immersed in carbon tetrachloride in some of the cells.[5]

Figure 1 illustrates the type of transmission curve obtained with powdered AgCN. Curve *A* represents the transmission of a typical sample, the dotted curve giving the estimated background due to scattering. Curve *B* shows the transmission of AgCN when corrected for scattering. It will be noted that there is an intense absorption band with maximum at 4.59μ. This band was observed for a number of different cells, and the frequency of maximum absorption was found to be 2178 cm^{-1}.

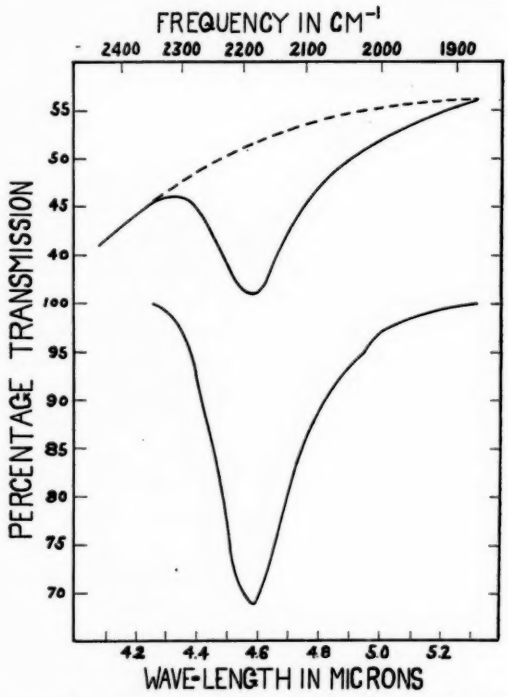

FIG. 1. The transmission of silver cyanide in the 2500–1800 cm^{-1} region.

TABLE I. The CN oscillational frequencies in various compounds.

Compound	Infra-red	Raman
NaCN	2080 GW	2085 K
KCN	2080 GW	2081 P–SG
AgCN	2178 PS	—
$Ba(CN)_2$	2080 GW	—
$Hg(CN)_2$	—	2192 K
CH_3NC	2183 GW	2161 B
C_2H_5NC	2159 GW	2146 B
CH_3CN	2285 GW	2250 P–SG
C_2H_5CN	2258 GW	2246 DK

K—Krishnamurti, Ind. J. Phys. **5**, 633 (1930).
P–SG—Pal and Sen Gupta, Ind. J. Phys. **5**, 13 (1930).
DK—Dadieu and Kohlrausch, Wien Ber. **139**, 165 (1930).
B—Bhagavantam, Ind. J. Phys. **5**, 48 (1930).
GW—W. Gordy and D. Williams, J. Chem. Phys. **3**, 664 (1935); **4**, 85 (1936).
PS—Present study.

[5] Carbon tetrachloride has no absorption bands in the range 2500–1800 cm^{-1} which was studied.

Table I summarizes the pertinent infra-red and Raman data for several types of cyanides. It will be noted that the CN frequency in AgCN is almost 100 cm^{-1} higher than for NaCN and KCN. This result is in accord with the suggestion that increasing homopolarity is accompanied by increases in the CN frequency. It might be mentioned in passing that the AgCN frequency actually falls in the range of the organic isocyanide, NC, frequencies, although many factors render unjustifiable any suggestion of similarity in structure from spectroscopic evidence. Included in the table are data for two divalent cyanides, $Ba(CN)_2$ and $Hg(CN)_2$. In this case also the compound having the higher degree of homopolarity has the higher CN frequency. It will be observed from the table that none of the inorganic cyanides yet studied has as great a CN frequency as that characteristic of the organic cyanides.

Second Virial Coefficients and the Forces Between Complex Molecules

J. O. HIRSCHFELDER, F. T. MCCLURE, AND I. F. WEEKS
Department of Chemistry, University of Wisconsin, Madison, Wisconsin

(Received November 28, 1941)

The second virial coefficients of ethane, propane, *n*-butane, *n*-heptane, ammonia, methyl chloride, and the freons are computed from available experimental data. The causes for sizeable errors in second virial coefficients are considered. At temperatures above the critical, the second virial agrees with the theorem of corresponding states. Below the critical temperature, molecules with dipoles have unusually large virials and the values of their reduced dipole moment, $\mu/(T_cV_c)^{\frac{1}{2}}$, determine the discrepancy. The data for isomeric hydrocarbons show that the second virial is not sensitive to the shape of the molecule. This makes it impossible to determine the exact laws of intermolecular interaction from the temperature variation of the second virial. The imperfections of a gas are considered to arise from the presence of double molecules which exist for the duration of a collision. The equilibrium constant for the formation of double molecules is related to the second virial and its temperature variation gives the entropy ΔS and the energy ΔE of their formation. These may be interpreted qualitatively in terms of the intermolecular forces. The second virial coefficient for all substances fits the equation: $B(T)=b_a(1-c\exp(-\Delta E/RT))$ where b_a, c, and ΔE are taken as constants. Here $b_ac=\exp(\Delta S/R)$. A corresponding states equation is given for estimating second virials when no experimental data are available.

IN this paper we investigate the significance of second virial coefficients for complex molecules. The treatment is divided into three parts: (1) the determination and probable accuracy of experimental values; (2) the qualitative interpretation of second virials from the theorem of corresponding states; and (3) a quantitative interpretation in terms of the energy and entropy of formation of instantaneous double molecules. Unfortunately it is difficult to distinguish the characteristic properties of the molecules because the second virials may have errors of ten cc/mole. At temperatures above the critical, the second virial agrees with the theorem of corresponding states. Below the critical temperature, molecules with dipoles have unusually large virials and the value of their reduced dipole moment, $\mu/(T_cV_c)^{\frac{1}{2}}$, determines the discrepancy. An examination of Roper's second virial coefficients for the isomeric hydrocarbons shows that the second virial coefficient is not sensitive to the shape of the molecule.

For the practical interpretation of the second virial coefficients of complex molecules, it is useful to exploit an idea of Fowler and Guggenheim.[2] Consider an imperfect gas as an equilibrium mixture of single, double, triple, etc. molecules. The double, triple, etc. species are complexes which exist only for the duration of a collision, but their number is determined by the usual type of chemical equilibrium constant. The equilibrium constant for the formation of *double molecules* is related to the second virial coefficient, and its temperature dependence gives the energy and entropy of their formation. This energy and entropy of formation of double molecules may be roughly interpreted in terms of intermolecular forces. To determine these forces quantitatively, we would require more accurate experimental data.

I. THE DETERMINATION OF SECOND VIRIAL COEFFICIENTS

The equation of state of a gas at moderate pressures can be written in the form:

$$pV=RT+pB(T)+p^2C(T)+\cdots. \qquad (1)$$

This is called the virial form of the equation of state since Clausius first derived it by equating the total kinetic energy of the molecules to the total virial of the system, $-\frac{1}{2}\sum_i(x_iF_{x_i}+y_iF_{y_i}+z_iF_{z_i})$. Here x_i is the x coordinate of the ith particle, and F_{x_i} is the x component of the force acting on the ith molecule, etc. The term pV arises from the forces exerted on the walls of the containing vessel, RT comes from the kinetic energy of the molecules, and all of the other terms arise from the mutual interactions between the molecules. $B(T)$ is called the second virial

[1] E. E. Roper, J. Phys. Chem. **44**, 835 (1940).
[2] R. H. Fowler and E. A. Guggenheim, *Statistical Thermodynamics* (Cambridge University Press, 1939), Chap. 7.

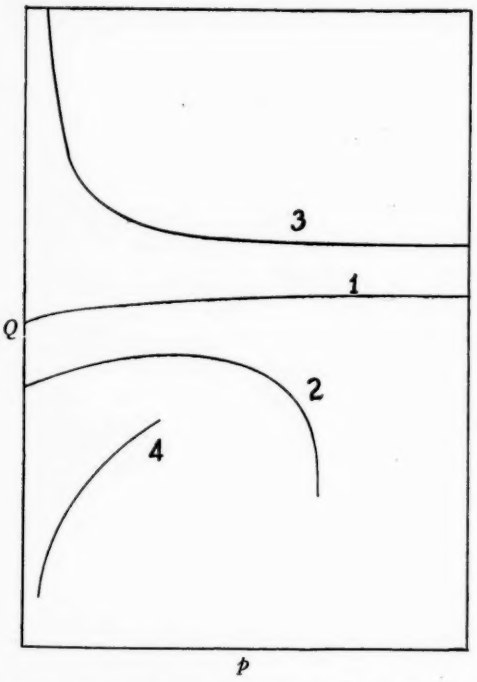

FIG. 1. The four types of curves obtained by plotting the experimental values of $Q=V-RT/p$ as a function of pressure.

coefficient, $C(T)$ is the third virial coefficient, etc. The second virial coefficient is particularly useful for our purposes because it arises only from collisions between two molecules at a time and is related rigorously to the energy of interaction between pairs of molecules.

The easiest way of determining $B(T)$ from experimental p, V, T data is to plot $Q=(pV-RT)/p$ as a function of pressure. Since

$$Q=(pV-RT)/p=B(T)+C(T)p+\cdots, \quad (2)$$

the second virial coefficient is the limit of Q as the pressure approaches zero:

$$B(T)=\lim_{p\to 0}\left(\frac{pV-RT}{p}\right). \quad (3)$$

The third virial coefficient is the slope of Q at zero pressure, etc. When we plot actual experimental data in this manner, we get four types of curves as shown in Fig. 1. Curve (1) is typical of substances above their critical temperature where the third and higher virial coefficients do not become important until rather high pressures are reached. Curve (2) is typical of substances below their critical temperature, the sharp break in the curve occurring when the pressure approaches the vapor pressure. Curve (3) could correspond to a gas which dissociates at low pressures to give n molecules. In such a case, pV approaches nRT at low pressures and $Q=(pV-RT)/p$ approaches infinity. However, curves of the form (3) can correspond to even small experimental error in the determination of the volume of the apparatus. Curve (4) must always correspond to errors of this nature. When the experimental details are available, it is sometimes possible to make a single correction to the volume of the apparatus such that the curves for Q now resemble either curves (1) or (2) for all temperatures. Otherwise it is necessary to extrapolate Q to zero pressure from the experimental data at moderate pressures where a small error in the volume of the apparatus has only a slight effect. Either of these processes naturally reduces the accuracy of the second virial coefficient. Unfortunately many of Sage and Lacey's measurements of p, V, T for hydrocarbons lead to curves of the form of (4) and are therefore unsuitable for the determination of second virial coefficients. This behavior was also manifested by the data for steam which Keenan and Keyes tabulated in the first edition of their "Steam Tables" but this has been corrected in their later editions.[3] We believe that accurate values of the second virial coefficients can best be obtained from specially constructed low pressure apparatus such as Roper[1] used in his excellent work on the olefins.

The second virial coefficients which we computed from the original experimental data are given in Table I. We were surprised at the lack of accurate low pressure p, V, T measurements of the paraffins. Only Deschner and Brown's[4] measurements for propane went to pressures as low as one atmosphere. The ethane, butane, and heptane results as well as the Beattie, Kay, and Kaminsky[5] values for propane were extrapolated from pressures as high as 25 atmospheres. The virial coefficients for steam and for ammonia

[3] J. H. Keenan and F. G. Keyes, *Thermodynamic Properties of Steam* (Wiley, 1936).
[4] W. W. Deschner and G. G. Brown, J. Ind. Eng. Chem. **32**, 836 (1940).
[5] Beattie, Kay, and Kaminsky, J. Am. Chem. Soc. **59**, 1589 (1937).

should be quite accurate. The data for methyl chloride seem to be quite reliable. Of the freons, CCl_2F_2—Freon 12, is the least accurate since the temperature measurements were uncertain to 1°. Second virial coefficients for other boiler fluids and refrigerants can be obtained from a study of similar commercial publications. The virials for the olefins are given directly in a paper of Roper[1] and are therefore not reproduced here.

It is difficult to obtain the second virial coefficients to within 10 cc/mole. For this accuracy we should know $Q(T)=V-RT/p$ to within 10 cc/mole. At room temperature, V is of the order of 24,000 cc/mole when p is of the order of one atmosphere. Thus the density of the gas, the pressure in the chamber, and the absolute temperature must all be measured to within one part in 2400. This is feasible with carefully built apparatus. Often we lose sight of the fact that the molecular weight and the gas constant must be known to the same accuracy, and the difference between two published sets of virial coefficients may be due to the different values of these constants which were used. Thus second virial coefficients for organic molecules published prior to 1937 when the atomic weight of carbon was thought to be 12.00 may differ very considerably from those in which the present atomic weight of carbon, 12.01 is used. However, for the saturated hydrocarbons where the older molecular weights were used,[5-8] the errors due to this cause would be inappreciable since all of the measurements were at high pressures. When Amagat units are used, molecular weights are not required and it is only necessary to know the gas constant R with reasonable accuracy. In recent years there has been some controversy as to whether the ice point is 273.16°K or 273.13°K. In the former case, $R=82.054$ atmos. cc per mole per deg. instead of 82.060 and the difference in $B(T)$ is approximately 3 cc/mole. Holborn and Otto (1925) and Kammerlingh-Onnes (1910) avoided serious errors in the virials for argon by using Amagat units and not relying on the faulty atomic weights available then. Often two good sets of data such as Deschner and Brown's and Beattie, Kay, and Kaminsky's for propane (see Table I) differ by a constant independent of temperature. Presumably this is because of small differences in the constants used or in the calibration of the thermometers. Joule-Thomson measurements are inherently more accurate than second virial coefficients because they do not require taking the difference of two large quantities. Also, Joule-Thomson coefficients are just as easy to interpret as the virials.

Often second virial coefficients are estimated from empirical equations of state such as the Beattie-Bridgman. This method has the advantage of being quick and easy, but it is sometimes unreliable. The constants for empirical

TABLE I.

Second virial coefficient, $B(T)$, in cc/mole

			Propane			
T°K	Ethane[a]	T°K	BKK[b]	DB[c]	T°K	n-Butane[d]
298.16	−191	303.16		−384	423.16	−324
323.16	−160	348.16		−293	448.16	−288
348.16	−139	369.97	−260		473.16	−256
373.16	−122	373.16	−247	−256	498.16	−224
398.16	−108	398.16	−211	−224	523.16	−198
423.16	− 94	423.16	−183	−197	548.16	−176
448.16	− 86	448.16	−160		573.16	−159
473.16	− 77	473.16	−139	−155		
498.16	− 71	498.16	−121			
523.16	− 60	523.16	−109			
		526.38		−108		
		548.16	− 96			
		570.46		− 89		

						Methyl Chloride[g]
T°K	n-Heptane[e]	T°K	Ammonia[f]		T°K	CH_3Cl
548.16	−569	273.16	−345		238.71	−764
573.16	−503	298.16	−261		249.82	−668
598.16	−449	323.16	−209		255.38	−637
623.16	−399	373.16	−142		283.16	−500
		423.16	−101		310.94	−401
		473.16	− 75		338.71	−320
		523.16	− 58		366.49	−265
		573.16	− 44		394.27	−214
					422.05	−184
					449.82	−155

	Freon −11[h]	Freon −21[i]	Freon −12[j]	Freon −113[k]
T°K	CCl_3F	$CHCl_2F$	CCl_2F_2	$CCl_2F-CClF_2$
238.71	−1150	−766	−637	
244.27			−604	
249.82	−1070	−734	−586	
255.38			−560	
283.16	− 862	−616	−454	−1080
310.94	− 720	−528	−347	− 944
338.71	− 617	−446		− 795
366.49	− 523	−403		− 737
394.27	− 459	−354		− 654
422.05	− 381	−310		− 561
449.82	− 328	−271		− 495

[a] See reference 6.
[b] See reference 5.
[c] See reference 4.
[d] See reference 7.
[e] See reference 8.
[f] C. H. Meyers and R. S. Jessup, Refrig. Eng. 11, 345 (1925).
[g] *Methyl Chloride* (E. I. du Pont de Nemours and Co., The R. and H. Chemicals Department, 1940), fifth edition.
[h] *Thermodynamic Properties of Trichloromonofluoromethane* (Kinetic Chemicals, Inc., 1938).
[i] *Thermodynamic Properties of Dichloromonofluoromethane* (Kinetic Chemicals, Inc., 1939).
[j] *Thermodynamic Properties of Dichlorodifluoromethane*, Circular No. 12, Am. Soc. Refrig. Eng. (1931).
[k] *Thermodynamic Properties of Trichlorotrifluoroethane* (Kinetic Chemicals, Inc., 1938).

[6] Beattie, Hadlock and Poffenberger, J. Chem. Phys. **3**, 93 (1935).
[7] Beattie, Simard, and Su, J. Am. Chem. Soc. **61**, 26 (1939).
[8] Smith, Beattie, and Kay, J. Am. Chem. Soc. **59**, 1587 (1937).

equations of state are usually made to fit high pressure measurements and therefore there is no guaranty that the equation really fits at low pressures. Furthermore, Michels and Michels[9] have shown from their work on CO_2 that there is an intrinsic difference between the virial coefficients which fit low pressure and those which fit high pressure experiments. This behavior can be explained by the presence of exponential terms such as $\exp(-cV)$ in the true equation of state. Such a term is asymptotically zero for large volumes and therefore no trace of its existence would appear in the low pressure measurements. However, at high pressures, $\exp(-cV)$ can be expanded in an ordinary power series to give the anomalous virial coefficients. On both theoretical and experimental grounds, such an exponential term might exist in the internal energy U and therefore appear in the equation of state. The exponential form of the quantum-mechanical exchange integrals together with the volume dependence of the internal energy of crystals suggests that:

$$U = U_0 - a/V - d\exp(-vV)$$

and this form is in good agreement with the experimental observations of Hildebrand[10] and others.

The usefulness of second virial coefficients for theoretical purposes depends on the rigorous statistical mechanical relation:

$$B(T) = \frac{N}{16\pi^2}\int\cdots\int[1-\exp(-E/kT)]d\Omega d\tau, \tag{5}$$

where

$$d\Omega = \sin\theta d\theta d\phi d\psi$$
$$0<\theta<\pi, \quad 0<\phi<2\pi, \quad 0<\psi<2\pi$$
$$d\tau = dxdydz.$$

Here E is the energy of a pair of molecules expressed as a function of the distance between the molecules and the relative orientations. In carrying out the integrations we can suppose that one molecule is held fixed at the center of a coordinate system and the second molecule is allowed to traverse all space with its center at x, y, z. The angles θ, ϕ, and ψ are the Eulerian angles which the second molecule makes with respect to the first. Since E does not involve the temperature, we may regard Eq. (5) as an integral equation for E as a function of the coordinates in terms of B as a function of temperature. The remainder of this paper is concerned with the solutions of this equation.

The potential energy of interaction of spherically symmetrical non-polar molecules can be approximated by the form:

$$E(r) = 4E_m[(r_0/r)^{12} - (r_0/r)^6]. \tag{4}$$

Here E_m is the maximum energy of attraction of the two molecules and r_0 is the collision diameter corresponding to $E(r_0)=0$. Lennard-Jones carried out the integration of Eq. (5) with this form of the potential energy and obtained:

$$B(T) = b_0 F_{12}(E_m/kT). \tag{5}$$

Here $b_0 = 2\pi N r_0^3/3$, is the van der Waals constant for the collision diameter r_0. The function $F_{12}(E_m/kT)$ is a power series which can be calculated readily for any desired value of E_m/kT. Table II shows the values of F_{12} from which it is possible to graph the function and interpolate to obtain the values of F_{12} for any other values of the argument.

Recently, Stockmayer showed how to calculate the second virial coefficient for spherical mole-

TABLE II.†

E_m/kT	$F_{12}(E_m/kT)$	E_m/kT	$F_{12}(E_m/kT)$	E_m/kT	$F_{12}(E_m/kT)$
.0025	.3247	.1986	.2468	.6280	−1.0624
.0158	.4949	.2079	.2236	.7046	−1.3398
.0315	.5258	.2500	.1154	.7906	−1.6668
.0628	.5148	.3147	−.0621	.9953	−2.5171
.0791	.4945	.3296	−.1044	1.1025	−3.0064
.0995	.4617	.3614	−.1969	1.3225	−4.1171
.1253	.4128	.3962	−.3012	1.5625	−5.5184
.1577	.3433	.4988	−.6237	2.2500	−11.0328

E_m/kT	$H_{12}(E_m/kT)$	$J_{12}(E_m/kT)$	$K_{12}(E_m/kT)$	$L_{12}(E_m/kT)$
.1225	−.0072	−.00001		
.1555	−.0113	−.00002		
.1936	−.0173	−.00004		
.2025	−.0189	−.00005		
.2500	−.0288	−.00011	$-.00\times10^{-4}$	$-.000\times10^{-5}$
.3025	−.0424	−.00023	$-.01\times10^{-4}$	$-.001\times10^{-5}$
.3600	−.0607	−.00045	$-.03\times10^{-4}$	$-.002\times10^{-5}$
.4900	−.1174	−.00152	$-.19\times10^{-4}$	$-.018\times10^{-5}$
.6400	−.2137	−.00453	$-.88\times10^{-4}$	$-.135\times10^{-5}$
.7225	−.2844	−.00758	-1.82×10^{-4}	$-.348\times10^{-5}$
.8100	−.3731	−.01237	-3.64×10^{-4}	$-.845\times10^{-5}$
1.0000	−.6324	−.03160	-13.85×10^{-4}	-4.698×10^{-5}

E_m/kT	$M_{12}(E_m/kT)$	$N_{12}(E_m/kT)$
.4900	$-.001\times10^{-6}$	
.6400	$-.017\times10^{-6}$	$-.02\times10^{-6}$
.7225	$-.052\times10^{-6}$	$-.06\times10^{-6}$
.8100	$-.151\times10^{-6}$	$-.22\times10^{-6}$
1.0000	-1.195×10^{-6}	-2.38×10^{-6}

† Many of the values of $F_{12}(E_m/kT)$ were given to us by Lennard-Jones.

[9] A. Michels and C. Michels, Proc. Roy. Soc. **A160**, 348 (1937).

[10] J. H. Hildebrand, *Solubility* (Reinhold, 1936), second edition.

cules in which a dipole μ is imbedded. In this case he assumes that the potential energy between pairs of molecules has the form:

$$E(r)=4E_m\left[\left(\frac{r_0}{r}\right)^s-\left(\frac{r_0}{r}\right)^6\right]$$
$$-\frac{\mu^2}{r^3}[2\cos\theta_1\cos\theta_2-\sin\theta_1\sin\theta_2\cos\phi]. \quad (6)$$

Here, of course, r_0 and E_m have a slightly different interpretation from those in the equation for non-polar gases. Stockmayer[11] makes most of his calculations on the assumption that either s is 24 or infinite. We believe that it is more reasonable to take $s=12$ which is in better accord with the repulsive forces in non-polar gases. Then, the second virial coefficient becomes:

$$B(T)=b_0[F_{12}(E_m/kT)+xH_{12}(E_m/kT)+x^2J_{12}(E_m/kT)+x^3K_{12}(E_m/kT)+x^4L_{12}(E_m/kT)+x^5M_{12}(E_m/kT)+x^6N_{12}(E_m/kT)+\cdots]. \quad (7)$$

Here $x=\mu^4/E_m^2r_0^6$ is the significant variable which gives the effect of the dipole. We can express H_{12}, J_{12}, K_{12}, L_{12}, etc. in terms of the derivatives of $F_{12}(E_m/kT)$. Remembering that extensive tables[12] are available for

$$G_{12}(E_m/kT)=T^2\frac{d}{dT}\left(\frac{F_{12}}{T}\right),$$

we obtain:

$$H_{12}=-\frac{1}{6}\left(\frac{5}{4}F_{12}+G_{12}\right)(E_m/kT), \quad (7a)$$

$$J_{12}=-\frac{1}{200}(3F_{12}+2G_{12})(E_m/kT)^3, \quad (7b)$$

$$K_{12}=-\frac{29}{88{,}200}\left[\left(\frac{5}{4}F_{12}+G_{12}\right)(E_m/kT)^4+(3F_{12}+2G_{12})(E_m/kT)^5-\left(\frac{5}{4}F'_{12}+G'_{12}\right)(E_m/kT)^5\right], \quad (7c)$$

$$L_{12}=-\frac{11}{793{,}800}\left[\left(2F_{12}+\frac{3}{2}G_{12}\right)(E_m/kT)^6+\left(3F_{12}+2G_{12}-2F'_{12}-\frac{3}{2}G'_{12}\right)(E_m/kT)^7\right], \quad (7d)$$

$$M_{12}=-\frac{312}{77(11!)}\left[\left(\frac{5}{2}F_{12}+2G_{12}\right)\left(\frac{E_m}{kT}\right)^7+\left(11F_{12}+8G_{12}-\frac{5}{2}F'_{12}-2G'_{12}\right)\left(\frac{E_m}{kT}\right)^8+\left(12F_{12}+8G_{12}-11F'_{12}-8G'_{12}+\frac{5}{4}F''_{12}+G''_{12}\right)\left(\frac{E_m}{kT}\right)^9\right], \quad (7e)$$

$$N_{12}=\frac{-1.045{,}109}{12!}\left[\left(\frac{13}{2}F_{12}+5G_{12}\right)\left(\frac{E_m}{kT}\right)^9+\left(14F_{12}+10G_{12}-\frac{13}{2}F'_{12}-5G'_{12}\right)\left(\frac{E_m}{kT}\right)^{10}+\left(12F_{12}+8G_{12}-14F'_{12}-10G'_{12}+\frac{13}{4}F''_{12}+\frac{5}{2}G''_{12}\right)\left(\frac{Em}{kT}\right)^{11}\right]. \quad (7f)$$

The single and double primes indicate first and second derivatives with respect to E_m/kT. In Table II the numerical values of these functions are tabulated, so that it is a simple matter to obtain the effect of a dipole moment on the second virial coefficient. Fitting the second virial coefficient of water, we find $x=10$, $E_m/k=400°$, and $b_0=22.9$ cc. When $T=400°$K the non-polar contribution, $b_0F_{12}(E_m/kT)$, is only 17 percent of the total second virial coefficient. At 500°K, it is 24 percent and at 1000°K it is 28 percent. At 400°K, the term $x^4L_{12}(E_m/kT)$ which contains the 16th power of the dipole moment still contributes 3.1 percent to the second virial but at 575°K it is reduced to 0.6 percent. Because of the importance of the

[11] W. H. Stockmayer, J. Chem. Phys. **9**, 398, 863 (1941).
[12] J. O. Hirschfelder, R. B. Ewell, and J. R. Roebuck, J. Chem. Phys. **6**, 205 (1938).

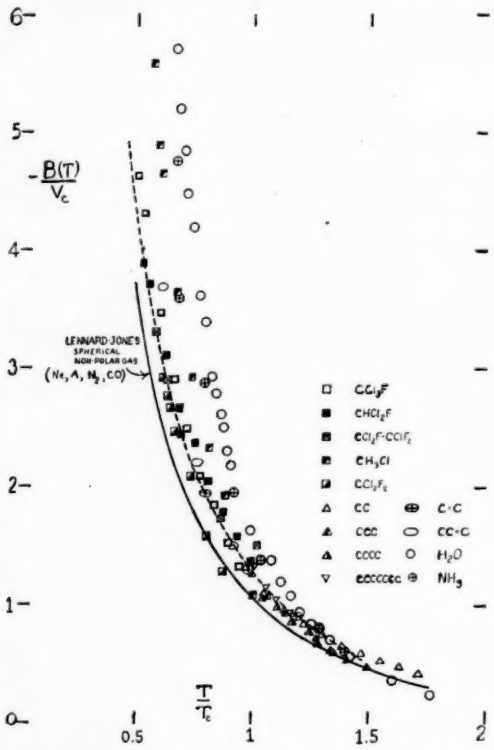

FIG. 2. Reduced second virial coefficients as a function of reduced temperature. The *CC*, *CCC*, ··· are for the saturated hydrocarbons ethane, propane, etc.; *C=C* is ethene and *CC=C* is propene.

dipole terms, the second virial coefficients really provide a sensitive method for the determination of dipole moments.

II. GENERAL PROPERTIES OF SECOND VIRIAL COEFFICIENTS OF COMPLEX MOLECULES

In making a general survey of the second virial coefficients of complex molecules, our first question is how well does the equation of corresponding states hold. In Fig. 2 we have plotted the reduced second virial coefficients, $B(T)/V_c$, of twelve substances as a function of their reduced temperatures, T/T_c, where V_c and T_c are the critical volume and temperature, respectively. The data for some of the freons, as for example CCl_2F_2 (where the temperature of the measurements is uncertain to one degree) may not be very accurate. However, a number of qualitative conclusions may be drawn:

1. The equation of corresponding state holds well for temperatures above the critical. Below the critical temperature there is a considerable spread in the values of the reduced second virials.

2. Molecules with large dipole moments have unusually large reduced second virial coefficients. However, from our previous section we see that the important quantity is not the dipole moment itself but $x=\mu^4 E_m^{-2} r_0^{-6}$. Since E_m is proportional to T_c and r_0^3 is proportional to V_c, we should expect that the important reduced dipole variable should be

$$z=(\mu^4/T_c^2 V_c^2)10^{80}. \tag{8}$$

Thus, the reduced second virial coefficients of H_2O, NH_3, and CH_3Cl do not fall in the order of their dipole moments: 1.83×10^{-18} e.s.u., 1.47×10^{-18} e.s.u., and 1.89×10^{-18} e.s.u., respectively. But rather, they occur in the order of their values of z: $z_{H_2O}=1.32$, $z_{NH_3}=.54$, and $z_{CH_3Cl}=.40$.

3. The shape of the molecules does not greatly affect the reduced second virial coefficients until the temperature becomes considerably lower than the critical point. The curve marked "Lennard-Jones spherical non-polar gas" is the reduced second virials for Ne, A, N_2, and CO

$$B(T)_{\substack{\text{Lennard-Jones}\\ \text{spherical non-polar}}}=0.68F_{12}(0.77T_c/T). \tag{9}$$

Deviations from this curve may be attributed to lack of symmetry of the molecules, the presence of dipole moments, or any other deviations from the form which Lennard-Jones assumed for the intermolecular forces. Actually the hydrocarbons and only slightly polar substances have reduced second virial coefficients which lie more nearly along the dotted curve:

$$B(T)/V_c=0.89[F_{12}(0.73T_c/T) - 0.0042z\exp(4.4T_c/T)]. \tag{10}$$

The development of the previous section makes it clear that the use of just the first power of z in the second virial cannot hold at low temperatures for molecules with large dipoles. Actually, the deviation of individual molecules from these predictions usually exceeds the experimental errors so that it is necessary to fit each molecule as a special case.

There are considerable experimental data for the olefin and paraffin series of hydrocarbons

which we can use to obtain additional generalities. For example, by comparing the virials for the four butene isomers which were studied by Roper, we see that the shape of the molecule does not greatly affect the second virials:

	$B(225°K)$ cc/mole	$B(280°K)$ cc/mole	$B(335°K)$ cc/mole	
2-methyl propene	−1436	−782	−483	
1-butene	−1432	−777	−478	(11)
trans-2-butene	−1504	−854	−551	
cis-2-butene	−1645	−868	−517	

Apparently the second virial coefficients for olefins are almost the same as for the corresponding paraffin. This is shown by a comparison at $T=335°K$:

$$\begin{aligned} &B(\text{ethene})-B(\text{ethane}) &&= -118+149=31 \text{ cc/mole},\\ &B(\text{propene})-B(\text{propane}) &&= -274+317=43, \qquad (12)\\ &B(\text{1-butene})-B(n\text{-butane}) &&= -478+516=38. \end{aligned}$$

Perhaps the most curious hydrocarbon regularity is that the second virials are proportional to the square of the number of carbon atoms. Strict proportionality would be in contradiction to the theorem of corresponding states and seems quite unlikely. This is shown in Table III. All of these regularities seem to hold better at the higher temperatures. Before attempting an explanation, we should have experimental data for the higher hydrocarbons and for temperatures above the critical so that we can be more positive about our facts.

III. THE IMPERFECT GAS AS AN ASSOCIATION PROBLEM

An imperfect gas may be considered to be an equilibrium mixture of readily interconvertible single, double, triple, etc. molecules. Fortunately,

TABLE III.

	n	$B(448°K)/n^2$	$B(523°K)/n^2$	
1. Paraffins				
Ethane	2	−21.6	−15.0	
Propane	3	−17.8	−12.1	
n-Butane	4	−18.0	−12.4	
n-Heptane	7	−17.9*	−12.9*	
2. Olefins	n	$+B(225°K)/n^2$	$+B(280°K)/n^2$	$+B(335°K)/n^2$
Ethene	2	−62.3	−41.6	−29.6
Propene	3	−72.3	−44.1	−30.4
2-Methyl-Propene	4	−89.7	−48.9	−30.2
1-Butene	4	−89.5	−48.6	−29.9
trans-2-Butene	4	−94.0	−53.4	−34.4
cis-2-Butene	4	−102.8	−54.2	−32.3

* Extrapolated from 548°K.

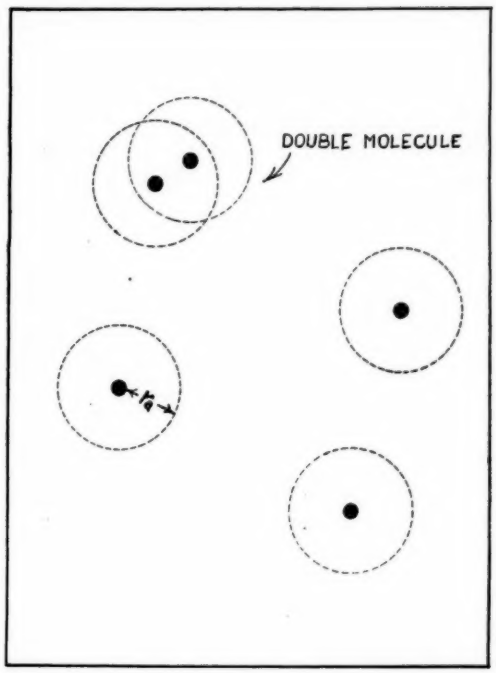

FIG. 3. An imperfect gas as a mixture of single and double molecules (or collision complexes).

only the double molecules can affect the second virial coefficient. In order to define the double molecules unambiguously, it is necessary to postulate that there exists a range of interactions such that whenever two molecules lie within this range, the energy of interaction is appreciable compared to kT and whenever they lie outside of this range their energy of interaction is negligible. If a molecule comes within the interaction range of another molecule the pair is considered to form a double molecule. This is illustrated in Fig. 3. The single molecules behave like molecules of a perfect gas until they collide with other molecules, whereupon we treat them separately as double molecules. The free volume in which the single molecules move like a perfect gas is $V-b_a$ where V is the molar volume of the system and b_a differs from the usual van der Waals b in having the range of interaction of the attractive forces substituted for the smaller collision diameter. Subtracting b_a from V corresponds to the fact that single molecules are excluded from the definitional domain of the double molecules. It is true that double molecules behave like a perfect gas in a

volume slightly different from $V-b_a$ but this difference can affect only the third and higher virial coefficients. From these considerations, we see that up to the third virial coefficient, the equation of state of an imperfect gas may be written:

$$p(V-b_a)=(n_1+n_2)RT, \tag{13}$$

where n_1 is the number of moles of single molecules and n_2 is the number of moles of double molecules. The numbers of single and double molecules are determined by an ordinary equilibrium constant for association

$$K(T)=n_2V/n_1^2. \tag{14}$$

In the limit that V is very large, n_1 approaches unity and n_2 approaches the value $K(T)/V$. Rearranging the equation of state (13) into the virial form, it is evident that

$$B(T)=b_a-K(T). \tag{15}$$

It is easy to derive this expression for the second virial coefficient directly from the fundamental statistical mechanical relation:

$$B(T)=\frac{N}{16\pi^2}\int\cdots\int(1-\exp(-E/kT))d\Omega d\tau.$$

While this integration is to be carried out over the whole range of the variables, the predominant part of the integral comes from that range over which the molecules have an appreciable effect on one another. This is the same interaction range which we were discussing in the previous paragraph. Thus:

$$B(T)=\frac{N}{16\pi^2}\int_{\text{interaction range}}\cdots\int(1-\exp(-E/kT))d\Omega d\tau$$
$$=b_a-K(T), \tag{16}$$

where now

$$b_a=\frac{N}{16\pi^2}\int_{\text{interaction range}}\cdots\int d\Omega d\tau \tag{17}$$

and

$$K(T)=\frac{N}{16\pi^2}\int_{\text{interaction range}}\cdots\int\exp(-E/kT)d\Omega d\tau. \tag{18}$$

It is evident that b_a and $K(T)$ have the physical significance which we attributed to them in the above discussion. The equilibrium constant $K(T)$ for the formation of double molecules is the ratio of the partition function for double molecules to the square of the partition functions for the single molecules. Since very few of the double molecules exist in discrete vibrational or rotational levels, we may treat the problem classically. In the classical approximation, it is evident that the internal degrees of freedom, the rotation of the double molecules, and the translational kinetic energy parts of the partition functions all cancel out of the equilibrium constant, leaving us with just the part of the phase integral for double molecules which is concerned with the translational potential energy. The additional factor of $\frac{1}{2}$ arises from the symmetry number of the double molecule. Thus b_a and $K(T)$ are just the expressions to which our simplified discussion leads.

Since $K(T)$ is an ordinary chemical equilibrium constant, we can also express it in terms of the

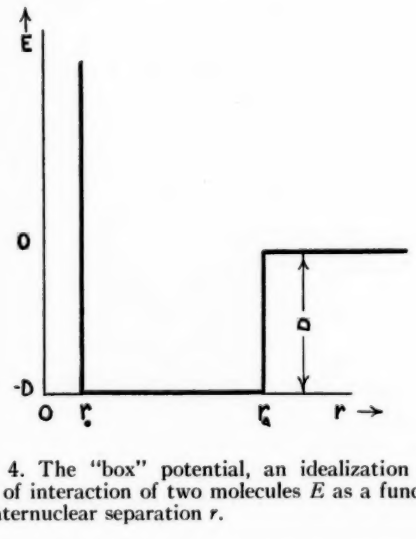

FIG. 4. The "box" potential, an idealization of the energy of interaction of two molecules E as a function of their internuclear separation r.

entropy ΔS and the energy ΔE of formation of the double from the single molecules.

$$K(T)=\exp(\Delta S/R-\Delta E/RT). \tag{19}$$

In general, ΔS and ΔE will depend somewhat on the temperature, but for comparatively small temperature ranges they may be considered to be constants. If we let $b_ac=\exp(\Delta S/R)$, the dependence of $B(T)$ on temperature assumes the

functional form:

$$B(T)=b_a(1-c\exp(-\Delta E/RT)). \quad (20)$$

Here b_a, c, and ΔE may be considered as three constants to be evaluated from the experimentally observed temperature variation of $B(T)$.

The physical significance of these constants is clarified by considering a hypothetical "box" potential for which we can calculate $B(T)$ in simple closed form. Here we assume that the molecules are spherically symmetrical; there is no energy of attraction until the molecules come a distance r_a apart; between r_a and the collision diameter r_0 there is a constant energy of attraction D; and it is impossible for the molecules to get any closer together than r_0. Figure 4 makes this clear. Substituting this potential into Eq. (5), we get:

$$B(T)=\frac{2\pi N r_a^3}{3}\left[1-\left(\frac{r_a^3-r_0^3}{r_a^3}\right)\exp(D/kT)\right]. \quad (21)$$

Comparing this with Eq. (15) we see that:

$$b_a=2\pi N r_a^3/3,\quad c=(r_a^3-r_0^3)/r_a^3,\quad \Delta E=-D. \quad (22)$$

Here we see once more that b_a is the van der Waals constant corresponding to the range of the attractive forces r_a and ΔE is the energy of formation of the double molecules. However, a consideration of this box potential brings out the significance of c; it is the ratio of the free volume v_f within the definitional domain of the double molecule to the total volume of the double molecule. Looking at these constants from a slightly different angle; $b_a c=v_f$ and so $\Delta S=R\ln v_f$, an expression similar to that which has become familiar in the theory of liquids. This interpretation of c in terms of a free volume is a general concept which should hold for any type of potential well. In case the molecule is asymmetrical, hindered rotation of the two molecules with respect to one another within the definitional domain of the double molecules will decrease the free volume and c. The extent of this decrease might be indicated by a "free-angle" factor equal to the average solid angle through which the molecules can rotate in the double molecule divided by 4π. This would be analogous to the treatment of Kincaid and Eyring[13] of the theory of liquids made up of asymmetrical molecules. We must be cautious in our interpretations of c, as unusually small or unusually large values may be due to force fields of a peculiar nature as well as to shape factors.

The exact second virial coefficient, $B(T)=b_0F_{12}(E_m/kT)$, for the spherical non-polar molecules which satisfy the Lennard-Jones potential (4) can be curve fitted to approximate $B(T)=b_a(1-c\exp(-\Delta E/RT))$. If we take $b_a=4.75b_0$, $c=0.835$, and $\Delta E/R=-0.608E_m/k$, the fit is perfect for $E_m/kT=0.4988$, 0.7046, and 0.9953 and is better than one part in one hundred over the whole useful temperature range. Going back to the equation of corresponding states, we could write these constants: $b_a=3.23V_c$, $c=0.835$, and $E/R=0.463T_c/T$. The constant $c=0.835$ is characteristic of the Lennard-Jones potential and complex molecules may have values quite different. Because of this variation in c we must depart from the equation of corresponding states when we come to fitting the experimental values to within their experimental error.

Unfortunately there are only a few molecules for which the experimental data are sufficiently accurate and cover a sufficiently large temperature range so that three constants b_a, c, and $\Delta E/R$ can be uniquely determined. For example in the case of ethane, we might take:

$b_a=135$ cc/mole, $c=0.731$,
and $-\Delta E/R=356$ deg.

or

$b_a=470$ cc/mole, $c=0.841$,
and $-\Delta E/R=153$ deg.

Either set of constants would fit the experimental data to within five percent for a two-hundred-degree temperature range. It is therefore necessary to legislate arbitrarily the value of one of the constants, say b_a. Making the most careful fits of the hydrocarbons and freons, we find that the average value of $b_a=1.75V_c$. The value of $b_a=3.23V_c$ of the Lennard-Jones gases is definitely too large and would lead to rather large deviations from the experimental values. This may not be apparent from our graph for

[13] J. Kincaid and H. Eyring, J. Chem. Phys. **6**, 620 (1938).

TABLE IV.

	b_a cc/mole	c	$-\Delta E/R$ degrees K	Fraction double molecules at 1 atmos. and 298°K	Ref. expt. data
Ethane	251	0.778	244	0.018	6
Propane	341	.681	347	.030	5
n-Butane	452	.689	387	.047	7
n-Heptane	749	.559	629	.141	8
Ethene	223	.788	222	.015	1
Propene	316	.679	339	.027	1
Propadiene	300*	.614	382	.027	1
1-Butene	430†	.487	492	.045	1
2-Methyl-Propene	430†	.493	490	.045	1
trans-2-Butene	430†	.569	465	.047	1
cis-2-Butene	430†	.443	537	.047	1
Freon−11 CCl_3F	434	.729	399	.049	h
Freon−21 $CHCl_2F$	345	.920	306	.036	i
Freon−12 CCl_2F_2	381	.631	345	.031	j
Freon−113 $CCl_2F-CClF_2$	569	.888	335	.064	k
Methyl Chloride CH_3Cl	239	.582	469	.027	g
Ammonia	62.8‡	.509	692	.013	f
Steam	38.5‡	.420	1260	.045	3

* Estimated from propane and propene.
† Estimated from ethene and propene.
‡ b_a was varied so as to fit the experimental data best, all other values of b_a in the table take $b_a = 1.75V_c$.

the reduced second virial coefficient because of the small scale in which the points are plotted. By assuming a definite value of b_a, the other two constants may be uniquely determined and have significance.

In Table IV we have tabulated the best values of the constants b_a, c, and $\Delta E/R$ for the hydrocarbons, freons, ammonia, steam, and methyl chloride. Let us interpret these results:

1. Paraffins

(a). $\Delta E/R$ increases with increasing number of carbon atoms. This corresponds to the long range of the van der Waals forces which enable distant atoms in a molecule appreciably to contribute to the energy of attraction of a molecule during collision.

(b). The value of c decreases with increasing number of carbon atoms. This agrees with our expectation that c should decrease as the molecule becomes more unsymmetrical.

(c). At one atmosphere pressure and room temperature, the fraction of double molecules increases with the number of carbon atoms. This may be considered a tendency for the higher hydrocarbons to cluster in the vapor phase. However, the hydrocarbons very nearly satisfy the theorem of corresponding states, so that this tendency would be the same if we compared the hydrocarbons at the same value of their reduced temperature, T/T_c.

2. Olefins

(a). The value of $\Delta E/R$ increases and c decreases as we increase the number of carbon atoms. This is similar to the paraffin series.

(b). cis-2-butene has a small dipole moment and its value of c is less than for the others.

3. Freons

(a). All of the freons have large values of c and approximately the same values of $\Delta E/R$.

(b). Because of the comparatively large errors in the experimental values, it was impossible to choose the values of c and of $\Delta E/R$ such that all of the experimental points were fitted to within 5 percent. For the other substances tabulated, the maximum errors in the curve fitting were of the order of 1 percent.

4. The Dipole Molecules: Steam, Ammonia, and Methyl Chloride

(a). Methyl chloride has a large value of $\Delta E/R$ for a small molecule but otherwise its constants appear normal. Because it has such a small reduced dipole moment (even though its actual dipole is larger than that of water) it shows no extreme dipole behavior.

(b). The values of b_a for steam and for ammonia are less than their critical volumes or about one-half of the normal values. If we had used larger values of b_a, we would have obtained a considerable deviation from the experimental observations.

(c). The values of $\Delta E/R$ for steam and ammonia are very large for such small molecules.

(d). The values of c for steam and ammonia are abnormally small. This is to be expected since small values of c are a manifestation of hindered rotation.

The large number of instantaneous double molecules in an imperfect gas is an interesting feature of our viewpoint. The fact that 4.5

percent of butane or 14 percent of heptane molecules at room temperature and one atmosphere pressure in the vapor phase are in a state of collision should have some interesting consequences. We should expect deviations from Beer's law for certain frequencies. Also, as H. Beutler and A. Turkevitch have suggested to us in a private discussion, some of the spectroscopic absorption bands which are present in the liquid but lacking in the molecular spectra should appear in the imperfect gas with an intensity proportional to the number of double molecules or proportional to the square of the pressure.

We would like to express our appreciation to the Wisconsin Alumni Research Foundation for the financial support of one of us (I.F.W.) during the course of this work.

APRIL, 1942 JOURNAL OF CHEMICAL PHYSICS VOLUME 10

Co-Precipitation of Radium and Barium Salts as a Function of Temperature and Acidity

W. B. PIETENPOL
Department of Physics, University of Colorado, Boulder, Colorado

(Received December 11, 1941)

Co-precipitation of radium and barium salts which accompanies the cooling of a solution results in the deposition of a percentage of radium largely in excess of that of barium. Under similar conditions of cooling the relative amounts of radium and barium deposited have been determined at different temperatures throughout the cooling process and curves have been plotted. Determinations of the above nature have been made with radium-barium solutions containing different concentrations of hydrobromic acid, and the variation in the form of the curves is shown. The first crystals formed in the solution contain a larger percentage of radium than succeeding crystals. It is pointed out that the efficiency of the refining process may be increased by separating liquor and crystals at a point above room temperature. In this way the factor of enrichment is increased, thereby hastening the process. Factor of enrichment curves for solutions of different acidity show that for cooling from boiling to room temperature an increase in acidity decreases the crystallization factor. However the inverse relationship is shown to be true when the solution is cooled through a small temperature interval. The rate at which the solution cools is a factor in the relative amounts of radium and barium deposited. With rapid cooling a smaller percentage of radium is precipitated than with slow cooling.

INTRODUCTION

IN the commercial refining of radium, the radium salts are commonly purified by fractional crystallization of a radium-barium solution. The chlorides and bromides are usually employed and the details of the method have been fully described.[1] In a series of crystallizations it has been pointed out[2] that the crystal fractions are progressively enriched with radium, while the liquor fractions are progressively impoverished. The concentration of the radium at any step in the positive direction is expressed by the relation

$$C = AK^n,$$

where A is the initial concentration of the radium salt, n the number of crystallizations, and K the factor of enrichment or crystallization factor. K is defined as the ratio of the concentration of radium crystals separated to the concentration of radium in the original crystals.

Nierman[3] working with mesothorium and radium-barium bromide solutions, found that the crystallization factor is independent of the concentration of hydrobromic acid. He also concluded that for varying concentration of mesothorium up to 2 mg per gram of salt, the crystallization factor remains constant. Unfortunately he made no reference to what precautions were taken in keeping the temperature limits constant, neither did he state that the rates of cooling of his solutions were uniform. As will be shown

[1] Bull. U. S. Bur. Mines, No. 104 (1915).
[2] Clarence E. Scholl, J. Am. Chem. Soc. **42**, 889 (1925).
[3] John L. Nierman, J. Phys. Chem. **24**, 192 (1920).

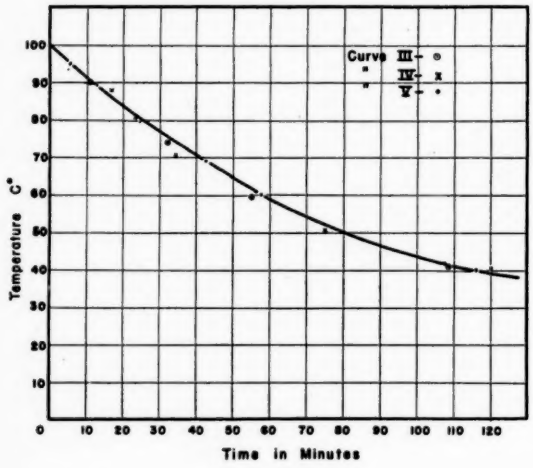

FIG. 1.

later these are two important conditions to be considered in the determination of the factor of enrichment.

Scholl[2] carrying out a fractional crystallization process with the radium-barium bromides and chlorides found that the value of K depended upon the temperature of maximum heating and minimum cooling, the speed of cooling, and the acidity of the solution. Scholl cooled his solutions saturated at 95°C by placing the crystallizing dishes for a period of 20 hours in a room of constant temperature at 20°C. He concluded that the greater the acidity the greater was the quantity of crystals formed and the smaller the factor of enrichment. Furthermore the effect of low concentrations of radium salt was found to be very marked if occurring with high concentrations of acid. With these conditions it was indicated that the enrichment of radium is reversed, more radium occurring in the mother liquid than in the crystals. Scholl's conclusions may now be interpreted in terms of the results presented in this paper.

EXPERIMENTAL PROCEDURE

A stock solution of radium-barium bromide was used, containing approximately 20 mg of radium per ton. 450 cc of this solution was placed in a beaker and heated in a bath the temperature of which could be controlled. This solution was heated to 95°C and under constant stirring was allowed to evaporate until saturation was obtained. The technique used to determine saturation was to allow a slight stream of air to strike the surface of the solution and observe the formation of crystals. After many trial experiments this was found to be a satisfactory method of indicating saturation.

At the point when crystallization was initiated samples were drawn by means of a graduated pipette to determine the radium-barium ratio. Because of the experimental difficulty in drawing two samples simultaneously, separate identical runs were made to determine the radium and the barium contents. For the radium determination, when the activity was high, proper dilution was made in order to obtain the correct amount for the most accurate measurement. The sample was then boiled gently to remove occluded radon gas, sealed in a flask under partial vacuum, and allowed to grow for a definite period. The amount of radium per cc of solution drawn was then measured in the usual way by an emanation electroscope of the Lind type. For the determination of the barium in solution the samples drawn were evaporated to dryness under gentle heat and allowed to stand in a dry atmosphere for about two days before weighing.

After the initial samples were drawn the solution was allowed to cool at a controlled rate. During the cooling the solution was constantly stirred and succeeding samples were drawn at spaced temperature intervals. However, preced-

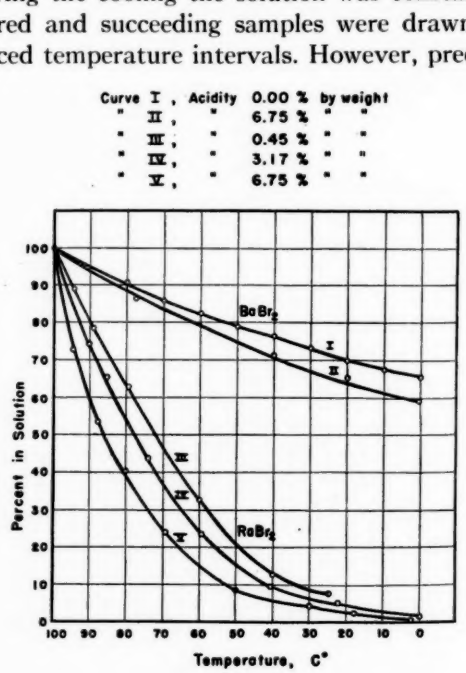

FIG. 2.

ing the drawing of a sample the stirring was temporarily discontinued to avoid the removal of minute crystals in suspension. Since the rate of cooling is a factor in the co-precipitation process, the cooling rate was reproduced as far as was possible in succeeding runs. The degree to which this was accomplished is shown by the curves in Fig. 1 covering the most critical portion of the temperature range.

The acidity of the solution was changed by the addition of a certain percentage of hybromatic acid. While this gave an approximate value, it was not considered reliable because of the evaporation of water in initially reducing the solution to the point where it was saturated with barium bromide. A sample was therefore drawn at the end of each run by means of which the maximum acidity was determined.

RESULTS

The results of the experimental determination of the co-precipitation of radium and barium bromides as related to temperature and acidity are shown by curves in Fig. 2. In this figure, the percentages of radium and of barium remaining in solution are plotted as a function of temperature. From these results the amounts of radium and barium precipitated in the form of crystals may readily be obtained and the factors of enrichment determined. For the various values of acidity in percentage by weight these factors are plotted in Fig. 3 as a function of the temperature in degrees C to which the solution was cooled.

The conclusions to be drawn from the author's results are obvious. In the first place, it is apparent that the factor of enrichment, as determined by the radium-barium ratio in the crystal fractions, is greatly increased when the cooling process is stopped and the liquor is separated from the crystals at a temperature far above room temperature. Such procedure results in a far greater concentration ratio and, in addition, introduces a time saving factor, since under ordinary conditions the time rate of cooling is more rapid at high temperatures than in the neighborhood of room temperatures.

The rate of formation of barium crystals is, however, a factor which cannot be neglected in the co-precipitation of radium. As an indication of this, the following experiments were performed. A radium-barium solution was heated and evaporated to saturation as in the previous experiments. Samples were drawn to determine the initial radium and barium content. One-half of this solution was cooled rapidly by passing through a water cooler and the other half was cooled slowly as represented by the time curve in Fig. 1. After cooling through the same temperature interval samples were taken to determine the radium-barium ratio and the acidity of the solution. In these tests the acidity was 1.14 percent by weight.

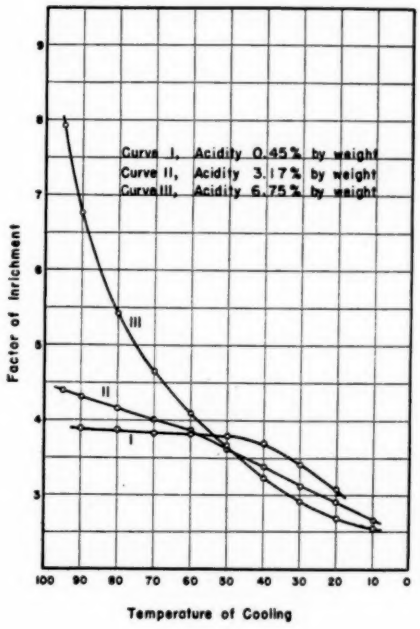
Curve I, Acidity 0.45% by weight
Curve II, Acidity 3.17% by weight
Curve III, Acidity 6.75% by weight
Factor of Inrichment
Temperature of Cooling
100 90 80 70 60 50 40 30 20 10 0

FIG. 3.

Test No. 1. Initial radium content at saturation, 426.8×10^{-10} curie per cc.

	Temperature interval	Factor of enrichment
Cooled rapidly	96.5° to 22°C	2.52
Cooled slowly	96.5° to 22°C	3.29

Test No. 2. Initial radium content at saturation, 451.8×10^{-10} curie per cc.

	Temperature interval	Factor of enrichment
Cooled rapidly	100° to 25°C	2.66
Cooled slowly	100° to 25°C	3.31.

The results show that with slow cooling a larger percentage of radium bromide is deposited with the barium bromide crystals. In terms of co-precipitation as an adsorption process these results are significant. However, in the commer-

cial refining process the variation in the crystallization factor with time rate of cooling may not be of great importance.

The conclusions of previous experimenters working in the fractional crystallization of radium and barium salts may now be interpreted in the light of the author's results. Nierman's conclusions that the factor of enrichment is independent of the concentration of hydrobromic acid and that the separation can be conducted advantageously in neutral or slightly acid solutions of the bromides, may be explained by reference to the curves of Fig. 3. Without careful control of the temperature interval through which the solution has been cooled no fair conclusion concerning the effect of acidity on the factor of enrichment may be drawn. Furthermore, Scholl's statement that "the greater the acidity the greater the quantity of crystals and the smaller the factor" is confirmed by the present results for the special case, as in his experiments, when the solution was cooled from 95°C to room temperature at 20°C. It may be mentioned that in the author's experiments the concentration ratio is constantly changing with change in temperature. Work on the co-precipitation of radium and barium salts as affected by temperature and concentration ratio, and the nature of the adsorption process is in progress.

In conclusion the author wishes to express his deep appreciation to Dr. O. C. Lester who suggested the problem and gave very valuable assistance in the experimental technique involved.

APRIL, 1942 JOURNAL OF CHEMICAL PHYSICS VOLUME 10

Intramolecular Energy Transfer

The Fluorescence of Complexes of Europium

S. I. WEISSMAN*
Department of Chemistry, University of California, Berkeley, California

(Received December 17, 1941)

The characteristic line fluorescence of trivalent europium is excited in certain organo-europium compounds by irradiation with light absorbed only by the organic part of the compound. The efficiency of excitation varies greatly with the nature of the compound, temperature, and solvent. Under optimum conditions, i.e., solution of a covalent compound at liquid-air temperature, almost unit efficiency has been obtained. The decay time of the fluorescence is independent of quenching; quenching prevents excitation of the europium ion. There seems to be a steady gradation of efficiency of transfer from covalent to ionic compounds.

ABSORPTION of energy by the trivalent ions of certain of the rare earths is often followed by emission of characteristic line luminescence. In most instances of rare earth fluorescence hitherto reported, the excitation has been accomplished by illumination of the material with light containing frequencies which are absorbed directly by the rare earth ions.[1] As we shall see, the excitation may be accomplished, under suitable conditions, through light absorption by other constituents of the rare earth compound with subsequent transfer of energy to the rare earth ion. Indeed, in some cases excitation with wave-lengths in the near ultraviolet and the visible violet yields "forbidden" rare earth fluorescence as bright as that of fluorescein under similar excitation.

Experiments with compounds of europium only will be discussed here, although observations with samarium and terbium have shown that the phenomena occur in compounds of these substances also.

---

* National Research Council Fellow, 1941–1942.

[1] O. Deutschbein and R. Tomascheck, Ann. d. Physik **29**, 311 (1937); H. Gobrecht, Ann. d. Physik **28**, 673 (1937). Except for the continuous absorption at wave-lengths lower than 2500A, the rare earth ion absorptions are weak and narrow, and as a result excitation of moderate intensities of luminescence require great intensities of exciting light.

Comparison of the fluorescence of crystals of europium salicylaldehyde[2] and of europium chloride hexahydrate illustrate the phenomenon. A monochromatic (30–40A wide) beam of light provided by a continuous source (the sun) and a Hilger quartz monochromator were focused first on a mass of crystals of $EuCl_3 \cdot 6H_2O$. As the dial of the monochromotor was turned through the 3000A–4000A region, bursts of the characteristic red orange fluorescence of europium[3] appeared at wave-lengths of exciting light 3920A and 3200A. These are the locations of the only fairly strong absorptions of europium ion in this region. When the europium chloride was replaced by a mass of crystals of europium salicylaldehyde, a compound possessing an intense and continuous absorption band between 3200A and 4400A, characteristic europium fluorescence of almost uniform intensity appeared at all wave-lengths of exciting light between these limits. Although sharp localization of the act responsible for this intense absorption may not be possible, the internal $(4f)^6$ electronic system of the europium is certainly not involved since the same band appears in the salicylaldehydes of colorless ions such as lanthanum and gadolinium. Hence it seems certain that excitation of the internal electronic system of the europium is provoked by light absorption in a region external to it.

The yield of fluorescence under this mode of excitation, in all cases thus far studied, has been strongly dependent on temperature and, in solution, on the nature of the solvent. The intensity of fluorescence from a 5×10^{-4} molar benzene solution of europium salicylaldehyde increases by a factor of 5.1 as the solution is cooled from 45°C to 6°C.[4] A solution of europium nitrate in water shows a change of only a few percent in its fluorescence intensity under the same temperature change. The fluorescence yield from solid europium salicylaldehyde increases about 150-fold as the material is cooled from 300°K to 90°K; the yield from crystalline europium chloride hexahydrate increases by a factor of 2 at most over the same temperature range.

The sensitivity of the fluorescence yield to the type of compound in which the transfer occurs may be seen from the data of Table I; here are given the intensities (in arbitrary units) at different temperatures of the fluorescence from 2×10^{-4} molar solutions in benzene of europium metanitrobenzoylacetonate and europium salcylaldehyde. The measurements were made under comparable conditions of total absorption of the 3650A radiation of a mercury arc. It will be noted that in the temperature range studied the fluorescence from the nitrobenzoylacetonate is brighter than that from the salicylaldehyde but that the salicylaldehyde fluorescence increases more rapidly with decreasing temperature.

TABLE I. Temperature dependence of fluorescence.

t°C	I_1	I_2	I_1/I_2
6.5	233	46	5.1
19.0	183	26	7.0
32.0	106	14	7.6

I_1 = Galvanometer deflection from fluorescence of europium nitrobenzoylacetonate.
I_2 = Deflection from europium salicylaldehyde.

Further, the yields from solutions of a given compound vary greatly from solvent to solvent. The fluorescence at room temperature from a 10^{-4} molar alcohol solution of europium benzoylacetonate, excited by radiation from a high pressure mercury arc, is barely visible in the dark, while the same material in benzene or toluene exhibits a fluorescence easily visible in a fully lighted room. However, the fluorescence from the alcohol solution increases very rapidly with decreasing temperature and at −80°C becomes as bright as the fluorescence from the toluene solution. Indeed, the fluorescence intensities from solutions at low temperatures of many compounds seem roughly equal. We would naturally suspect that in these cases unit quantum efficiency is approached. Measurement of the yield of the brightest fluorescence yet encountered supports this suspicion. The measurement was made by comparison with the intensity of fluorescence from a fluorescein

[2] $Eu(C_6H_4CHOO)_3$, a non-ionic compound, insoluble in water, very soluble in benzene.
[3] A line at 5790A, a group at 5880A, a group at 6100A.
[4] The measurements were made with a Weston photronic cell Model 594, type 2. The solution was contained in a Pyrex cell 1 cm deep; in such a cell there is total absorption of the exciting radiation—the 3200A–4000A region from a high pressure mercury arc.

TABLE II. Relative efficiencies of fluorescence of various compounds.‡

Compound	Formula of negative constituent	Solid room temp.	Solid liquid air	Benzene solution room temp.	Soln. in a. e. i.* room temp.	Soln. in a. e. i.* liquid air
Salicylaldehyde	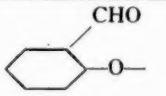	1	3	2	—	—
Benzoylacetonate	$\varphi-CO^{-}=CH-CO-CH_3$	2	3	2	1	3
Metanitrobenzoylacetonate	$NO_2\varphi-CO^{-}=CH-CO-CH_3$	2	3	2	1	3
Dibenzoylmethide	$\varphi-CO^{-}=CH-CO-\varphi$	2	3	2	1	3
o-hydroxy acetophenone	$-O-\varphi-COCH_3$	2	3	2	—	—
5 nitrosalicyl aldehyde	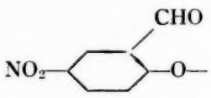	3	3	—	2	3
3 nitrosalicyl aldehyde	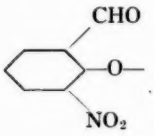	1	2	—	0	2
3 nitrosalicylate	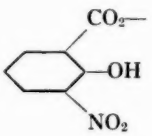	0	2	—	0	2
5 nitrosalicylate	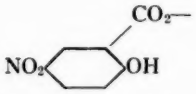	0	2	—	0	2
picrate	$(NO_2)_3\varphi-O-$	1	2	—	0	2
o-nitrophenolate	$NO_2\varphi-O-$	*a*	*a*	—	0	2
m-nitrophenolate	$NO_2\varphi-O-$	*a*	*a*	—	0	1–2
p-nitrophenolate	$NO_2\varphi-O-$	*a*	*a*	—	0	2
2-4-6 trinitro benzoate	$(NO_2)_3\varphi-CO_2-$	0	1	—	0	0
Platinocyanide	$Pt(CN)_6^{=}$	0	0	—	—	—

a = not isolated as a solid.
* The alcohol-ether-isopentane mixture.
‡ Details concerning the spectra and preparation of the individual compounds will be given in another communication.

solution.[5] A 2.8×10^{-4} molar solution of europium metanitrobenzoylacetonate in a 2–5–5 mixture by volume of ethyl alcohol, diethyl ether, and isopentane[6] illuminated at liquid-air temperature by the 3650A line of a mercury arc yielded fluorescence 0.86 as intense as that given by a 6×10^{-4} molar solution of fluorescein in alcohol. Total absorption of the exciting radiation took place in each case. If the quantum yield of fluorescence of the fluorescein solution is 0.9, the yield for the europium solution is 0.85.[7]

[5] S. I. Vavilov has made measurements of the absolute yield from fluorescein solutions. S. I. Vavilov, Zeits. f. Physik **22**, 266 (1924).

[6] This solvent has been extensively used in this laboratory by Professor Lewis and Dr. Lipkin. See G. N. Lewis, T. T. Magel, and D. Lipkin, J. Am. Chem. Soc. **62**, 2973 (1940).

[7] This is a quantum efficiency; account has been taken of the frequencies of the fluorescein and europium luminescences.

In those situations in which the quantum yield is less than unity, it is desirable to locate the fluorescence quenching act in the sequence of events after the initial absorption of light. Measurements of the variation of the lifetime of fluorescence with efficiency provide information on this point. The transitions responsible for the europium fluorescence are of the forbidden type, and we would expect an afterglow of duration 10^{-3}–10^{-2} sec. Vavilov and Sevchenko[8] have found for aqueous solutions of inorganic europium salts τ (the decay constant) $=0.84\times10^{-3}$ second. With a Becquerel phosphoroscope, I have found for the organic europium compounds described here values of τ from 0.7×10^{-3} to 1.0×10^{-3} second.

The phosphoroscope consisted of two 25-cm disks each containing four symmetrically spaced 1-cm wide slots. The disks were driven at thirty revolutions per second by a synchronous motor which maintained them in exact synchronism with the flashes from a high pressure mercury arc. This synchronism is necessary so that the illuminating slots encounter the light beam at the same position in each cycle. For detection of changes in decay time—the point in which we are especially interested—two settings of the disks were used; at one setting the slots were staggered by 4.2×10^{-4} sec., at the other by 18×10^{-4} sec. The relative intensities of afterglow at these times were measured with a photronic cell and galvanometer.

Following are a set of intensity readings taken on 1.4×10^{-4} molar solution of europium meta-nitrobenzoylacetonate in the ether-alcohol-isopentane mixture at -50°C and at -190°C.

$t=4.2\times10^{-4}$ sec.	$t=18\times10^{-4}$ sec.
$-$ 50°C 8.8	2.2
$-$190°C 19.5	5.0

The ratios of the intensities at the beginning and end of an interval 1.4×10^{-3} sec. long (two half-lives) differ by only two percent, while there is over a twofold change in efficiency at the two temperatures.

[8] S. I. Vavilov and A. N. Sevchenko, Comptes rendus acad. sci. U. R. S. S. **27**, 541 (1940).

Similar experiments on europium picrate solutions in the alcohol-ether-isopentane solvent in which the intensities were compared by a visual polarization photometer, showed that as the efficiency changed by over fifty-fold the decay constant changed no more than thirty percent. These results indicate that the major part at least of the quenching of fluorescence is accomplished by some dissipative process occurring previous to the excitation of the rare earth ion. There seems to be remarkably little deactivation by non-radiation processes of those rare earth ions which do receive excitation energy.

The dependence of the efficiency of energy transfer on the type of compound in which the europium ion and absorbing group are linked has already been mentioned. I have examined the fluorescence of the europium compounds listed in Table II. Estimates are given of the efficiencies of transfer of the solids and approximately 10^{-4} molar solutions in the alcohol-ether-isopentane mixture at room temperature and liquid-air temperature; estimates on benzene solutions, where it has been possible to prepare them, are also included. The entire zero to unity range of efficiencies has been arbitrarily divided into four regions; fluorescence yields of twenty-five percent or higher are labeled 3, zero yield 0, and intermediate yields 2 and 1.

A steady decrease in efficiency of energy transfer from the covalent, benzene soluble, benzoylacetonates, to the ionic crystals of the platinocyanide is apparent. Evidently energy does not easily cross ionic bonds. Just what conditions of conjugation and resonance are necessary for ready transfer across non-ionic bonds has not yet been established. Further work on this point is in progress.

ACKNOWLEDGMENTS

All the europium used in this research was supplied by Dr. H. N. McCoy. A portion had been originally given to Dr. Simon Freed from whom I borrowed it, and the rest was given me by Dr. McCoy. It is a pleasure to acknowledge the generosity of Drs. McCoy and Freed.

Frequency Spectrum of Crystalline Solids

ELLIOTT W. MONTROLL*
Sterling Chemistry Laboratory, Yale University,† New Haven, Connecticut
(Received January 2, 1942)

It is generally accepted that a normal crystalline solid can be pictured at absolute zero as an assembly of molecules arranged at periodically placed lattice points. Since at higher temperatures each molecule becomes a harmonic oscillator about its lattice point, in order to calculate thermodynamic properties of the crystal it is necessary to know the distribution of its internal normal modes of vibration. On the basis of the Born-von Kármán model these normal modes of vibration are roots of a secular determinant. In this paper it is shown that the $2n$th moment of the distribution function of normal modes is proportional to the trace of the nth power of the matrix of the Born-von Kármán determinant. By expressing the distribution function as a linear combination of Legendre polynomials it is shown that the coefficient of each polynomial is a linear combination of the moments. The frequency distribution function of a two-dimensional simple cubic lattice is calculated by the above method and turns out to have two maxima. Usually the equation for a thermodynamic function $F(T)$ involves the integral of the product of the frequency distribution function $g(\nu)$ and a known function $K(T, \nu)$. We show here that when $F(T)$ is a known function of T an integral equation results with $g(\nu)$ under the integral sign. This integral equation can be solved for $g(\nu)$ by use of Fourier transforms.

I. INTRODUCTION

ONE of the failures of classical mechanics and classical statistics was their inability to explain even qualitatively the decrease in specific heat of solids with decreasing temperatures; and one of the selling points of Planck's original quantum theory had its source in the success of Einstein's[1] application of Planck's "quantized oscillators" to the lattice vibrations of a solid. By Einstein's method the vibrational factor of the partition function of a normal crystal is

$$Q=\prod_{i=1}^{3N}\frac{\exp(-h\nu_i/2kT)}{1-\exp(-h\nu_i/kT)} \qquad (1)$$

and the Einstein assumption of equal numerical value of all $3N$ frequencies of a crystal explains the observed decrease of the specific heat below the Dulong-Petit value of $3NkT$ at low temperatures. Here h = Planck's constant, k = Boltzmann's constant, T = absolute temperature, ν_i = frequency of the ith normal mode of vibration, N = number of lattice points.

Refinements in specific heat measurements in the first decade of this century demonstrated that the agreement between experiments and Einstein's theory was not quantitative at low temperatures; and Debye[2] and Born and von Kármán[3] pointed out that the discrepancies were probably due to the existence of a distribution of normal modes of vibration instead of a single "Einstein frequency." Thus, for example, the temperature dependent vibrational contribution per lattice point to the free energy should be written[4]

$$F_V(T)=-kT\int_0^\infty g(\nu)\log(1-e^{-h\nu/kT})d\nu, \qquad (2)$$

where $g(\nu)d\nu$ is the fraction of normal modes with frequencies between ν and $\nu+d\nu$.

Debye's proposition to treat the solid as a continuum with the same elastic properties led to a frequency distribution proportional to ν^2 and to equations of physical quantities in terms of a parameter $\Theta=h\nu_L/k$ which theoretically should be a constant for a given crystal. The term ν_L is the largest frequency of the normal modes of vibration, and Θ is usually referred to as the Debye or characteristic temperature. Unfortunately this development which mathematically is quite simple is insufficient, for experiments

* Sterling Research Fellow in Chemistry.
† Present address: Baker Chemistry Laboratory, Cornell University, Ithaca, New York.
[1] A. Einstein, Ann. d. Physik **22**, 180 (1906); **34**, 170 (1911).
[2] P. Debye, Ann. d. Physik **39**, 789 (1912).
[3] M. Born and T. von Kármán, Physik. Zeits. **13**, 297 (1912); **14**, 15 (1913).
[4] For a general discussion of theory of normal solids cf. E. Schroedinger, *Handbuch der Physik* (1926), Vol. 10; M. Born and M. Göppert-Mayer, *Handbuch der Physik* (1933), Vol. 24; R. Fowler, *Statistical Mechanics* (1936), Chap. 4.

show that Θ is not constant over a large temperature range.

The extension of Born and von Kármán of Einstein's work afforded a more accurate physical picture than that suggested by Debye. However, it led to a mathematical problem which could be solved analytically for a one-dimensional solid but which required tedious numerical calculations in two- and three-dimensional crystals. In the Born-von Kármán theory one sets up the equations of motion for a set of coupled oscillators with the same coupling and force constants as those of the crystal, and shows that the normal modes of vibration are the characteristic roots of a secular determinant of order N^3. Actually the determinant can be factored into secular determinants of very small order, but to find $g(\nu)$ by present methods the roots of all the resulting equations (and there are $O(N^3)$ of these) must be calculated and the number of roots in every small frequency interval must be determined. Even though it seems reasonable to base the $g(\nu)$ computations on the solution of a large random sample of cubic equations, the lack of popularity of the Born-von Kármán approach is understandable.

The first part of this paper will be devoted to developing an analytical method of finding $g(\nu)$ in a Born-von Kármán crystal. This method will depend on the matrix theorem that the sum of the kth powers of the characteristic values of a matrix is equal to the trace of the kth power of the matrix. Noticing that the sum of the kth powers of the characteristic values of the Born-von Kármán matrix is proportional to the kth moment of $g(\nu)$, and that a continuous distribution function defined in a finite interval can be expanded as a linear combination of Legendre polynomials, it is apparent that the coefficients of the Legendre polynomials can be expressed as linear combinations of the moments of $g(\nu)$. This means that $g(\nu)$ can be expressed analytically as a function of the lattice constants of the crystal.

These observations will be applied in detail to a two-dimensional cubic lattice, postponing to some later date the application (which is not much more difficult) to real three-dimensional crystals.

The second part of this paper will concern the determination of $g(\nu)$ from experimental specific heat data by use of Fourier transforms.

II. $g(\nu)$ FOR THE BORN-VON KÁRMÁN MODEL

1. Mathematical Techniques

The possible frequencies of normal modes of vibration in a Born-von Kármán crystal will be shown in the next section to be roots of a secular determinant (see Eq. (17a)) and two approaches to the problem of deriving their distribution from the determinant are: (a) by calculating all or a large random sample of its roots and counting the number in each small frequency interval; (b) by evaluating the moments of the distribution function and from the moments determining the distribution.

Blackman's[5] researches have demonstrated that the first method involves the solution of a large collection of quadratic or cubic equations and thus an enormous amount of tedious numerical work—and further, they show that the computation must be repeated for every set of lattice parameters, so method (a) cannot easily show the influence of changes in lattice parameters on changes in physical properties. Here we shall devise a technique based on the second approach which avoids tedious numerical work.

Let $\mathbf{M}$ be the matrix of a symmetrical secular determinant whose roots are $\{\lambda_i\}$. Then

$$\mathbf{M}\psi_i=\lambda_i\psi_i, \tag{1}$$

where ψ_i is the ith characteristic vector of the matrix, and λ_i is the corresponding characteristic value. Multiplication of both sides of (1) by $\mathbf{M}$ yields

$$\begin{aligned}\mathbf{M}^2\psi_i&=\mathbf{M}\lambda_i\psi_i=\lambda_i\mathbf{M}\psi_i\\&=\lambda_i^2\psi_i\end{aligned}$$

and in general

$$\mathbf{M}^k\psi_i=\lambda_i^k\psi_i. \tag{2}$$

Thus λ_i^k is the characteristic value corresponding to the characteristic vector ψ_i of $\mathbf{M}^k$. Now it is well known[6] that the trace of a matrix is the sum of its characteristic values, so

$$\text{Trace } \mathbf{M}^k=\textstyle\sum_i \lambda_i^k. \tag{3}$$

Since the total number of characteristic values (where a characteristic value of degree of degeneracy d is counted d times) is equal to the

---

[5] M. Blackman, Proc. Roy. Soc. **148**, 365, 384 (1935); **159**, 416 (1937); see also P. Fine, Phys. Rev. **56**, 355 (1939).

[6] Cf. Rojansky, *Introductory Quantum Mechanics* (New York, 1938), p. 324.

order of the matrix, which we shall assume to be m, the average values of powers of the characteristic values of $\mathbf{M}$ are

$$\sum \lambda_i^k/m = (\text{Trace } \mathbf{M}^k)/m. \tag{4}$$

But this is exactly the kth moment of the distribution function of the characteristic values and will be abbreviated by μ_k.

We must now find a way of expressing the distribution function $g(\lambda)$ in terms of the set of moments $\{\mu_k\}$. Let λ_S and λ_L be, respectively, the smallest and largest characteristic values of $\mathbf{M}$ (since the matrix is finite they actually exist; also, since the matrix was assumed to be symmetrical, the λ's are all real) and let us assume that the elements of the set $\{\lambda_i\}$ are densely distributed.

Suppose the distribution function is expanded as a linear combination of Legendre polynomials

$$g(\lambda) = \sum_{n=0}^{\infty} a_n P_n\left(\frac{2\lambda-(\lambda_L+\lambda_S)}{\lambda_L-\lambda_S}\right), \tag{5}$$

where

$$P_n(x) = \frac{1}{2^n n!}\frac{d^n}{dx^n}(x^2-1)^n \tag{6a}$$

and

$$\int_{-1}^{1} P_k(x)P_j(x)dx = 2\delta_{kj}/(2k+1). \tag{6b}$$

To evaluate the coefficients $\{a_k\}$ multiply both sides of (5) by

$$P_k\left(\frac{2\lambda-\lambda_L-\lambda_S}{\lambda_L-\lambda_S}\right)d\lambda$$

and integrate from λ_S to λ_L

$$\int_{\lambda_S}^{\lambda_L} g(\lambda)P_k\left(\frac{2\lambda-\lambda_L-\lambda_S}{\lambda_L-\lambda_S}\right)d\lambda$$

$$= \sum_{n=0}^{\infty} a_n \int_{\lambda_S}^{\lambda_L} P_n\left(\frac{2\lambda-\lambda_L-\lambda_S}{\lambda_L-\lambda_S}\right)P_k\left(\frac{2\lambda-\lambda_L-\lambda_S}{\lambda_L-\lambda_S}\right)d\lambda.$$

Letting $x = (2\lambda-\lambda_L-\lambda_S)/(\lambda_L-\lambda_S)$

$$\frac{(\lambda_L-\lambda_S)}{2}\int_{-1}^{1} g(\lambda)P_k(x)dx$$

$$= \sum_{n=0}^{\infty} a_n \int_{-1}^{1} \frac{(\lambda_L-\lambda_S)}{2} P_n(x)P_k(x)dx$$

$$= a_k(\lambda_L-\lambda_S)/(2k+1).$$

Therefore

$$a_k = \frac{(2k+1)}{2}\int_{-1}^{1} g\left(\frac{(1+x)\lambda_L+(1-x)\lambda_S}{2}\right)P_k(x)dx. \tag{7}$$

If we define

$$u_k = \int_{-1}^{1} x^k g(\lambda)dx$$

$$= \frac{2}{(\lambda_L-\lambda_S)^{k+1}}\int_{\lambda_S}^{\lambda_L} (2\lambda-\lambda_L-\lambda_S)^k g(\lambda)d\lambda$$

$$= \frac{2}{(\lambda_L-\lambda_S)^{k+1}}\int_{\lambda_S}^{\lambda_L} (\text{polynomial in } \lambda)g(\lambda)d\lambda, \tag{8}$$

it is apparent that the a_k's can be written as linear combinations of the u_k's. Furthermore, the definition of $g(\lambda)$ implies that its moments are

$$\mu_i = \int_{\lambda_S}^{\lambda_L} g(\lambda)\lambda^i d\lambda$$

$$= (\text{Trace } \mathbf{M}^i)/m, \tag{9}$$

so the u_k's are linear combinations of μ_i's and therefore the coefficients a_k are also linear combinations of the moments (or the traces of $\mathbf{M}^i$) μ_i of $g(\lambda)$.

In the theory of frequency spectrum of solids the frequencies of normal modes are proportional to the square root of the roots of the secular equation, so the smallest frequency is the negative of the largest, and the odd moments of the distribution function are zero. Considering this case in detail we have:

$$g(\lambda) = \sum_{n=0}^{\infty} a_n P_n(\lambda/\lambda_L) \tag{10a}$$

with

$$a_n = \frac{(2n+1)}{2}\int_{-1}^{1} g(x\lambda_L)P_n(x)dx. \tag{10b}$$

If

$$u_k = \int_{-1}^{1} g(x\lambda_L)x^k dx, \tag{11}$$

then

$$\mu_k = \int_{-\lambda L}^{\lambda_L} g(\lambda)\lambda^k d\lambda$$

$$= \lambda_L^{k+1} u_k. \tag{12}$$

Therefore

$$a_0=\frac{1}{2}\int_{-1}^{1}g(x\lambda_L)\cdot 1dx$$

$$=\mu_0/2\lambda_L$$

$$a_1=\frac{3}{2}\int_{-1}^{1}g(x\lambda_L)\cdot xdx$$

$$=\frac{3}{2}(\mu_1/\lambda_L{}^2)=0.$$

Similarly, since the odd Legendre polynomials involve only odd powers of x, and since the odd moments of $g(\lambda)$ are zero:

$$a_1=a_3=\cdots=a_{2n+1}=0,$$

$$a_2=\frac{5}{2}\int_{-1}^{1}g(x\lambda_L)\left(\frac{3}{2}x^2-\frac{1}{2}\right)dx,$$

$$=5(3\mu_2-\mu_0\lambda_L{}^2)/4\lambda_L{}^3,$$

$$a_4=9(35\mu_4-30\mu_2\lambda_L{}^2+3\mu_0\lambda_L{}^4)/16\lambda_L{}^5,$$

$$a_6=13(231\mu_6-315\mu_4\lambda_L{}^2+105\mu_2\lambda_L{}^4-5\lambda_L{}^6)/32\lambda_L{}^7,$$

and in general

$$a_{2k}=\frac{4k+1}{(2k)!2^{2k+1}}\int_{-1}^{1}g(x\lambda_L)\left[\frac{d^{2k}}{dx^{2k}}(x^2-1)^{2k}\right]dx$$

$$=\frac{4k+1}{(2k)!2^{2k+1}\lambda_L}\left\{\frac{d^{2k}}{dy^{2k}}(y^2-1)^{2k}\right\}_{y^k=\mu_k/\lambda_L{}^k}, \tag{13}$$

where after the differentiation is performed in the last expression, y^k is replaced by $\mu_k/\lambda_L{}^k$.

2. Two-Dimensional Cubic Lattice

Here we shall apply the Moment-Trace method to a two-dimensional one-component cubic lattice of the Born-von Kármán type which includes interactions between nearest and next nearest neighbors. Let α be the binding force between two nearest neighbors whose distance of separation is a and let γ be that for two next nearest neighbors whose distance of separation is $a\sqrt{2}$. If there are $2N\times 2N$ particles of mass M in our square lattice, each atom can be specified by two letters l, m $(1\leq l, m\leq 2N)$ and its displacement components along rows and columns can be represented by $u_{l,m}$ and $v_{l,m}$, respectively. The motion of the particle (l, m) is described by the simultaneous differential equations[5]

$$M\ddot{u}_{l,m}+\alpha(u_{l,m}-u_{l+1,m}+u_{l,m}-u_{l-1,m})+\gamma(u_{l,m}+v_{l,m}-u_{l+1,m+1}-v_{l+1,m+1}+u_{l,m}+v_{l,m}$$
$$-u_{l-1,m-1}-v_{l-1,m-1}+u_{l,m}-v_{l,m}-u_{l+1,m+1}+v_{l+1,m-1}+u_{l,m}-v_{l,m}-u_{l-1,m+1}+v_{l-1,m+1})=0 \tag{14a}$$

and

$$M\ddot{v}_{l,m}+\alpha(v_{l,m}-v_{l+1,m}+v_{l,m}-v_{l-1,m})+\gamma(u_{l,m}+v_{l,m}-u_{l+1,m+1}-v_{l+1,m+1}+u_{l,m}+v_{l,m}$$
$$-u_{l-1,m-1}-v_{l-1,m-1}+u_{l,m}-v_{l,m}-u_{l+1,m-1}+v_{l+1,m-1}+u_{l,m}-v_{l,m}-v_{l-1,m+1}+v_{l-1,m+1})=0. \tag{14b}$$

By assuming the periodic solutions

$$u_{l,m}=u'\exp i(2\pi\nu t+l\varphi_1+m\varphi_2), \tag{15a}$$

$$v_{l,m}=v'\exp i(2\pi\nu t+l\varphi_1+m\varphi_2), \tag{15b}$$

$$\varphi_1=\pi a_1/N;\quad \varphi_2=\pi a_2/N, \tag{15c}$$

where a_1 and a_2 are integers satisfying

$$-N\leqq a_1, a_2\leqq N,$$

and substituting (15) into (14) one can easily show that the frequencies of the normal modes of vibration of the crystal must be roots of the characteristic equations

$$\begin{vmatrix} A(\varphi_1,\varphi_2)-4\pi^2M\nu^2 & B(\varphi_2,\varphi_1) \\ B(\varphi_1,\varphi_2) & A(\varphi_2,\varphi_1)-4\pi^2M\nu^2 \end{vmatrix}=0, \tag{16}$$

when

$$A(\varphi_1,\varphi_2)=2\alpha(1-\cos\varphi_1)+4\gamma(1-\cos\varphi_1\cos\varphi_2),$$
$$B(\varphi_1,\varphi_2)=4\gamma\sin\varphi_1\sin\varphi_2.$$

Henceforth it will be assumed that ν is measured in units of $2\pi\sqrt{M}$ so that the factor $4\pi^2M$ can be omitted. If the matrix of the determinant (16) is represented by $M^2(a_1, a_2)$, the matrix of the entire characteristic determinant is

$$\mathbf{M}^2=\begin{pmatrix} M^2(-N,-N) & 0 & \cdots & 0 & 0 \\ 0 & M^2(-N,-N+1) & \cdots & 0 & 0 \\ \cdots & \cdots & \cdots & \cdots & \cdots \\ 0 & 0 & \cdots & M^2(N,N-1) & 0 \\ 0 & 0 & \cdots & 0 & M^2(N,N) \end{pmatrix} \tag{17a}$$

(the submatrices are represented as squares because the roots of their characteristic determinants are proportional to the squares of the frequencies of the normal modes of vibration). Of course:

$$\mathbf{M}^{2k}=\begin{pmatrix} M^{2k}(-N,-N) & 0 & \cdots & 0 & 0 \\ 0 & M^{2k}(-N,-N+1) & \cdots & 0 & 0 \\ \cdots & \cdots & \cdots & \cdots & \cdots \\ 0 & 0 & \cdots & M^{2k}(N,N-1) & 0 \\ 0 & 0 & \cdots & 0 & M^{2k}(N,N) \end{pmatrix}. \tag{17b}$$

Since all the small $M^2(a_1, a_2)$ matrices are of the same form, namely

$$M^2(a_1, a_2)=\begin{pmatrix} A & B \\ B & A^* \end{pmatrix} \tag{18}$$

(where $A=A(\varphi_1, \varphi_2)$; $A^*=A(\varphi_2, \varphi_1)$; $B=B(\varphi_1, \varphi_2)=B(\varphi_2, \varphi_1)$),

$$\text{Trace } \mathbf{M}^{2k}=\sum_{a_1=-N}^{N}\sum_{a_2=-N}^{N}\text{Trace } M^{2k}(a_1, a_2) \tag{19}$$

and we first need only to find traces for one general pair (a_1, a_2). Now

$$\text{Trace } M^2(a_1, a_2)=A(\varphi_1, \varphi_2)+A(\varphi_2, \varphi_1)$$

and

$$\begin{aligned}\text{Trace } \mathbf{M}^2&=\sum_{a_1, a_2}[A(\pi a_1/N, \pi a_2/N)+A(\pi a_2/N, \pi a_1/N)]\\ &=2\sum_{a_1, a_2}A(\pi a_1/N, \pi a_2/N).\end{aligned} \tag{20a}$$

Since

$$\begin{aligned}M^4(a_1, a_2)&=M^2(a_1, a_2)\cdot M^2(a_1, a_2)\\ &=\begin{pmatrix} A & B \\ B & A^* \end{pmatrix}\begin{pmatrix} A & B \\ B & A^* \end{pmatrix}\\ &=\begin{pmatrix} A^2+B^2 & B(A+A^*) \\ B(A+A^*) & B^2+(A^*)^2 \end{pmatrix}\end{aligned}$$

$$\begin{aligned}\text{Trace } \mathbf{M}^4&=\sum_{a_1, a_2}[A^2+B^2+B^2+(A^*)^2]\\ &=2\sum_{a_1, a_2}(A^2+B^2).\end{aligned} \tag{20b}$$

Continuation of this process leads to

$$\text{Trace } \mathbf{M}^6 = 2\sum_{a_1, a_2} (A^3 + 3AB^2), \tag{20c}$$

$$\text{Trace } \mathbf{M}^8 = 2\sum_{a_1, a_2} (A^4 + 4A^2B^2 + 2B^2AA^* + B^4), \tag{20d}$$

$$\text{Trace } \mathbf{M}^{10} = 2\sum_{a_1, a_2} (A^5 + 5A^3B^2 + 5A^2B^2A^* + 5AB^4). \tag{20e}$$

These Traces will be sufficient to yield a $g(\nu)$ correct to the 10th Legendre polynomial. In general the sum of the diagonal elements of the matrix

$$M^{2k}(a_1, a_2) = \underbrace{\begin{pmatrix} A & B \\ B & A^* \end{pmatrix}\begin{pmatrix} A & B \\ B & A^* \end{pmatrix}\cdots\begin{pmatrix} A & B \\ B & A^* \end{pmatrix}}_{k \text{ matrices}}$$

is Trace $M^{2k}(a_1, a_2)$.

Actually

$$\text{Trace } \mathbf{M}^2 = 2\sum_{a_1, a_2} \{2\alpha(1-\cos\varphi_1) + 4\gamma(1-\cos\varphi_1\cos\varphi_2)\}$$

$$= 2\{\sum_{a_1, a_2} (2\alpha+4\gamma) - 4\alpha\sum_{a_1, a_2}\cos\varphi_1 - 8\gamma(\sum_{a_1}\cos\varphi_1)^2\}.$$

But as shown in the appendix

$$\sum_{a_1=-N}^{N} \cos\varphi_1 = -1.$$

Therefore

$$\frac{\text{Trace } \mathbf{M}^2}{2(2N+1)^2} = (2\alpha+4\gamma) + \frac{2\alpha}{(2N+1)} - \frac{4\gamma}{(2N+1)^2}.$$

Since N is very large, and since this is exactly the second moment of $g(\nu)$:

$$\mu_2 = \frac{\text{Trace } \mathbf{M}^2}{2(2N+1)^2} = (2\alpha+4\gamma). \tag{21a}$$

To find μ_4 we must first calculate

$$\text{Trace } \mathbf{M}^4 = 2(\sum A^2 + \sum B^2).$$

For this calculation we find

$$\sum A^2 = \sum_{a_1, a_2} \{4\alpha^2(1-2\cos\varphi_1+\cos^2\varphi_2) + 16\alpha\gamma(1-\cos\varphi_1)(1-\cos\varphi_1\cos\varphi_2)$$

$$+16\gamma^2(1-2\cos\varphi_1\cos\varphi_2+\cos^2\varphi_1\cos^2\varphi_2)\}.$$

But from the appendix:

$$\sum_{a_2}\cos^2\varphi_2 = N+1, \quad \sum_{a_1}\cos\varphi_1 = -1,$$

so

$$\sum_{a_1, a_2} A^2 = 4\alpha^2(2N+1)^2 + 4\alpha^2(2N+1)(N+1) + 16\alpha\gamma(2N+1)^2 + 16\gamma^2(2N+1)^2 + 16\gamma^2(N+1)^2 + O(N)$$

and

$$\sum A^2/(2N+1)^2 = 4(\alpha+2\gamma)^2 + 2(\alpha^2+2\gamma^2) + O(1/N).$$

Also,

$$\sum_{a_1, a_2} B^2 = 16\gamma^2(\sum_{a_1}\sin^2\varphi_1)^2,$$

but from the appendix $\sum a_1 \sin^2 \varphi_1 = N$, therefore

$$\sum B^2/(2N+1)^2 = 4\gamma^2.$$

Since

$$\mu_4 = (\text{Trace } \mathbf{M}^4)/2(2N+1)^2, \quad \mu_4 = 4(\alpha+2\gamma)^2+2(\alpha^2+4\gamma^2)+O(1/N). \tag{21b}$$

In a similar manner some of the higher moments can be shown to be (to within terms of order $1/N$)

$$\mu_6 = 8(\alpha+2\gamma)^3+12(\alpha+2\gamma)(\alpha^2+4\gamma^2), \tag{21c}$$

$$\mu_8 = 16(\alpha+2\gamma)^4+48(\alpha+2\gamma)^2(\alpha^2+4\gamma^2)+6(\alpha^2+4\gamma^2)^2+40\alpha^2\gamma^2, \tag{21d}$$

$$\mu_{10} = 32(\alpha+2\gamma)^5+160(\alpha+2\gamma)^3(\alpha^2+4\gamma^2)+120\gamma^2(\alpha+2\gamma)(7\alpha^2+8\gamma^2) + 40\alpha^2\gamma^2(\alpha+\gamma)+60\alpha^4(\alpha+2\gamma). \tag{21e}$$

Using the results of the previous section, if we assume

$$g(\nu) = \sum_{n=0}^{\infty} a_{2n} P_{2n}(\nu/\nu_L) \tag{22}$$

(ν_L = largest frequency of a normal mode) the first few coefficients are

$$a_0 = 0.5/\nu_L,$$

$$a_2 = 5(6\alpha+12\gamma-\nu_L^2)/4\nu_L^3,$$

$$a_4 = 9[140(\alpha+2\gamma)^2+70(\alpha^2+4\gamma^2)-60(\alpha+2\gamma)\nu_L^2+3\nu_L^4]/16\nu_L^5.$$

The number of parameters involved in the a's can immediately be reduced by one, for as Blackman[5] has shown, the largest normal mode ν_L results from the 2×2 determinant in which $\varphi_1 = 0$ and $\varphi_2 = \pi$ (or vice versa, $\varphi_2 = \pi$ and $\varphi_2 = 0$); therefore by (16).

$$\nu_L^2 = 4(\alpha+2\gamma).$$

This means

$$\nu_L a_0 = \tfrac{1}{2},$$

$$\nu_L a_2 = \tfrac{5}{8},$$

$$\nu_L a_4 = 9(9\alpha^2-104\alpha\gamma+36\gamma^2)/8(\alpha+2\gamma)^2, \quad \text{etc.}$$

Since the purpose of this paper is more to introduce new methods than to obtain particular results, let us limit ourselves to the special case $\gamma = 0.05\alpha$. This α, γ relationship is of special interest because it is the one used by Blackman in his detailed calculations—and may therefore give us an opportunity to compare the results of the trace-moment approach with those obtained by Blackman in his detailed root calculations. In this case $\nu_L^2 = 4.4\alpha$.

The first six even moments in the special case $\gamma = 0.05\alpha$ are[7] (of course the odd moments are all zero)

$$\mu_0 = 1, \qquad \mu_6 = 0.28150826\nu_L^6,$$

$$\mu_2 = 0.5\nu_L^2, \qquad \mu_8 = 0.23560495\nu_L^8,$$

$$\mu_4 = 0.35433884\nu_L^4, \quad \mu_{10} = 0.20316225\nu_L^{10}$$

and the corresponding Legendre coefficients of (22) are

$$\nu_L a_0 = 0.5, \qquad \nu_L a_6 = 0.3704,$$

$$\nu_L a_2 = 0.625, \qquad \nu_L a_8 = -0.3182,$$

$$\nu_L a_4 = 0.2260, \quad \nu_L a_{10} = -0.0133.$$

[7] The large number of significant figures is necessary because one must take differences of multiples of the μ's in order to find the a's.

The resulting function $\nu_L g(\nu)$ is plotted in Fig. 1. It qualitatively resembles the equivalent curve of Blackman as obtained by direct numerical computation of a random sample of normal modes. Blackman's first peak is sharper and is displaced a little more to the left. The quantitative disagreement may be the result of Blackman's smoothing process, or it may have its source in the existence of a large value for one or more of the coefficients of the higher Legendre polynomials that have been neglected here. Since our $g(\nu)$ is not quite zero at $\nu=0$ as it should be, we must be omitting some contribution of the higher polynomials.

The calculation of physical quantities from a frequency distribution of the form (22) offers no special difficulty. For example the specific heat is in general

$$C=k\int_0^{\nu_L}\frac{h^2\nu^2 g(\nu)d\nu}{4k^2T^2\sinh^2 h\nu/2kT},$$

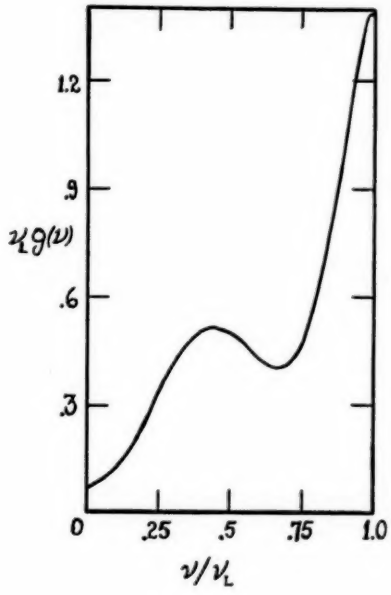

FIG. 1.

so in a low temperature region where one may expand $(\sinh^2 h\nu/2kT)^{-1}$ as an exponential series, elementary integrals of the form

$$\int_0^{\nu_L} e^{-nh\nu/kT}\,(\text{polynomial in }\nu)d\nu$$

are all that are involved, while at higher temperatures where it would be desirable to use a power series expansion for $(\sinh^2 h\nu/kT)^{-1}$ one encounters only sums of integrals of the form

$$\int_0^{\nu_L}(\text{polynomials in }\nu)d\nu.$$

Before concluding this section it might be worth while reminding the reader that the expressing of $g(\nu)$ as a linear combination of Legendre polynomials is somewhat arbitrary. Any other artifice which allows one to express $g(\nu)$ as a function of the moments would be equally valid. The Legendre development merely seemed to be the most straightforward and simplest approach which occurred to the author.

III. FREQUENCY DISTRIBUTION FROM EXPERIMENTAL DATA

If in a crystal of N structureless atoms or in a complex molecule of N atoms, the frequency distribution function $g(\nu)$ is defined so that $3Ng(\nu)d\nu$ is the number of normal modes of vibration in the frequency interval ν and $\nu+d\nu$, the logarithm of the partition function (per normal mode) is given by

$$\log Z(T)=-\int_0^{\infty} g(\nu)\log(1-e^{-h\nu/kT})d\nu \tag{23a}$$

under the restriction

$$\int_0^{\infty} g(\nu)d\nu=1. \tag{23b}$$

Formally a knowledge of $Z(T)$ at all temperatures permits (23a) to be regarded as an integral equation in which $g(\nu)$ occurs as the unknown function. Also, the average energy per normal mode is

$$\bar{E}(T)=kT^2\partial \log Z/\partial T$$
$$=\int_0^\infty \frac{h\nu g(\nu)d\nu}{e^{h\nu/kT}-1}. \tag{24}$$

(using for zero energy the state of lowest energy of the system including the residual energy $h\nu/2$ per normal mode) and by definition the specific heat is

$$C_v(T)=(\partial E/\partial T)_v$$
$$=k\int_0^\infty \left(\frac{h\nu}{2kT}\right)^2 \frac{g(\nu)d\nu}{\sinh^2(h\nu/2kT)}. \tag{25}$$

Making the substitution $\theta=h/kT$ and writing

$$\log Z(T)=\boldsymbol{Z}(\theta);\quad \boldsymbol{E}(\theta)=\theta E(T/h;\quad \boldsymbol{C}(\theta)=C_v(T)/k,$$

we have the three fundamental integral equations

$$\boldsymbol{Z}(\theta)=-\int_0^\infty g(\nu)\log(1-e^{-\theta\nu})d\nu, \tag{26}$$

$$\boldsymbol{E}(\theta)=\int_0^\infty g(\nu)\theta\nu d\nu/(e^{\theta\nu}-1), \tag{27}$$

$$\boldsymbol{C}(\theta)=\int_0^\infty \frac{\theta^2\nu^2 g(\nu)d\nu}{4\sinh^2(\theta\nu/2)},$$

all of which are of the form

$$f(\theta)=\int_0^\infty g(\nu)K(\theta\nu)d\nu. \tag{28}$$

It is quite clear that if the partition function, the internal energy or the specific heat of a given system could be found at all temperatures, and if the above integral equation could be inverted[8] so that $g(\nu)$ would be a function of the measurable quantities it would be possible to compute $g(\nu)$ and perhaps get a better understanding of the internal structure of a given crystal or complex molecule.

As has been demonstrated in Appendix II, the formal solution of (28) is

$$g(\nu)=\frac{1}{2\pi}\int_{-\infty}^\infty \frac{du}{I(u)}\int_0^\infty f(\theta)(\nu\theta)^{iu}d\theta, \tag{29}$$

where

$$I(u)=\int_0^\infty x^{iu}K(x)dx.$$

Inasmuch as[9]

$$\int_0^\infty x^{iu}\log(1-e^{-x})dx=-\zeta(2+iu)\Gamma(1+iu)$$

[8] Inversions of the partition function have been made before by S. Bauer, J. Chem. Phys. **6**, 403 (1938); **7**, 1097 (1939).

[9] These integrals are easily evaluated by expanding the transcendental functions in the integrands as sums of powers of e^{-x}.

($\zeta(z)$ is the Riemann zeta-function defined by $\zeta(z)=\sum_{n=1}^{\infty} n^{-z}$)

$$\int_0^\infty \frac{x^{iu+1}dx}{e^x-1}=\zeta(2+iu)\Gamma(2+iu), \quad \int_0^\infty \frac{x^{iu+2}dx}{4\sinh^2 x/2}=\zeta(2+iu)\Gamma(3+iu),$$

the formal equations for $g(\nu)$ are

$$g(\nu)=\frac{1}{2\pi}\int_{-\infty}^{\infty}\frac{du}{\zeta(2+iu)\Gamma(1+iu)}\int_0^\infty \boldsymbol{Z}(\theta)(\nu\theta)^{iu}d\theta, \tag{30}$$

$$g(\nu)=\frac{1}{2\pi}\int_{-\infty}^{\infty}\frac{du}{\zeta(2+iu)\Gamma(2+iu)}\int_0^\infty \boldsymbol{E}(\theta)(\nu\theta)^{iu}d\theta, \tag{31}$$

$$g(\nu)=\frac{1}{2\pi}\int_{-\infty}^{\infty}\frac{du}{\zeta(2+iu)\Gamma(3+iu)}\int_0^\infty \boldsymbol{C}(\theta)(\nu\theta)^{iu}d\theta. \tag{32}$$

As is to be expected, substitution of the Debye specific heat formula

$$\boldsymbol{C}(\theta)=C_v(T)/NK=3\left(\frac{12}{\theta^3{\nu_L}^3}\int_0^{\theta\nu_L}\frac{x^3dx}{e^x-1}-\frac{3\theta\nu_L}{e^{\theta\nu_L}-1}\right)$$

into (32) can be shown to yield the frequency distribution

$$g(\nu)=\begin{cases}9\nu^2/{\nu_L}^3 & \text{if } \nu<\nu_L\\ 0 & \text{if } \nu>\nu_L.\end{cases} \tag{33}$$

For actual calculation of $g(\nu)$ from (32) there seem to be several possible approaches. One might integrate (32) numerically after substitution of the experimental $\boldsymbol{C}(\theta)$ values derived from specific heat measurements. However, since most specific heat curves are almost of the Debye form, one might divide $\boldsymbol{C}(\theta)$ into a Debye and a residual portion. The Debye portion would contribute the amount (33) to $g(\nu)$ and the rest of $g(\nu)$ might be found either by numerical integration or by obtaining empirical equations for the residual $\boldsymbol{C}(\theta)$. In the latter case one would attempt to fit a power series in θ to the high temperature part and a power series in $e^{-\theta}$ in the low temperature region. Then (32) could probably be integrated analytically. Another possibility would be to assume that $g(\nu)$ could be expanded in Legendre polynomials and finding the coefficients by applying the orthogonality property of the polynomials to the assumed equation (32).

In conclusion the author would like to thank Professor J. G. Kirkwood for his discussions concerning this problem.

APPENDIX I. SUMMATION FORMULA

In the main part of this paper the following trigonometric sums are needed

$$C_k=\sum_{a=-N}^{N}\cos^k\frac{\pi a}{N}; \quad S_k=\sum_{a=-N}^{N}\sin^k\frac{\pi a}{N}.$$

To sum C_k and S_k it is convenient to find first

$$E_k=\sum_{a=-N}^{N}\exp(ik\pi a/N).$$

If $x=\exp(ik\pi/N)\neq 1$ when $0<k<N$,

$$E_k=\sum_{a=-N}^{N}x^a=x^{-N}(1-x^{2N+1})/(1-x)$$

$$=e^{-i\pi k}(1-e^{2\pi ik}e^{ik\pi/N})/(1-e^{ik\pi/N}).$$

Since

$$e^{-i\pi k}=(-1)^k,$$

$$E_k=(-1)^k \quad \text{when} \quad 0<k<N.$$

Obviously $E_0=2N+1$.

Now

$$C_k=\frac{1}{2^k}\sum_{a=-N}^{N}(e^{i\pi a/N}+e^{-i\pi a/N})^k$$

$$=\frac{1}{2^k}\sum_{m=0}^{k}\frac{k!}{m!(k-m)!}\sum_{a=-N}^{N}e^{i\pi(2m-k)/N}.$$

When k is odd, $2m-k$ is also odd and

$$\sum_{a=-N}^{N}\exp\{i\pi(2m-k)/N\}=-1.$$

So

$$C_{k(\text{odd})}=-\frac{1}{2^k}\sum_{m=0}^{k}\frac{k!}{m!(k-m)!}=-1.$$

When k is even $(2m-k)$ is also even and it is zero when $k=2m$; so

$$C_{k(\text{even})}=\left\{\sum_{m=0}^{(k/2)-1}\frac{k!}{m!(k-m)!}+\sum_{(k/2)+1}^{k}\frac{k!}{m!(k-m)!}+\frac{(2N+1)k!}{(k/2)!(k/2)!}\right\}$$

$$=\frac{1}{2^k}\left\{\sum_{m=0}^{k}\frac{k!}{m!(k-m)!}+\frac{2Nk!}{(k/2)!(k/2)!}\right\}$$

$$C_{k(\text{even})}=1+2^{1-k}N(k!)/(k/2)!(k/2)!.$$

To find S_k we proceed in essentially the same manner:

$$S_k=\frac{1}{(2i)^k}\sum_{a=-N}^{N}(e^{i\pi a/N}-e^{-i\pi a/N})^k$$

$$=\frac{1}{(2i)^k}\sum_{a=-N}^{N}\frac{k!}{m!(k-m)!}\sum_{a=-N}^{N}(e^{i\pi a/N})^{k-m}(-e^{-i\pi a/N})^m$$

$$=\frac{1}{(2i)^k}\sum_{m=0}^{\infty}\frac{k!(-1)^m}{m!(k-m)!}\sum_{a=-N}^{N}e^{i\pi a(k-2m)/N}.$$

When k is odd $k-2m$ is odd and

$$S_{k(\text{odd})}=\frac{-1}{(2i)^k}\sum_{m=0}^{k}\frac{(-1)^m k!}{m!(k-m)!}$$

$$=-\frac{1}{(2i)^k}(1-1)^k=0.$$

If k is even $k-2m$ is also even

$$S_{k(\text{even})}=\frac{1}{(2i)^k}\left\{\sum_{m=0}^{k/2-1}\frac{k!(-1)^m}{m!(k-m)!}+\sum_{m=(k/2)+1}^{k}\frac{k!(-1)^m}{m!(k-m)!}+\frac{(-1)^{k/2}(2N+1)k!}{(k/2)!(k/2)!}\right\}$$

$$=\frac{1}{(2i)^k}\left\{\sum_{m=0}^{k}\frac{k!(-1)^m}{m!(k-m)!}+\frac{i^k(2N)k!}{(k/2)!(k/2)!}\right\}$$

$$S_{k(\text{even})}=\frac{N(k!)}{2^{k-1}(k/2)!(k/2)!}.$$

The first few C_k's and S_k's are

k	C_k	S_k
0	$2N+1$	$2N+1$
1	-1	0
2	$N+1$	N
3, 5, 7, 9	-1	0
4	$1+(3N/4)$	$3N/4$
6	$1+(5N/8)$	$5N/8$
8	$1+(35N/64)$	$35N/64$

APPENDIX II

Formal Solution of $f(\theta)=\int_0^\infty g(\nu)K(\theta\nu)d\nu$

Here we shall find the formal solution $g(\nu)$ of the integral equation

$$f(\theta)=\int_0^\infty g(\nu)K(\theta\nu)d\nu, \tag{A}$$

when $f(\theta)$ and $K(\theta\nu)$ are assumed to be known functions. The Fourier transform method to be used is modeled on that of Payley and Wiener[10] (the formal solution is also a simple consequence of some operations with Mellin transforms of f, g, and K.[11] Let us make the substitutions

$$\theta=e^{-\eta}, \quad \nu=e^{\alpha} \tag{B}$$

in (A) yielding

$$e^{-\eta}f(e^{-\eta})=\int_{-\infty}^{\infty}g(e^{\alpha})e^{\alpha-\eta}K(e^{\alpha-\eta})d\alpha. \tag{C}$$

Multiplying by

$$e^{-iu\eta}d\eta/\sqrt{2\pi}$$

and integrating:

$$\frac{1}{\sqrt{2\pi}}\int_{-\infty}^{\infty}e^{-\eta}f(e^{-\eta})e^{-iu\eta}d\eta$$

$$=\frac{1}{\sqrt{2\pi}}\int_{-\infty}^{\infty}g(e^{\alpha})e^{-i\alpha u}d\alpha\int_{-\infty}^{\infty}e^{\alpha-\eta}e^{-iu(\eta-\alpha)}K(e^{\alpha-\eta})d\eta.$$

Now let $\eta-\alpha=\beta$

$$\frac{1}{\sqrt{2\pi}}\int_{-\infty}^{\infty}e^{-\eta}f(e^{-\eta})e^{-iu\eta}d\eta$$

$$=\frac{1}{\sqrt{2\pi}}\int_{-\infty}^{\infty}g(e^{\alpha})e^{-iu\alpha}d\alpha\int_{-\infty}^{\infty}e^{-\beta}e^{-iu\beta}K(e^{-\beta})d\beta.$$

---

[10] R. Payley and N. Wiener, *Fourier Transforms* (New York, 1934), p. 38.

[11] Titchmarsh, *Theory of Fourier Transforms* (Oxford, 1937), p. 315.

Define

$$I(u)=\int_{-\infty}^{\infty}e^{-\beta(iu+1)}K(e^{-\beta})d\beta$$
$$=\int_{0}^{\infty}x^{iu}K(x)dx.$$

Then

$$\frac{1}{\sqrt{2\pi}}\int_{-\infty}^{\infty}e^{-\eta}f(e^{-\eta})e^{-iu\eta}d\eta=\frac{I(u)}{\sqrt{2\pi}}\int_{-\infty}^{\infty}g(e^{\alpha})e^{-i\alpha u}d\alpha$$

and taking Fourier transforms

$$g(e^{\alpha})=\frac{1}{2\pi}\int_{-\infty}^{\infty}\frac{e^{iu\alpha}du}{I(u)}\int_{-\infty}^{\infty}f(e^{-\eta})e^{-\eta(1+iu)}d\eta.$$

By applying (B)

$$g(\nu)=\frac{1}{2\pi}\int_{-\infty}^{\infty}\frac{du}{I(u)}\int_{0}^{\infty}f(\theta)(\theta\nu)^{iu}d\theta.$$

APRIL, 1942 JOURNAL OF CHEMICAL PHYSICS VOLUME 10

The Viscosity of Certain "Ferric Oxide" Hydrosols *†

LEON M. GREENSTEIN AND ARTHUR W. THOMAS
Columbia University, New York, New York

(Received December 11, 1941)

(1) The changes produced in the viscosities of "ferric oxide" hydrosols by aging, heating, and the addition of a number of electrolytes and a non-electrolyte have been studied, in some instances together with the attendant changes in the *p*H values and specific conductances of the systems. (2) Agreement with Poiseuille's law has been demonstrated for typical cationic and anionic hydrosols. (3) The decrease in viscosity of hydrosols on aging and heating is accompanied by an increase in specific conductance. This conductance increase in the case of cationic sols is due almost entirely to the increase in hydrogen ion activity which occurs during the reaction. This is not so for anionic hydrosols, where the conductance increase is explained by the conversion of coordinated citrato groups to citrate ions. (4) The addition of salts and acids to these hydrosols first results in a viscosity decrease, followed by an increase in viscosity at higher electrolyte concentrations. (5) The viscosity increase occurs at lower salt concentrations for those salts which are potent precipitants than for those which are weak. For cationic hydrosols, salts of both weakly and strongly coordinating anions have the same effect in depressing the viscosity; in the case of anionic hydrosols, potassium citrate is less effective in this respect than potassium sulfate and nitrate. (6) The effects of acids in decreasing the viscosity of a sol, either cationic or anionic, was found to be the same for all acids used, when compared at the same *p*H values. The more powerful precipitants caused the subsequent viscosity increase to occur at lower electrolyte concentrations. (7) Acids are less effective than salts in decreasing the viscosities of cationic hydrosols. (8) Large concentrations of acetone produced a decrease in the relative viscosity of cationic hydrosols; this effect is, however, negligible in comparison with the magnitude of the changes caused by electrolytes. (9) The viscosity decrease produced by aging, heating, and the addition of electrolytes may be attributed in each case partly to the increase in electrolyte concentration of the system. (10) The viscosity resulting from these reactions is considered to be dependent also upon the micellar charge: the lower the charge, the lower the viscosity. (11) The viscosity increase at higher electrolyte concentrations may be ascribed to agglomeration of dispersed particles. (12) A mechanism based upon a Donnan equilibrium between the dispersed particle and the dispersion medium has been proposed to account for the effects observed.

INTRODUCTION

THE addition of electrolytes to hydrosols has long been known to cause changes in the viscosities of the colloidal system. Farrow[1] showed that the viscosity of hydrosols of sodium palmitate is decreased by the addition of sodium chloride or sodium hydroxide, but passes through a minimum, increasing with further increase in electrolyte concentration. Woudstra[2] demonstrated that curves of similar shape were obtained upon the addition of electrolytes to ferric oxide hydrosols, and Pauli[3] found electrolyte addition to lower the viscosity of ceric oxide hydrosols. In the ferric oxide system, viscosity decreases were obtained also on heating, and in the ceric, on aging. The extensive investigations of Loeb[4] on gelatin indicated that the depression

* Presented at the Atlantic City meeting of the American Chemical Society, September, 1941, and published with the permission of the Society.

† Dissertation submitted by Leon M. Greenstein in partial fulfillment of the requirements for the degree of Doctor of Philosophy in the Faculty of Pure Science, Columbia University. Publication assisted by the Ernest Kemptom Adams Fund for Physical Research of Columbia University.

[1] F. D. Farrow, J. Chem. Soc. **101**, 347 (1912).

[2] H. W. Woudstra, Kolloid Zeits. **8**, 73 (1911).

[3] W. Pauli and A. Fernau, Kolloid Zeits. **20**, 20 (1917).

[4] J. Loeb, *Proteins and the Theory of Colloidal Behavior* (McGraw-Hill Book Co., 1924), second edition.

of the viscosity of gelatin chloride dispersions was dependent upon the valence of the anion of the added salt: the greater the valence, the greater the depression. Similarly, the viscosity decrease for dispersions of gelatin on the alkaline side of the isoelectric point was found to depend on the valence of the cation of the added electrolyte.

More recently, Thévenet and Boutaric have demonstrated the influence of the valence of the cation of the added salt on the lowering of the viscosity of arsenious sulfide hydrosols (anionic micelles),[5] while showing the valence of the anion to be of importance in the case of cationic micellar ferric oxide sols.[6] In the latter case, as in that of gelatin chloride,[4] the greater depression resulted upon the addition of the anion of higher valence.

The problem of the viscosity of dispersions was early considered by Einstein, who derived the equation

$$\eta_r = \eta/\eta_0 = 1 + 2.5\varphi \qquad (1)$$

for dilute dispersions of non-charged, very small, rigid spheres, which are large in comparison with the molecules of solvent.[7,8] Here η_r is the relative viscosity, η is the viscosity of the dispersion, η_0 the viscosity of the medium, and φ the ratio of the volume of the dispersed phase to the volume of the dispersion. The constant 2.5 assumes greater values for particles which have shapes other than the spherical.

Smoluchowski[9] presented an equation for the case of charged spheres by adding a term to correct for the "electroviscous" effect:

$$\eta_r = 1 + 2.5\varphi\left[1 + \frac{3}{2\lambda\eta_0 r^2}\left(\frac{D\zeta}{2\pi}\right)^2\right]. \qquad (2)$$

In addition to the symbols used above, λ is the specific conductance of the dispersion, r the radius of the spherical particle, D the dielectric constant of the medium, and ζ the "electrokinetic potential of the double layer." The factor $\frac{3}{2}$ of the final term did not appear in Smoluchowski's original equation, but was added in a re-derivation by Krasny-Ergen.[10] The conditions necessary for the derivation, as given by the latter, include:

1. The tiny spheres must have uniformly charged surfaces.
2. They must be complete insulators.
3. The diffuse layer, or ionic atmosphere, must be very thin in comparison with the radius of the particle.

The equation predicts that, for constant values of φ, the viscosity of the dispersion will be greater the greater the charge on the particle and the smaller the conductance of the dispersion. The equation has been used by Kruyt and his co-workers[11,12] to explain the decrease in viscosity produced by added electrolyte, since this addition both decreases ζ and increases λ. Consideration of these two variables alone, however, represents an oversimplification of the systems which they investigated, because these were hydrophilic, rather than hydrophobic, dispersions. The particles are expected to be highly hydrated, and no assurance can be obtained that the hydration, and therefore φ, will not vary in the presence of electrolytes. Kruyt and Tendeloo[12] themselves found that the viscosity and ζ for gum arabic dispersions varied in opposite directions, and assumed therefore that φ was not constant. They suggest that the dispersed particles are surrounded by a shell of water, whose thickness changes in the presence of electrolytes.

The Smoluchowski equation has been applied by Briggs[13] to measurements on sodium gum arabic and caseinate dispersions, which contained various concentrations of sodium chloride. Values of $\eta_0/(\eta-\eta_0)$ were plotted against $\zeta^2/[\lambda(\eta-\eta_0)]$, since this choice of coordinates should yield, if hydration changes do not occur, a straight line whose slope is dependent only upon r^2. Although straight lines were obtained, the calculated value of the radius of the particle was found to decrease as the concentration of the dispersed phase increased. This variation in the value of the radius is not in agreement with the equation.

[5] A. Boutaric and S. Thévenet, Comptes rendus **205**, 862 (1937).
[6] S. Thévenet, Comptes rendus **207**, 68 (1938).
[7] A. Einstein, Ann. d. Physik (4) **19**, 289 (1906).
[8] E. Guth, Kolloid Zeits. **74**, 147 (1936).
[9] M. V. Smoluchowski, Kolloid Zeits. **18**, 190 (1916).
[10] W. Krasny-Ergen, Kolloid Zeits. **74**, 172 (1936).
[11] H. G. B. de Jong, Rec. trav. chim. **43**, 189 (1924).
[12] Kruyt and Tendeloo, Kolloidchem. Beihefte **29**, 413 (1929).
[13] D. R. Briggs, J. Chem Phys.. **45**, 866, 943 (1941).

TABLE I. Description of hydrosols.

No.	Method of prep.	Micellar charge	Appearance of sol	Time of dialysis*	Total conc. Fe: meq. Fe^{+++}/l.	Total conc. Anion meq. X^-/l.	Conc. ratio: Fe/X	Rel. viscos.†	pH†
1	IAa	Pos.	Dark red-brown, slightly turbid to reflected light	8 days	1,219	54.9	22.2	1.570	——
2	IAb	Pos.	Clear, very dark red-brown	14 days	935	48.2	19.4	1.37	——
3	IAb	Pos.	Similar to sol 1	16 days	556	15.1	36.8	1.208	——
4	IAb	Pos.	Clear, very dark red-brown	3 days	1,898	102.6	18.5	1.731	3.44
5	IB	Pos.	Clear dark red-brown	5 days	546	18.4	29.7	1.113	——
6	II	Pos.	Clear red-brown	31 days	726	28.2	25.8	1.305	4.64
7	II	Pos.	Clear red-brown	31 days	641	24.9	25.8	1.267	4.6
8	III	Pos.	Very turbid red-brown by reflected, clear deep red by transmitted light	17 hours at 70°C, 5 days at room temp.	744	5.6	132	1.186	4.2
9	IV	Neg.	Clear dark red-brown	2 days	800	——	——	1.306	6.67
10	IV	Neg.	Clear dark red-brown	36 hours	1,019	——	——	1.285	5.97

* Approximately four liters of distilled water were used per day.
†Fresh sol, diluted: 1 ml water to 10 ml sol.

Loeb has made use of change in hydration as the mechanism for viscosity variations in gelatin dispersions. He determined that, using *p*H values as abscissae, curves of the same shape were obtained whether the ordinate was swelling of gelatin granules, or the osmotic pressure or viscosity of gelatin dispersions. All these properties are at a minimum at the isoelectric point. The osmotic pressure curve was explained on the basis of a Donnan equilibrium, and the swelling and viscosity curves by considering the distribution of ions which result from such an equilibrium when the charged gelatin particle is immersed in an electrolyte solution. The Donnan equilibrium predicts the hydration of the particle to be greatest when the charge is greatest and the electrolyte concentration of the solution smallest. Since the viscosity of the dispersion will vary in the same direction as the hydration of the dispersed phase, these are the same conditions as those required for maximum viscosity by the Smoluchowski equation. The mechanisms, however, are quite different.

The increase in viscosity which occurs when greater quantities of electrolyte are added is considered to be due to an agglomeration of individually dispersed particles. Smoluchowski points out that, for spherical particles, even the closest possible packing must produce an increase in the relative volume of the dispersed phase.[9] Should a looser packing occur, with more occluded water, the increase in relative volumes, and consequently in viscosity, must be still greater. Freundlich[14] has used this increase in viscosity as a means of measuring the rate of coagulation of aluminum hydroxide sols on the addition of various salts.

Reports on the viscosity of "iron oxide" hydrosols[2, 6, 15, 16] have been brief, and do not afford a knowledge of the factors upon which the viscosities of these systems depend. It is the purpose of this investigation to determine these factors by the study of a number of variables which influence the viscosities of these sols, and to propose a mechanism through which the changes in viscosity occur.

EXPERIMENTAL

Methods of Preparation of Hydrosols

I. (A) One mole of ferric chloride was treated with excess ammonia. Each portion of the precipitate, after dividing among four half-liter

[14] H. Freundlich and C. Ishizaki, Trans. Faraday Soc. **9**, 66 (1913).
[15] G. H. Ayres and C. H. Sorum, J. Phys. Chem. **34**, 2826 (1930).
[16] J. H. Yoe and E. Freyer, J. Phys. Chem. **30**, 1389 (1926).

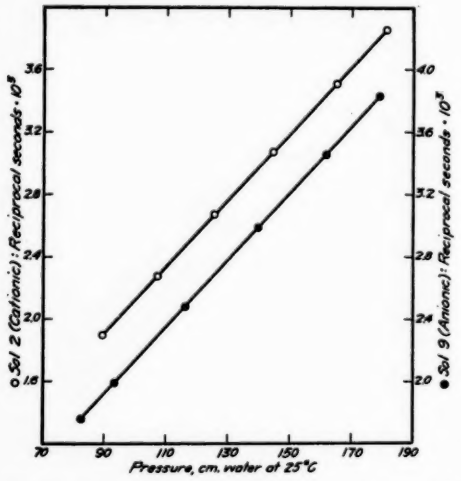

FIG. 1. Variation of time of flow of sols 2 and 9 with pressure.

centrifuge cups, was washed centrifugally with eight portions of distilled water of 250 ml each. The precipitate was then suspended in distilled water, the volume of the suspension being one liter. Peptization was effected by adding either (a) 1*M* ferric chloride or (b) concentrated hydrochloric acid, to the extent of approximately 0.1 equivalent of added electrolyte per equivalent of precipitated iron. (B) The same procedure was followed using ferric nitrate, and peptizing with 1*M* ferric nitrate. About 0.25 equivalent of ferric nitrate was added for each equivalent of precipitated iron.

II. To an aqueous 2*M* solution of ferric chloride was added slowly, with agitation, concentrated ammonia equivalent to two-thirds of the ferric ion.

III. 0.5 liter of 0.5*M* solution of ferric nitrate was added dropwise with agitation to one liter of distilled water at 70 to 80°C. Dialysis was carried on simultaneously to remove the products of hydrolysis.

IV. A dialyzed sol (to absence of thiocyanate test for ferric ion on the diffusate) prepared by method II was precipitated and redispersed by adding, with agitation, potassium citrate solution.

Dialysis in each case was accomplished by placing the sol in a nitrocellulose bag which was immersed in a beaker through which distilled water was allowed to flow continuously.

The hydrosols are described in Table I.

Apparatus

Viscosity

A Bingham viscometer,[17] having a working volume of five milliliters, was used for the determination of outflow times of hydrosols under various pressures. The efflux time for water at 25.000±0.005°C was 215.0 seconds under a pressure of 164.0 cm of water. For all other viscometric measurements, Ostwald viscometers were used. At 25°C, these had outflow times of about ninety seconds when containing five milliliters of water. All measurements of viscosity were carried out at 25°±0.005°C.

*p*H *Values*

These were measured at 25.0±0.1°C by the glass electrode.

Conductance

Twenty-five ml of the sol were placed in an unplatinized platinum electrode conductivity

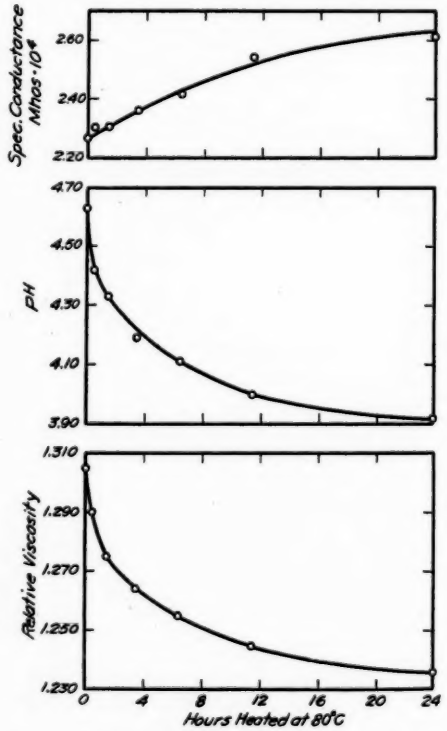

FIG. 2. Effect of heating on sol 6 (cationic).

[17] E. C. Bingham, *Fluidity and Plasticity* (McGraw-Hill Book Co., 1922), first edition, p. 76.

cell. The cell constant was determined at various resistances by the use of several concentrations of potassium chloride, the equivalent conductances of which are given by Shedlovsky.[18] Measurements were made at 25.000±0.005°C, using 1000-cycle alternating current and the modified Wheatstone bridge arrangement described by Dike.[19]

Determination of Nature of Flow

According to Poiseuille,

$$\eta = Cpt - C'\rho/t, \qquad (3)$$

where η is the viscosity of the liquid, p is the pressure causing flow, t is the time of outflow of a given volume through the capillary, C and C' are constants for a given viscometer, and ρ is the density of the liquid.[20] In order to show whether the sols investigated obeyed Poiseuille's law, their times of outflow through a Bingham viscometer were determined under various driving pressures. For large values of t, the second term becomes negligible, and

$$p = k(1/t), \qquad (4)$$

where $k = \eta/C$. The plot of $1/t$ against p in Fig. 1 demonstrates that typical cationic and anionic sols* exhibit viscous flow.

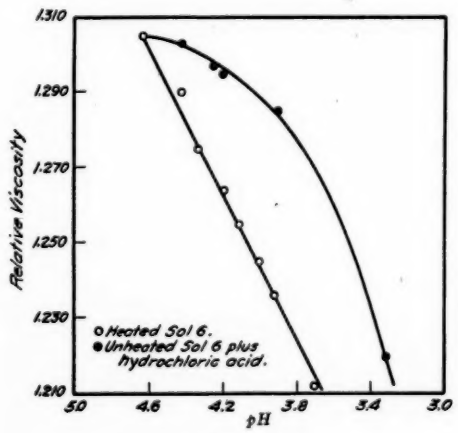

FIG. 3.

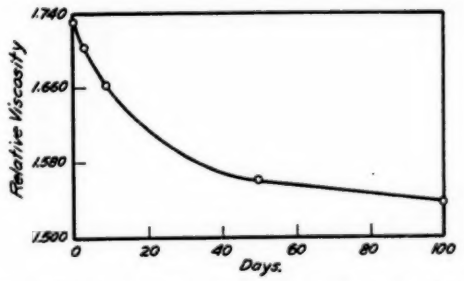

FIG. 4. Change in viscosity of sol 4 on aging at 25°C.

TABLE II. pH value and specific conductance of heated sol 6.*

1 Hr. heated at 80°C	2 pH	3 $a_{H^+}\cdot10^5$	4 $\Delta a_{H^+}\cdot10^5$	5 $\Delta\kappa_{calc}\cdot10^5$	6 $\kappa_{calc}\cdot10^5$	7 $\kappa_{obs}\cdot10^5$
0.0	4.63	2.34				22.7
0.5	4.42	3.80	1.46	0.51	23.2	23.0
1.5	4.33	4.68	2.34	0.82	23.5	23.1
3.5	4.19	6.46	4.12	1.44	24.1	23.6
6.5	4.11	7.76	5.42	1.90	24.6	24.2
11.5	4.00	10.00	7.66	2.68	25.4	25.5
24.0	3.92	12.02	9.68	3.39	26.1	26.2
72.0	3.70	20.0	17.6	6.17	28.9	29.0

κ = specific conductance

$\Delta a_{H^+} = a_{H^+} - a_{H^+_0}$; $a_{H^+_0} = 2.34\cdot10^{-5}$

$\Delta\kappa_{calc} = (0.350)\Delta a_{H^+}$

$\kappa_{calc} = \kappa + \kappa_0$; $\kappa_0 = 22.7\cdot10^{-5}$

* Sol diluted prior to heating: 10 ml water to 100 ml sol.

Heating and Aging

Portions of sol 6 (cationic), sealed in steamed seventy-five-ml Pyrex test tubes,† were placed in an 80±0.3°C-water thermostat. Test tubes were withdrawn from the bath at specific time intervals, and rapidly cooled in an ice-bath. The viscosity and pH value fall with time, while the conductance increases, all measurements being made at 25°C (Fig. 2).

The lower curve of Fig. 3 shows this viscosity and pH value data plotted against one another. The addition of hydrochloric acid to the unheated sol also lowers the viscosity and the pH value of the sol, and the effects of increasing concentrations of hydrochloric acid are shown by the upper curve of Fig. 3. The viscosity of the heated sol, at a given pH value, is seen to be distinctly lower than that of the unheated sol.

It is interesting to note that the change in specific conductance on heating may be accounted for largely on the basis of the change in

[18] T. Shedlovsky, J. Am. Chem. Soc. **54**, 1411 (1932).
[19] P. H. Dike, Rev. Sci. Inst. **2**, 379 (1931).
[20] Reference 17, p. 74.
* For brevity, hydrosols with positive micelles will be described simply as "cationic sols," and those with negative micelles as "anionic sols."

† Samples heated in tubes which had been treated with sulfuric acid-dichromate cleaning mixture, but had not been subsequently steamed, gave erratic results.

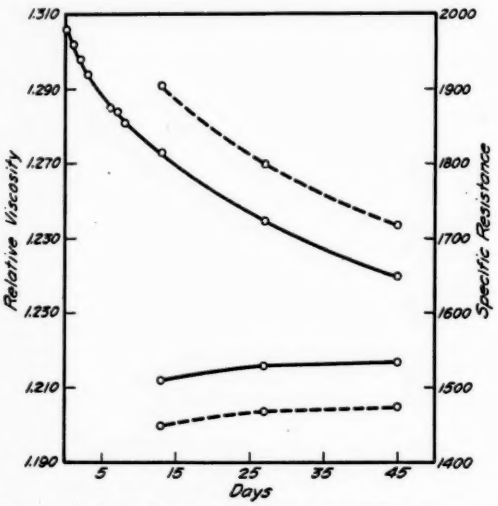

FIG. 5. Aging of sol 9 (anionic) at 25°C. Lower pair of curves: the aging at 25°C of a portion of the sol which had been heated at 90°C for 13.5 hours. Solid lines: viscosity. Broken lines: resistance.

TABLE III. Sol 4 (undiluted).

Age in days*	0	315
Rel. viscosity	1.843	1.587
*p*H	3.46	3.17
Spec. conduct. (Mho)	8.92×10^{-4}	10.35×10^{-4}

* Refers to time elapsed after removal from dialyzing bag.

hydrogen ion activity. Column 4 of Table II shows the increase of hydrogen ion activity of the heated portions of sol over the hydrogen ion activity of the original unheated sol, as calculated from the *p*H values. This increase in hydrogen ion activity should lead to the increase in specific conductance shown in column 5, assuming 350, the equivalent conductance of the hydrogen ion at infinite dilution (25°C),[21] to be the equivalent conductance of the hydrogen ion in this system. In column 6, these conductance increases are added to the specific conductance of the original sol, and in the last column are given the observed conductances for the heated portions of the sol.

The viscosity of cationic sols aging at room temperature follows a path similar to the heating curve discussed above. Figure 4 shows the change of viscosity of sol 4 with time.‡ That the *p*H value and specific conductance of the sol also change is shown by Table III.

[21] *Landolt-Bornstein Tabellen* (Julius Springer, 1936), Vol. 3, p. 2059.

‡ Sol diluted just before making measurements: 10 ml water to 100 ml sol.

The decrease, with time, of the viscosity of an anionic sol is shown in Fig. 5.‡‡ Heating a portion of this sol causes a much more rapid decrease in viscosity: 13.5 hours at 90°C causes the relative viscosity of the sol to fall from 1.273 to 1.212, and the *p*H value from 6.67 to 5.97, while the specific conductance increased from $5.25\cdot10^{-4}$ to $6.90\cdot10^{-4}$ mho, a change of $1.65\cdot10^{-4}$ mho. The change in hydrogen ion activity ($8.6\cdot10^{-7}$ mole/liter) will account for a change in conductance of only $0.0030\cdot10^{-4}$ mho. Thus it is necessary to conclude that ions other than hydrogen are mainly produced. These must be citrate ions.

It is to be noted that the aging of the heated portion of sol 9 produces some reversal of the effect of the heating, Fig. 5 indicating a small increase in viscosity and in electrical resistance.

Effect of Added Salts

To ten ml of the sol in a small glass-stoppered bottle was added one ml of salt solution. In Table IV are given the viscosities resulting from the addition of several concentrations of potassium sulfate solution to sol 4. Column 1 lists the viscosity immediately after the addition of the salt solution, and columns 2 and 3 the viscosities at subsequent intervals.

The aging of the sol to which potassium sulfate has been added is accompanied by a viscosity decrease. However, the decrease in viscosity with time is smaller for the sol—salt mixture than for the sol diluted only with water.

If larger concentrations of salt are present, or if the sol is one whose viscosity does not diminish rapidly with time, another effect becomes apparent. Figure 6 shows the aging of sol 3, in

TABLE IV. Addition of potassium sulfate to sol 4.

	Relative viscosity		
Final conc. of pot. sulfate	1 Immediately after addition	2 72 hours after addition	3 216 hours after addition
0.00 meq./l	1.731	1.703	1.663
0.91	1.600	1.575	1.549
1.82	1.535	1.518	1.495
3.64	1.442	1.438	1.432

‡‡ Aging experiment conducted on diluted sol: 10 ml water to 100 ml sol.

the presence of added potassium sulfate and potassium chloride. The viscosity increases with time, and the rate of increase is greater where the salt concentration is greater (curves *B* and *C*). It is evident also that for equal salt concentrations (curves *C* and *D*), the rate of viscosity increase is greater for potassium sulfate than for potassium chloride.

In order to obtain comparable viscosity values for viscosity-salt concentration curves, all values for a given experiment were determined either immediately after salt addition, or twenty-four hours after salt addition.* The viscosities in the presence of a given concentration of all salts were determined within a time sufficiently short to render insignificant differences due to the aging of the sol.

The effect of salts on the viscosity of cationic sols is shown in Figs. 7 and 8, and on anionic sols in Fig. 9.

In these figures, the upward trend in the curves is attained at lower salt concentrations for salts which are potent precipitants than for those which are weaker in this respect. (For sols in which the dispersed phase is positively charged, the potent precipitants are the salts of anions which are good coordinators with iron. For anionic sols, the order of precipitating ability is reversed, since strongly coordinating anions may augment the negative charge of the micelle, thus conferring greater stability upon the sol.) The decrease in viscosity, however, appears to be independent of the anion used in

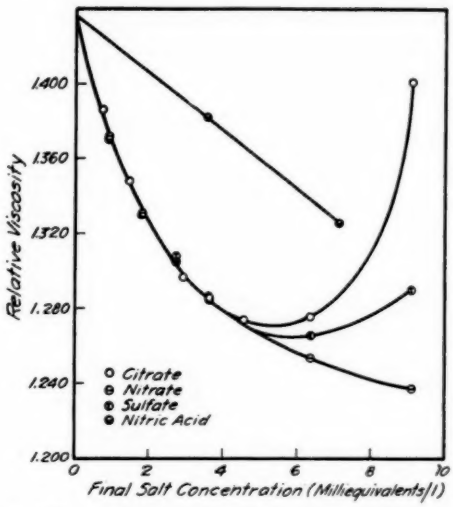

FIG. 7. Effect of potassium salts on viscosity of sol 1 (cationic).

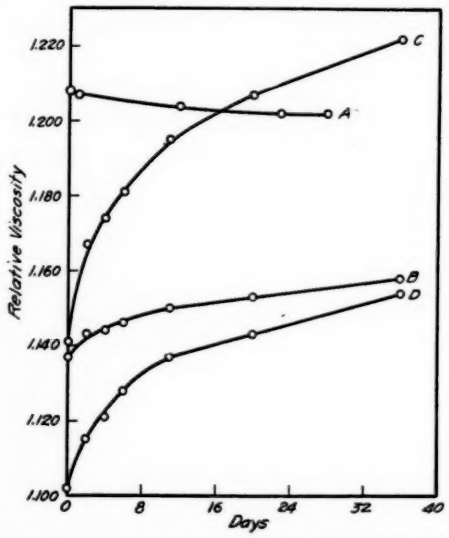

FIG. 6. Change of viscosity of sol 3 (cationic) with time at 25°C. *A*. No salt added. *B*. Added potassium sulfate, 1.14 milliequivalents/l. *C*. Added potassium sulfate, 2.28. *D*. Added potassium chloride, 2.28.

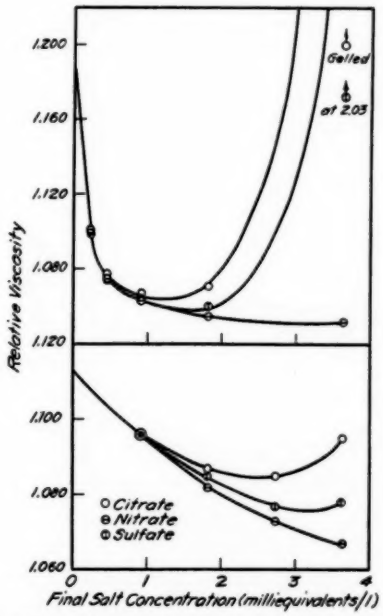

FIG. 8. Effect of potassium salts on viscosity of cationic sols 8 (upper) and 5 (lower). Points corresponding to viscosities outside the range of the plot are shown by arrows. The abscissa is indicated by the position on the graph, and the ordinate by the number beneath the arrow.

* Data for sols 8 and 9 were obtained immediately after salt addition; data for sols 1, 5, and 10 were obtained twenty-four hours after salt addition.

the case of positive sols. The curves shown in Figs. 7 and 8 are representative of those obtained for all positive sols in this research, whether preparation was by method I, II, or III. These disagree with the data of Thévenet,[6] who reported the decrease in viscosity to be in the order $K_4Fe(CN)_6 > K_3PO_4 > K_2SO_4 > KCl$. There is evident, nevertheless, a difference in the effect of various anions on the decrease of viscosity of anionic sols. Potassium citrate produces a smaller viscosity decrease than salts of the less strongly coordinating sulfate and nitrate ions.

Effect of Added Acids

The above procedure was followed, except that acid additions replaced the addition of salts. Figure 10A shows the results on plotting, as above, relative viscosity against final electrolyte concentration. (The acid curve which is included in Fig. 7 shows the relative efficiency of acids and salts in lowering the viscosity.) The order of the curves of Fig. 10A indicates that the stronger the acid, the greater the viscosity depression, which suggests that the smaller depressions are due to smaller actual ion concentrations. This was tested by plotting the viscosity of each sol-acid mixture against its *p*H value (Fig. 10B). At constant *p*H value, the viscosity decrease for this positive sol is apparently independent of the nature of the anion. Again, the strongly coordinating anions cause the viscosity increase to appear at lower electrolyte concentration. Similar data were obtained with an anionic sol (Fig. 11), there being a difference owing to various anions only for the ascending portions of the curves. The viscosity minimum is first produced by the acid with the most weakly coordinating anion, as in the case of salts on this sol (Fig. 9). A comparison of the effects of an acid and a potassium salt on sol 10 may be seen in the nitrate curves of Fig. 9.

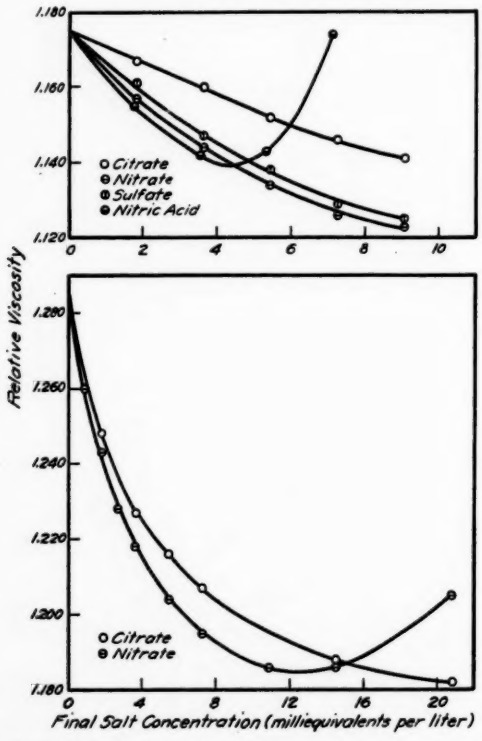

FIG. 9. Effect of potassium salts on viscosity of anionic sols 9 (lower) and 10 (upper).

Effect of Neutral Molecules

To forty ml of sol were added ten to sixty ml of acetone, and the volume made up to 100 ml. The relative viscosity of each solution was obtained by dividing the viscosity of the sol-acetone-water mixture by the viscosity of the acetone-water solution of the same acetone concentration. Although the viscosity is lowered by the addition of acetone (Table V), the effect is negligible when compared to the viscosity decrease produced by an electrolyte. The relative viscosity of this sol is reduced, for example, from 1.144 to 1.031 in the presence of 0.004*M* potassium nitrate.

TABLE V. The effect of acetone on sol 7.

Conc. acetone (moles/l)	Rel. viscosity
0.00	1.144
1.35	1.141
2.70	1.137
4.05	1.134
5.40	1.130
6.75	1.127
8.10	1.123

DISCUSSION

According to the mechanism proposed by the workers of this laboratory,[22] one of the types of

[22] A. W. Thomas and co-workers, J. Am. Chem. Soc. **60**, 2384 (1938); **58**, 2526 (1936); **57**, 1825, 2131 (1935); **57**, 1821, 2538 (1935); **57**, 4 (1935); J. Phys. Chem. **35**, 27 (1931); Kolloid Zeits. **86**, 279 (1939).

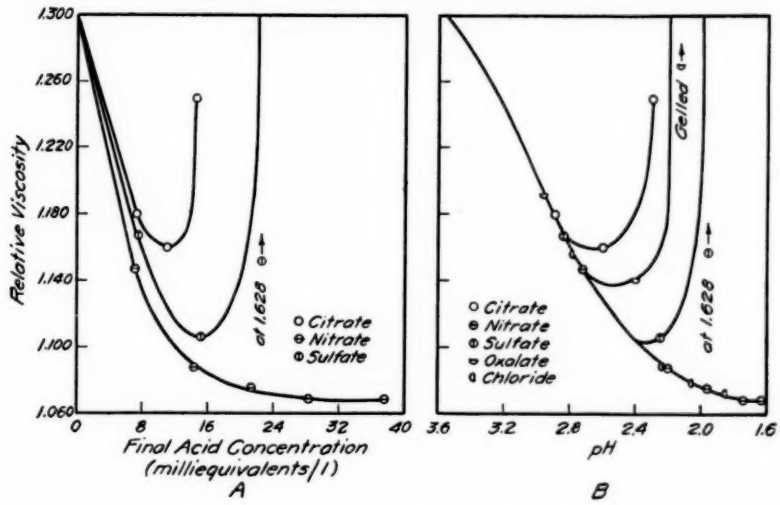

FIG. 10. Effect of acids on viscosity of sol 2 (cationic).

chemical changes occurring during the aging or heating of metal oxychloride dispersions may be formulated:†

$$\left[H_2O\ Cl\ OH\ H_2O\ H_2O\ Fe\ Fe\ H_2O\ H_2O\ OH\ H_2O\ H_2O\right]^{3+} + H_2O \rightleftharpoons H_3O^+ + \left[H_2O\ Cl\ OH\ H_2O\ OH\ Fe\ Fe\ H_2O\ H_2O\ OH\ H_2O\ H_2O\right]^{2+}.$$

This reaction explains the increase in the hydrogen ion activity and in the conductance of the sol. The experiments discussed above indicate that the addition of any electrolyte to an iron oxychloride, -nitrate, or -citrate sol diminishes the viscosity of the dispersion. The viscosity decrease which accompanies the heating and aging reaction may thus be accounted for partly by the increased hydrochloric acid concentration of the sol. A simultaneous result of the above reaction is a decrease in particle charge. Increased electrolyte concentration may be realized without the decrease in charge by the addition of hydrochloric acid to the unheated sol. The micellar charge may in fact be increased by reversing the above reaction. (Hazel and Ayres[23] have shown that the electrophoretic velocity of the particles in positive ferricoxychloride sols increases with the decrease in *p*H value produced by the addition of acid, suggesting an augmented positive charge.) At equal *p*H values, the heated and unheated sols have the same hydrochloric acid activities, and differences in the viscosity should be attributable

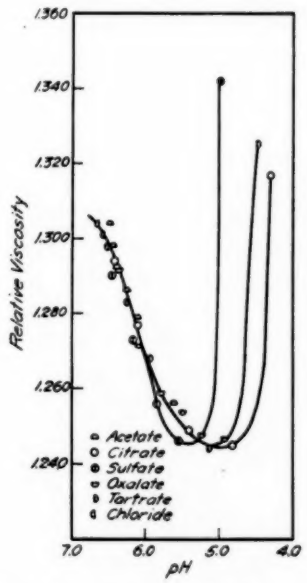

FIG. 11. Effect of acids on viscosity of sol 9 (anionic).

† The micelles of metal oxide dispersions are considered to be complex coordination structures containing a large number of metal atoms, linked to one another by means of ol or oxo bridges. Other coordination positions are occupied by anions, and by aquo and hydroxo groups.

[23] F. Hazel and G. H. Ayres, J. Phys. Chem. **35**, 2930 (1931).

to differences in micellar charge. Figure 3 demonstrates that the heated sol has, at a given *p*H value, a lower viscosity than the unheated, indicating that the viscosity is decreased when the micellar charge is lowered.

Another illustration of this point may be seen in Fig. 7, where the viscosity diminution produced by nitric acid is less than that caused by potassium nitrate, because of the increase in particle charge by reaction of the hydrogen ion with the micelle. A contributing factor in this instance, however, is the decrease in electrolyte concentration of the dispersion which results from the combination of some of the added hydrogen ion with the micelle.

The curves for the aging of the negative dispersion (Fig. 5) may be considered to be analogous to those for the positive, the main reaction being the hydrolysis of the micelle in such a manner as to replace coordinated citrato groups with aquo groups. That this occurs was indicated by the change in conductance which occurs on aging. This reaction decreases the negative charge of the particle and increases electrolyte concentration, producing the decrease in viscosity. The increase in viscosity and electrical resistance on aging after heating may be the result of recoordination of some of the citrate ions at the lower temperature.

Since the dependence of the viscosity of "ferric oxide" hydrosols on charge and electrolyte concentration has now been demonstrated, certain effects must be expected on the addition of salts to the dispersion. All salts will increase the electrolyte concentration; thus all salts may be expected to decrease the viscosity. Those salts which have strongly coordinating anions must decrease the charge of positive micelles to a greater extent than those with poorly coordinating anions, while those same salts will tend to augment the charge of negative micelles more than will the salts of the poorly coordinating anions. In the case of positive micelles, therefore, the better coordinators should produce a greater, and in the case of negative particles, a smaller, decrease in viscosity. The latter expectation is fulfilled (Fig. 9), while the former, in the present research, is not (Figs. 7 and 8). It will be seen in all these curves that the minimum in the viscosity-electrolyte concentration curve is attained at lower electrolyte concentrations for potent precipitants than for poor. Herein lies an explanation for the apparent similarity of effect of all anions on the viscosity decrease of cationic sols. The strongly coordinating anion reduces the positive charge of the micelle. This should produce a decrease in viscosity. The stability of the sol has at the same time been decreased by the decrease in charge, with the result that agglomeration of particles may occur, thus increasing the viscosity. (It was, in fact, possible in some instances to detect by eye very minute suspended particles in the citrate series, as the minimum in the curve was approached.) An indication of the effect of agglomeration may be seen in the slow increase of viscosity with time in Fig. 6. Where the salt concentrations are equal, as in curves *C* and *D*, the more strongly coordinating anion causes the more rapid viscosity increase. This balance of opposite forces produces a smaller decrease in viscosity upon the addition of good coordinators than would be the case were no agglomerating action present. Since both the viscosity-decreasing and the viscosity-increasing reactions have the same source (the lowering of the micellar charge by the coordination of anions), the variation with extent of coordination does not appear, and all the salt curves tend to coincide.

The same argument may be applied to the acid curves. Differences among the effects of various acids are obvious only at the ascending portions, and it is the tendency toward agglomeration in the presence of potent precipitants that masks the viscosity-decreasing effect at the lower acid concentrations.

In the one instance where differences in the descending parts of the curves are produced by different anions (the addition of potassium salts to anionic sols, Fig. 9), an electrolyte concentration factor, as well as a particle charge factor, may contribute to the result. The coordination of citrate ions will lower the actual electrolyte concentration of the dispersion, and thus the final equilibrium potassium citrate concentration will be smaller than the final salt concentration in the case of an equal quantity of added nitrate.

That the viscosity changes of the magnitude observed are due only to electrolyte influence is shown by Table V above, where acetone up to

sixty percent by volume caused a relatively small change in the viscosity. This viscosity decrease may possibly result from a lowering of the particle charge by increased association (in the Bjerrum sense[24]) of positive micelle and free chloride ions, through reduction of the dielectric constant of the dispersion medium by the addition of acetone.

Systems described by the Smoluchowski Eq. (2) would show a dependence of viscosity on electrolyte concentration and micellar charge, through the presence of the variables λ and ζ. Freundlich[25] points out, however, that iron oxide sols, in regard to their viscosity, are more closely related to the hydrophilic sols than to the hydrophobic. Since the hydration of the particles is great and unknown, no estimation of the value of φ of the Einstein (1) and Smoluchowski equations may be obtained, and the applicability of the equations to these systems cannot be ascertained. It is questionable, indeed, whether a ferric oxide dispersion is one composed of the rigid, non-conducting spheres, surrounded by relatively thin ionic atmospheres, for which the Smoluchowski equation was derived. According to the model to be presented below, which is based upon the properties of "ferric oxide" hydrosols, the particles would be neither rigid nor non-conducting. There has been evidence that the dispersed particles in these systems are non-spherical,[26] and may be disks or platelets in aged iron oxide sols.[27] Furthermore, the radius of the particle is believed not to be great in comparison with the thickness of its ionic atmosphere, in colloidal dispersions of low ionic concentration.[28] Freundlich states that the water content of the particles and the resultant "active volume" are nevertheless of great influence on the viscosity of sols, generally in the sense that with increasing water content the viscosity increases. It is therefore of interest to consider whether the extent of hydration may be related to the electrolyte concentration of the dispersion and the particle charge.

Let us assume a model for the positively charged micelle in a ferricoxychloride hydrosol. As a result of the positive charge, the distribution of ions in the solution will be such that an atmosphere of predominantly negative ions will surround the positive micelle. The micelle contains water, and water is free to diffuse into and out of it. Browne[29] has shown that all the water in a ferricoxychloride system acts as solvent water for added dextrose, as determined from the freezing point depression. Thus the ions of the intermicellar liquid must be considered free to diffuse into the water within the particle, and the ionic atmosphere, instead of originating at the particle boundary, is continuous from the intermicellar liquid through the particle. The larger the positive charge for a particle of given size, the more dense will this negative ionic atmosphere be, and the greater will be the concentration of negative ions in the liquid within and around the particle.

In the system under discussion, the negative ions are chloride ions, and the concentration of these ions within, and in the immediate vicinity of, the micelle is greater than in the bulk of the dispersion medium. In addition to chloride ions, the dispersion medium contains hydrogen ions. At equilibrium, as has been shown by Donnan,[30] the energy required to transport reversibly and isothermally δn moles of H^+ from a part of the intermicellar liquid (region 1) to a part of the dispersion medium which is within the particle (region 2) is equal to the energy which can be gained from the corresponding reversible and isothermal transport of δn moles of Cl^-. The diminution of free energy for this process is zero, hence

$$\delta nRT \ln \frac{a_{H^+_2}}{a_{H^+_1}} + \delta nRT \ln \frac{a_{Cl^-_2}}{a_{Cl^-_1}} = 0, \qquad (5)$$

or

$$a_{H^+_1}\, a_{Cl^-_1} = a_{H^+_2}\, a_{Cl^-_2}, \qquad (6)$$

where the subscripts denote the aforementioned regions. For simplicity, the equation of products may be approximated using concentrations in

[24] R. M. Fuoss, Chem. Rev. **17**, 27 (1935).
[25] H. Freundlich, *Colloid and Capillary Chemistry* (Methuen and Co., Ltd., 1926), trans. from the third German edition, p. 368.
[26] B. Lange, Zeits. f. physik. Chemie **132**, 1 (1928).
[27] H. Diesselhorst and H. Freundlich, Physik. Zeits. **17**, 117 (1916).
[28] D. C. Henry, Proc. Roy. Soc. **A133**, 106 (1931).
[29] F. L. Browne, J. Am. Chem. Soc. **45**, 297 (1923).
[30] F. G. Donnan, Zeits. f. Elektrochem. **17**, 572 (1911).

place of activities:

$$[H^+]_1[Cl^-]_1=[H^+]_2[Cl^-]_2. \quad (7)$$

Now, if $x=[H^+]_1=[Cl^-]_1$, $y=[H^+]_2=$ the concentration of chloride ions which balances these hydrogen ions, and $z=$ the concentration of excess chloride ions in region 2 which are held by the positive charge of the micelle, $[Cl^-]_2=y+z$, and

$$x^2=y(y+z), \quad (8)$$

$$y=\frac{-z+(z^2+4x^2)^{\frac{1}{2}}}{2}. \quad (9)$$

The difference in osmotic pressure between the two regions under discussion depends on the difference in ionic concentrations, or

$$P=(2y+z-2x)RT. \quad (10)$$

Substituting in this expression the value of y from (9) gives

$$P=[(z^2+4x^2)^{\frac{1}{2}}-2x]RT. \quad (11)$$

From (11) it may be seen that when z is not zero (this will be the case when the micelle is charged), the osmotic pressure will have positive values, whereas the decrease of the charge to zero gives

$$\lim_{z\to 0} P=[(4x^2)^{\frac{1}{2}}-2x]RT=0. \quad (12)$$

Adding hydrochloric acid to a ferricoxychloride sol may produce some increase in z, but x will increase to a greater extent, and once more

$$\lim_{z\to\infty} P=0.$$

A change in osmotic pressure will be followed by the diffusion of water into or out of the particle, causing a change in particle volume and in the fraction of the total volume occupied by the dispersed phase. Hence, a viscosity change occurs.

A similar treatment for the addition of an electrolyte without common ions, such as potassium nitrate, also predicts a viscosity decrease. This mechanism is consistent with the influence of micellar charge, since (11) indicates that the greater degree of swelling occurs when z has the greater value. Also explained is the lack of a primary effect on the addition of a non-electrolyte, acetone, which does not directly vary the ion concentrations, but merely substitutes throughout the system for water.

APRIL, 1942 JOURNAL OF CHEMICAL PHYSICS VOLUME 10

The Approximate Solution of Schrödinger Equations by a Least Squares Method

ARTHUR A. FROST
Department of Chemistry, Northwestern University, Evanston, Illinois

(Received December 12, 1941)

A method of approximation to the solution of a Schrödinger equation has been developed in which variation functions are used but no integrations are involved. The procedure involves the evaluation of the energy for a set of representative points in configuration space. The parameters in the variation function are then chosen by applying the condition that the mean square deviation of the energy from the average should be a minimum.

INTRODUCTION

THE calculation of the electronic energy levels of molecules requires the use of approximation methods. The hydrogen molecule ion, H_2^+, and the hydrogen molecule, H_2, are examples of molecules that have been solved with high accuracy.[1] Only rather crude approximations have been applied to more complicated molecules. It would be very desirable to have methods that could be used successfully in such cases.

Of the many approximation methods used in quantum mechanics[2] the best known are the

[1] For H_2^+, e.g. the work of G. Jaffe, Zeits. f. Physik **87**, 535 (1934); for H_2, H. M. James and A. S. Coolidge, J. Chem. Phys. **3**, 129 (1935).

[2] See, for example, L. Pauling and E. B. Wilson, *Introduction to Quantum Mechanics* (McGraw-Hill Book Company, New York, 1935), Chaps. 6 and 7. An example of a recently developed method is the numerical integration method of G. E. Kimball and G. H. Shortley, Phys. Rev. **45**, 815 (1934).

perturbation methods and the variation method. Perturbation methods are unsatisfactory for the calculation of electronic energy levels of molecules because the perturbations involved are much too large. On the other hand the variation method if pushed far enough will give results of sufficient accuracy. It is this method that was used by James and Coolidge[1] in their calculation of the hydrogen molecule.

The application of the variation method to more complicated systems is both difficult and tedious. Good variation functions may easily be chosen, but there is no straightforward method of evaluating the required integrals. If simpler functions are used so that the integrals become reasonable, then the determination of the best values of the parameters becomes a lengthy process. In this paper is described an attempt to develop a method which makes use of a variation function but in which no integrations are required. Numerical calculation here is more extensive than in the variation method but is put in such a form that machine methods may be used.[3]

GENERAL FORMULATION OF THE METHOD

Let the Schrödinger equation for the stationary states of the system be $H\varphi = E\psi$ where H is the Hamiltonian operator and ψ is a function of the coordinates. E is the energy parameter. Dividing both sides of the equation by ψ,

$$H\psi/\psi = E. \tag{1}$$

Since E is a constant, independent of coordinates, then if ψ is a solution, $H\psi$ divided by ψ must be a constant independent of coordinates even though $H\psi$ and ψ are both functions of the coordinates.

Suppose that φ is an approximate solution. $H\varphi/\varphi$ will in general be not a constant but a function of coordinates. As φ is varied to become more nearly a solution $H\varphi/\varphi$ becomes more nearly a constant which is equal to the energy of the particular state represented by φ.

Define

$$\epsilon \equiv H\varphi/\varphi. \tag{2}$$

ϵ may be evaluated at any point without difficulty because H is a differential operator. Now take as a criterion of the excellence of the approximate function φ the mean square deviation of ϵ from its mean value. To find the best solution, vary the parameters in φ until the mean square deviation of ϵ from its mean value is a minimum. Using the subscript $_{Av}$ to indicate the taking of mean values this condition may be written as

$$\text{Minimize } \langle(\epsilon - \epsilon_{Av})^2\rangle_{Av} \tag{3}$$

or after expansion

$$\text{Minimize } (\langle\epsilon^2\rangle_{Av} - \epsilon_{Av}^2). \tag{4}$$

The method of taking the mean value is not unique. For example ϵ_{Av} may be taken over a finite set of points so that $\epsilon_{Av} = \sum_i g_i\epsilon_i / \sum_i g_i$ where g_i is a weighting factor, or ϵ_{Av} may be taken as an integral over all points in configuration space. A special case of ϵ_{Av} represented as an integral is where $\varphi^*\varphi$ is used as a weighting factor. Then

$$\epsilon_{Av} = \int \varphi^*\varphi\epsilon d\tau \Big/ \int \varphi^*\varphi d\tau$$

or introducing the definition of ϵ

$$\epsilon_{Av} = \int \varphi^* H\varphi d\tau \Big/ \int \varphi^*\varphi d\tau.$$

In this case ϵ_{Av} is the usual quantum-mechanical expectation value or mean value of the energy for the system in the state φ. Where other weighting factors are used or where summation over a finite set of points is resorted to ϵ_{Av} may still be interpreted as a mean value of the energy and ϵ itself as the energy at a given point. As a result of this the condition (3) or (4) for the best function φ may be interpreted as requiring the energy to be as nearly as possible independent of the coordinates.

In the limit, for a correct solution, ϵ is a constant, and regardless of what weighting procedure is used the mean square deviation will be zero. This fact leads to the conclusion that a satisfactory method for taking the mean would be to use the mean over a set of representative points rather than to integrate over all possible points. Naturally the number and distribution of points would determine the accuracy with

[3] Punched-card machine methods are labor-saving where a long calculation involves many similar steps. For applications of punched-card machines see W. J. Eckert, *Punched Card Methods in Scientific Computation* (Columbia University, 1940).

which the approximation is made. However, the use of a set of points replaces integration by summation and therefore may eliminate an extremely difficult integration. It should be noted that this replacement of integration by summation is not just a numerical integration. In choosing the points for the summation there is no need to spread them evenly or by suitable weighting to cause the summation to approach to an integration.

THE METHOD APPLIED TO A LINEAR VARIATION FUNCTION

Let

$$\varphi=\sum_m C_m\varphi_m,$$

where the C_m's are coefficients in a linear combination of φ_m's. Since it is the energies of stationary states that are to be calculated the C_m's and φ_m's can be restricted to real numbers and real functions respectively. Substitution in (2) yields

$$\epsilon=\sum_m C_mH\varphi_m/\sum_m C_m\varphi_m$$

or

$$\epsilon(i)=\sum_m C_mH\varphi_m(i)/\sum_m C_m\varphi_m(i),$$

where the index i is used to refer to values of functions at a particular point and $H\varphi_m(i)$ means the value of $H\varphi_m$ at point i.

In order to obtain the least square deviation it is convenient to calculate $\langle\epsilon^2\rangle_{Av}$ and ϵ_{Av}^2 as used in condition (4). The weighting factor will be taken to be $p_i\varphi^2(i)$ since this results in a great simplification of the formulas due to the possibility of changing the order of summation. Then

$$\epsilon_{Av}=\frac{\sum_i p_i\varphi^2(i)\epsilon_i}{\sum_i p_i\varphi^2(i)}$$

$$=\frac{\sum_i p_i(\sum_m C_m\varphi_m(i))(\sum_n C_nH\varphi_n(i))}{\sum_i p_i(\sum_m C_m\varphi_m(i))(\sum_n C_n\varphi_n(i))}$$

and interchanging the order of summation over i and m and n, which is permissible since these are all finite summations,

$$\epsilon_{Av}=\frac{\sum_m\sum_n C_mC_n\sum_i p_i\varphi_m(i)H\varphi_n(i)}{\sum_m\sum_n C_mC_n\sum_i p_i\varphi_m(i)\varphi_n(i)}. \quad (5)$$

Likewise,

$$\langle\epsilon^2\rangle_{Av}=\sum_i p_i\varphi^2(i)\epsilon_i^2/\sum_i p_i\varphi^2(i)$$

$$=\frac{\sum_m\sum_n C_mC_n\sum_i p_iH\varphi_m(i)H\varphi_n(i)}{\sum_m\sum_n C_mC_n\sum_i p_i\varphi_m(i)\varphi_n(i)}. \quad (6)$$

To simplify the expressions three definitions are introduced:

$$\sum_i p_i\varphi_m(i)\varphi_n(i)\equiv D_{m,n},$$

$$\sum_i p_i\varphi_m(i)H\varphi_n(i)\equiv H_{m,n}. \quad (7)$$

$$\sum_i p_iH\varphi_m(i)H\varphi_n(i)\equiv K_{m,n}.$$

Formulas (5) and (6) then become

$$\epsilon_{Av}=\sum_m\sum_n C_mC_nH_{m,n}/\sum_m\sum_n C_mC_nD_{m,n}, \quad (8)$$

$$\langle\epsilon^2\rangle_{Av}=\sum_m\sum_n C_mC_nK_{m,n}/\sum_m\sum_n C_mC_nD_{m,n}. \quad (9)$$

Having chosen a set of functions φ_m and a set of points i the quantities $D_{m,n}$, $H_{m,n}$, and $K_{m,n}$ can be calculated. There remains the determination of the C_m's such that Eq. (4) with the aid of Eqs. (8) and (9) is satisfied. In general several choices of the relative values of the C_m's are possible corresponding to different energy states of the system.

THE DETERMINATION OF THE LEAST SQUARE DEVIATION

Minimizing the mean square deviation of ϵ in this method corresponds to minimizing the energy integral in the variation method. Whereas in the latter process the use of a linear variation function leads to a secular equation to be solved, the present method, if a similar procedure were followed, would lead to equations of great complexity. Instead, a method of successive approximations may be used for the determination of the values of the C_m's which minimize the mean square deviation of ϵ.

Given a set of approximate C_m's, the corresponding ϵ_{Av} and $\langle\epsilon^2\rangle_{Av}$ and mean square deviation $\langle\epsilon^2\rangle_{Av}-\epsilon_{Av}^2$ may be calculated from Eqs. (8) and (9). A single coefficient C_k is then changed by slight positive and negative values and $\langle\epsilon^2\rangle_{Av}-\epsilon_{Av}^2$ determined for each. A new value of C_k is then estimated which will roughly minimize $\langle\epsilon^2\rangle_{Av}-\epsilon_{Av}^2$. The procedure is repeated for each C_m in turn following through several cycles of all the C_m's until $\langle\epsilon^2\rangle_{Av}-\epsilon_{Av}^2$ shows no appreciable further decrease. The value of ϵ_{Av} for this final set of C_m's is then the desired approximate energy. Computational details of this procedure are to be found in the appendix.

CONVERGENCE OF THE METHOD AND THE CHOICE OF POINTS

That the convergence of the method is intimately bound up with the choice of points is shown by the following argument. For any arbitrary approximation function φ, ϵ will be a definite function of the coordinates. Now choose all the sets of coordinates or points for which ϵ has some constant value E'. The values of ϵ associated with this set of points are all equal and the mean square deviation of ϵ is zero. Therefore, if the set of points had been chosen originally as a basis for the present method of approximation, the mean square deviation of ϵ could be minimized to zero without the function φ being equal to the true solution ψ and without the value E' being equal to the correct value E, all of this despite the fact that the set of points may have been infinite in number. The method does not necessarily converge to the correct solution merely by taking a sufficiently large number of points. It is probable that for the process to converge to the correct solution the points must be so chosen that in the limit all possible points are included. It is obvious for this limiting case of all points included that the mean square deviation of ϵ can be zero only when φ is the correct solution and $\epsilon=E$. For suppose that the mean square deviation of ϵ is zero. Then $\epsilon\equiv H\varphi/\varphi$ must be constant, say E'. Therefore, $H\varphi=E'\varphi$ and φ must be a solution ψ and E' a value of the parameter E.

The best choice of points to be used could possibly be found by a method similar to the method of Gauss for the case of ordinary numerical integration.† However, physical intuition offers a simpler method. The form of the wave function, as long as it is constrained to satisfy the boundary conditions, is most important where its square is largest, i.e., where the probability amplitude is greatest. This, of course, will be the configurations where the electrons are not too far from the nuclei. However, points in configuration space corresponding to actual superposition of electrons on nuclei are to be avoided because at such points for any ordinary approximation functions ϵ is likely to become infinite or many-valued. In the practical application of the method probably the choice of points for a given problem will have to be determined through experience with similar problems.

† J. B. Scarborough, *Numerical Mathematical Analysis*, p. 131. I wish to thank the reviewer for reference to Gauss' method.

APPLICATION OF THE METHOD TO THE HYDROGEN MOLECULE-ION

The theory presented in the preceding sections gives no indication of the accuracy with which a problem may be solved after a set of points has been chosen. In this section is described a practical application which was carried out for the purpose of determining the approximate number of points and functions necessary to arrive at a solution of sufficient accuracy for a problem of the type under consideration. The problem of the normal state of the hydrogen molecule-ion was chosen for this purpose because of its simplicity and because of the fact that an accurate solution is known.

The Hamiltonian operator expressed in atomic units[4] is

$$H\equiv-(1/2)\nabla^2-(1/r_A)-(1/r_B),$$

r_A and r_B being the distances of the electron from nucleus A and nucleus B, respectively. For the normal state ψ may be expressed as a function of r_A and r_B as coordinates inasmuch as there is cylindrical symmetry about the internuclear axis. The operator ∇^2 may be expressed in terms of the coordinates r_A and r_B together with a third, angular, coordinate determining position about the axis. All derivatives with respect to this angular coordinate vanish since ψ is a constant so far as this coordinate is concerned. In these coordinates the Schrödinger equation becomes

$$-\frac{1}{2}\frac{\partial^2\psi}{\partial r_A^2}-\frac{1}{2}\frac{\partial^2\psi}{\partial r_B^2}-\cos AB\frac{\partial^2\psi}{\partial r_A\partial r_B}-\frac{1}{r_A}\frac{\partial\psi}{\partial r_A}-\frac{1}{r_B}\frac{\partial\psi}{\partial r_B}-\frac{1}{r_B}\psi-\frac{1}{r_B}\psi=E\psi,$$

where $\cos AB$ is the cosine of the angle between

[4] Unit of length—radius of 1st Bohr orbit of H; unit of mass—mass of electron; unit of time—$(1/2\pi)$ period of electron in first Bohr orbit of H. These result in the unit of charge being the electronic charge and the unit of energy being twice the ionization energy of an H atom with infinite nuclear mass.

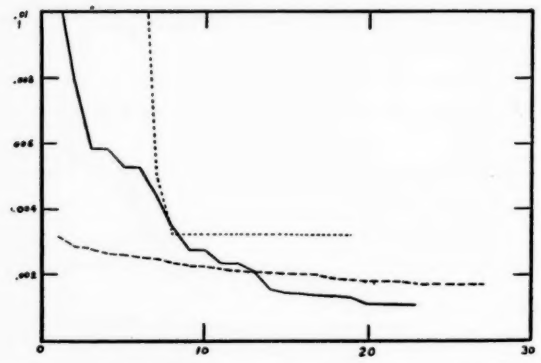

FIG. 1. Ordinate: $\langle\epsilon^2\rangle_{Av}-\epsilon_{Av}^2$, atomic units; abscissa: number of variations; dotted line: 6-point calculation; dashed line: 9-point calculation; full line: 15-point calculation.

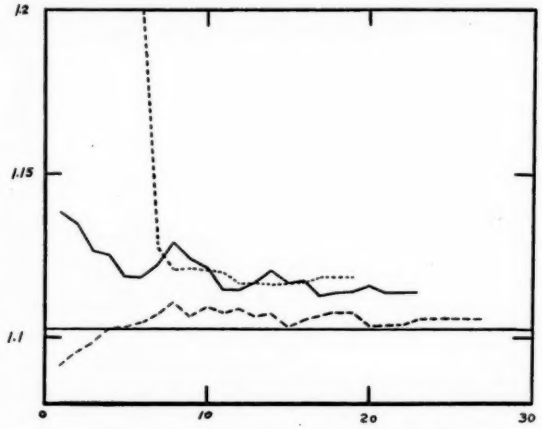

FIG. 2. Ordinate: $-\epsilon_{Av}$, atomic units; abscissa: number of variations; dotted line: 6-point calculation; dashed line: 9-point calculation; full line: 15-point calculation; horizontal line at $-\epsilon_{Av}=1.1026$ indicates known correct value.

the radius vectors from the electron to the two nuclei. This comes in through the relation

$$\cos AB=(r_A^2+r_B^2-R^2)/2r_Ar_B,$$

where R is the internuclear distance. The value of R will be taken as 2, corresponding to the minimum in the potential energy curve.

Although the equation is separable in elliptical coordinates and not separable in the coordinates r_A and r_B, the latter set will be used so as to have a system of calculation which can easily be generalized to more complicated molecules.

ψ will be approximated to by the function φ of the form

$$\varphi=\exp\left[-z(r_A+r_B)\right]F(r_A, r_B),$$

where

$$F(r_A, r_B)=\sum_k\sum_l c_{kl}r_A^k r_B^l.$$

Substitution in Eq. (2) yields

$$-\epsilon F=\sum_{k,l}c_{k,l}r_A^k r_B^l\Big\{z^2(1+\cos AB)-(z-1)\left(\frac{1}{r_A}+\frac{1}{r_B}\right)-k\frac{z}{r_A}(1+\cos AB)-l\frac{z}{r_B}(1+\cos AB)+k(k+1)\frac{1}{2r_A^2}+l(l+1)\frac{1}{2r_B^2}+kl\frac{\cos AB}{r_Ar_B}\Big\}. \quad (10)$$

Since the lowest state of H_2^+ is symmetrical with respect to an interchange of r_A and r_B, the set of approximation functions may be grouped as follows:

$$\begin{aligned}
&\varphi_1=\exp\left[-z(r_A+r_B)\right],\\
&\varphi_2=\exp\left[-z(r_A+r_B)\right](r_A+r_B),\\
&\varphi_3=\exp\left[-z(r_A+r_B)\right](r_A^2+r_B^2),\\
&\varphi_4=\exp\left[-z(r_A+r_B)\right]r_Ar_B,\\
&\varphi_5=\exp\left[-z(r_A+r_B)\right](r_A^3+r_B^3),\\
&\varphi_6=\exp\left[-z(r_A+r_B)\right](r_A^2r_B+r_Ar_B^2),\\
&\text{etc.}
\end{aligned} \quad (11)$$

The set of six functions above are used in this calculation together with F^2 as the weighting factor.

The parameter z could be varied as well as the coefficients c_m. However, in this calculation it was given a single constant value. A reasonable value of z was determined by applying the condition that ϵ must approach the correct value of the energy at distances far from the nuclei.

TABLE I. Final values of coefficients relative to c_1.

No. of variations	6-point calculation	9-point calculation	15-point calculation
c_1	1	1	1
c_2	0.448	0.369	0.308
c_3	.110	.100	.107
c_4	−.463	−.408	−.366
c_5		.0139	.0143
c_6		−.0082	−.0075

From Eq. (10) it is found that for F a finite series

$$\lim_{r_A,\, r_B\to\infty} \epsilon = -2z^2.$$

Equating this to the known value of $E=-1.1026$ atomic units gives $z=0.74$, which is the value used. A slightly different value of z would not be expected to decrease the accuracy of the method.

The coordinates of the points used are as follows: $(r_A, r_B)=(0.4, 1.6)$, $(0.4, 2.4)$, $(0.6, 1.8)$, $(0.6, 2.2)$, $(1, 1)$, and $(1, 2.8)$ for the first calculation. These six plus the following three were used in the second calculation: $(1.4, 1.4)$, $(1.5, 2)$ and $(1, 3)$. For the last calculation the following six points were taken in addition to the above nine: $(1.2, 1.2)$, $(1, 2)$, $(2, 2)$, $(2, 3)$, $(2, 3.5)$, and $(2, 4)$. It should be noted that no points need be taken where $r_B<r_A$ since the functions used are symmetrical in r_A and r_B.

By using Eq. (10) together with (7) the matrices $D_{m,n}$, $H_{m,n}$, and $K_{m,n}$ were calculated for each of the three sets of points to an accuracy of eight significant figures. For the first calculation with six points only the first four functions of (11) were used and the initial values of the coefficients were arbitrarily taken as $c_1=1$, $c_2=0.5$, $c_3=c_4=0$. Starting with c_3 and going on to c_4, c_1, c_2, c_3, c_4, etc., the coefficients were varied according to the procedure given in the appendix. After several cycles of single coefficient variations the values relative to c_1 arbitrarily taken as 1 were as indicated in the first column in Table I. The gradual decrease in the mean square deviation with successive variations in the coefficients is shown in Fig. 1 and the successive changes in the value of ϵ_{Av} in Fig. 2. For the 9-point and 15-point calculations the variation procedure was initiated using approximate values of the coefficients obtained in the previous calculations.

As was expected in each case as the value of ϵ_{Av} approaches to the correct value the mean square deviation of ϵ is minimized. The actual deviation of about 0.01 atomic unit for the 15-point calculation is somewhat less than would be expected from the lowest value of the root mean square deviation of 0.033. The fact that the 15-point calculation does not give the best answer for the energy is probably due to the particular choice of points. There is no doubt that with increasing number of points and functions the correct result could be obtained as closely as desired.

Application of the method to the H_3 problem is in progress.

APPENDIX

The Minimization of $\langle\epsilon^2\rangle_{Av}-\epsilon_{Av}^2$ by Successive Approximation

Given a set of approximate c_m's. Calculate the quantities

$$\left.\begin{aligned} D&=\textstyle\sum_m \sum_n c_m c_n D_{m,n}\\ H&=\textstyle\sum_m \sum_n c_m c_n H_{m,n}\\ K&=\textstyle\sum_m \sum_n c_m c_n K_{m,n}\end{aligned}\right\} \quad (12)$$

and

$$\left.\begin{aligned} D_k&=2\textstyle\sum_m c_m D_{m,k}\\ H_k&=\textstyle\sum_m c_m(H_{m,k}+H_{k,m})\\ K_k&=2\textstyle\sum_m c_m K_{m,k}\end{aligned}\right\} \quad (13)$$

$$\epsilon_{Av}=H/D, \quad \langle\epsilon^2\rangle_{Av}=K/D.$$

Primes will be used to indicate new values of each quantity. Let

$$c'_k=c_k+\Delta c_k.$$

Then

$$\left.\begin{aligned} D'&=D+D_k\Delta c_k+D_{kk}(\Delta c_k)^2\\ H'&=H+H_k\Delta c_k+H_{kk}(\Delta c_k)^2\\ K'&=K+K_k\Delta c_k+K_{kk}(\Delta C_k)^2\end{aligned}\right\} \quad (14)$$

and, of course,

$$\epsilon'_{Av}=H'/D' \quad \text{and} \quad \langle\epsilon^2\rangle'_{Av}=K'/D'.$$

The best value of Δc_k and therefore c'_k can be then obtained by passing a parabola through the resulting values of $(\langle\epsilon^2\rangle_{Av}-\epsilon_{Av}^2)'$ or with sufficient accuracy merely by inspection. The corresponding D', H', K' are calculated, and using the new value of c_k, everything is ready for the variation of the next c_m.*

* *Note added in proof:* The present method is closely related to that of D. H. Weinstein, Proc. Nat. Acad. Sci. **20**, 529 (1934), a fact called to my attention by Dr. L. Pauling.

Letters to the Editor

THIS section will accept reports of new work, provided these are terse and contain few figures, and especially few halftone cuts. The Editorial Board will not hold itself responsible for opinions expressed by the correspondents. Contributions to this section should not exceed 600 words in length and must reach the office of the Managing Editor not later than the 15th of the month preceding that of the issue in which the letter is to appear. No proof will be sent to the authors. The usual publication charge ($3.00 per page) will not be made and no reprints will be furnished free.

Surface Tension of Micelle-Forming Solutions

HANS M. CASSEL
Chicago, Illinois
February 16, 1942

THE capillary curves of some soaps[1] and other long chain molecules in aqueous solution exhibit a peculiar minimum of the surface tension (s.t.) at relatively low concentrations (less than 0.01 molar), the s.t. becoming smaller than half that of water. McBain in numerous publications,[2] as well as Nutting, Long, and Harkins,[3] believes that the observations correspond to true equilibria and that, according to Gibbs' equation, the adsorbed quantities vanish at the concentrations of the minima. In other words, it is assumed that there the composition of the surface layers equals that of the solutions. On the other hand, it can be proved by surface viscosity measurements and direct tests[4] that rather dense surface films do exist at the same concentrations. To reconcile the contradictory conclusions, McBain has recurred to postulating a void of solute in the deeper layers of the solutions. On this basis, the existence of very thin, double-faced structures, like soap bubbles, is hard to understand.

In writing Gibbs' equation: $d\sigma/dm = -\Gamma \cdot d\mu/dm$ (σ designates the s.t.; m, the concentration of solute; Γ, its superficial density; μ, its thermodynamic potential) one notices immediately that $d\sigma/dm$ will vanish when either one of the factors of the second member of the equation tends towards zero. Since a decrease of Γ is out of the question the alternative has to be considered that a gradual fading of the change in potential goes on as the concentration increases.

Unfortunately, there is not much information available about the activities of these solutions in the low concentration range and at the temperature of the s.t. measurements. Values derived by Randall, McBain, and White[5] from vapor pressure measurements show that Na palmitate and stearate start to approach constant activities above a molality of 0.3 at 90°C. Hence, it may be concluded that these and similar substances behave identically at room temperature in a much lower concentration range.

Such a behavior is not surprising in view of the fact that all solutions with which the s.t. minimum is encountered display definite signs, and are indeed typical examples, of micelle formation.[6] Some of these solutions are notoriously very close to being saturated. The conditions obtaining are analogous to certain features of monomolecular films spread on water. Langmuir[7] has put forward the theory that the almost horizontal portion following a kink in the A-F curves is due to the condensation of single molecules into two-dimensional micelles.

Also J. E. Mayer's ideas[8] on the condensation process in general seem to support the expectation that in certain cluster-forming systems at sufficiently low temperature the Gibbs potential tends to a limiting value as saturation is approached (Case "a" of Born and Fuchs[9]). This effect may be enhanced if the interfacial tension of the particles is very small.[10]

The above considerations, of course, do not account for the ascending branch of the capillary curve. It is probable that the surface films at higher concentrations assume a crystalline or liquid-crystalline structure. Unless such films are formed in a reversible way they are likely to be in a state of stress which, to be released, takes much longer periods of time than usually spent for the observations. A superposition of s.t. and surface stress may be reponsible for time effects also before the minimum concentration is reached.

[1] H. M. Cassel, J. Am. Chem. Soc. **57**, 2009 (1935).
[2] J. W. McBain and G. F. Mills, *Report on Progress in Physics* (1939) Vol. 5, p. 30.
[3] G. C. Nutting, F. A. Long, and W. D. Harkins, J. Am. Chem. Soc. **62**, 1496 (1940).
[4] J. W. McBain and L. A. Word, Proc. Roy. Soc. **A174**, 286 (1940).
[5] M. Randall, J. W. McBain, and A. M. White, J. Am. Chem. Soc. **48**, 2517 (1926).
[6] H. V. Tartar, V. Sivertz, and R. E. Reitmeier, J. Am. Chem. Soc. **62**, 2375 (1940).
[7] I. Langmuir, J. Chem. Phys. **1**, 756 (1933).
[8] J. E. Mayer and S. F. Harrison, J. Chem. Phys. **6**, 91 (1938).
[9] M. Born and K. Fuchs, Proc. Roy. Soc. **A166**, 391 (1938).
[10] M. Volmer in cooperation with the author, Zeits. f. physik. Chemie **125**, 156 (1927). See also J. Frenkel, J. Chem. Phys. **7**, 538 (1939).

Polarization of Luminescence in Crystals

B. V. THOSAR
College of Science, Nagpur, India
February 24, 1942

THE state of polarization[1] of the sharp red luminescent doublet of ruby at λ6936, and also of the anti-Stokes bands shifted from the doublet by 756 cm^{-1}, 523 cm^{-1}, and 368 cm^{-1}, respectively, has been quantitatively investigated. The technique usually employed for studying the polarization of Raman lines was used, the observations being made visually. The crystal was kept with its optic axis vertical, along OZ, and the intensity of luminescence polarized parallel to this direction was compared with that polarized perpendicular to it (along OX). Table I gives the

TABLE I.

Lines and bands	Intensity	$\rho = I_{OZ}/I_{OX}$
λ6936 (doublet)	sharp, intense	0.16
$\Delta\nu$ 756 cm^{-1}	intense, broad	0.70
523 cm^{-1}	v. intense, broad	0.37
368 cm^{-1}	weak	>1.00

ratio I_{oz}/I_{ox} of the intensities polarized parallel and perpendicular to the optic axis of the crystal.

When the crystal is mounted with the optic axis along the direction of observation OY the ratio ρ is unity for all the lines and bands listed above.

(1) The bands have been explained as due to the superposition of internal vibration frequencies in the crystal on the sharp line radiation. Since the latter is strongly linearly polarized perpendicular to the crystal axis, this is a case analogous to the excitation of Raman lines by initially polarized light. The degree of polarization of the bands would be of help in assigning them to the different possible modes of vibrations within the crystal.

(2) Regarding the polarization of the sharp doublet, it is to be noted that there is a striking resemblance between the above observations and the phenomena of polarization of resonance radiation of mercury, observed by Hanle.[2] The red luminescence lines of ruby behave as though the crystal is a natural resonance lamp with an inherent magnetic field along the optic axis. The examination of the x-ray structure of corundum shows that the fluorescent Cr^{+++} ion, which replaces the Al atom, is situated in crystalline fields of axial symmetry and in accordance with the theory[3] of paramagnetic crystals, the orbital moment of the ion should be quenched in all directions but one—the symmetry axis, i.e., the optic axis. The orbital moment being conserved only along the direction of the optic axis, the electric vector in the emitted radiation is confined to the orbital plane, i.e., the plane normal to the optic axis.

(3) The present evidence seems to show that the Cr^{+++} ions in ruby are subjected to external crystalline fields strong enough to break the L-S coupling but not strong enough to break the coupling of individual l's to give the resultant L and of individual spins to give S. The energy levels of Cr^{+++} ion available from Bowen's work[4] then explain the principal emission and absorption lines according to the following plan:

Transition	Bowen's value	Observed lines
$^4P \rightarrow {}^4F$	14200 cm^{-1}	λ6936 doublet (emission)
$^2G \rightarrow {}^4F$	15200 cm^{-1}	λ6580 doublet (absorption)
$^2H \rightarrow {}^4F$	21200 cm^{-1}	λ4752, λ4762 (absorption)
$^2D_a \rightarrow {}^4F$	20600 cm^{-1}	

This scheme is supported by the fact that $^4P \rightarrow {}^4F$ transition being between two quartet levels is much more probable and accounts for the large intensity of the red emission lines. The other lines caused by transitions between doublet and quartet levels are shown only in absorption.

(4) The occurrence of one or more lines for the $^4P \rightarrow {}^4F$ transition in Cr^{+++} ion, when it is bedded in different crystals[5] seems to be related either to the degree of symmetry of the crystalline field in which it is situated or to the number of non-equivalent positions in which it can replace the metal atom of the ground-lattice. In spinel-type crystals, which are regular, there is one line and in Al_2O_3 and Ga_2O_3, there are two. This point cannot further be discussed here.

I regard the above explanation of the polarization of luminescence of ruby as only a particular case of a more general interpretation of crystal luminescence, based on the following concepts:

(a) The polarization of luminescence is caused by the quenching of orbital moment of the "center" in all but one direction (or a few discreet ones) determined by the nature and symmetry of the crystalline fields.

(b) The absence or existence of luminescence is conditioned by the complete quenching of the orbital moment of a possible center or its conservation along one or more directions within the crystal.

Such an interpretation is being attempted.

[1] B. V. Thosar, Phys. Rev. **60**, 616 (1941); Phil. Mag. **26**, 878 (1938).
[2] Mitchell and Zemansky, *Resonance Radiation and Excited Atoms* (Cambridge, 1934), p. 262.
[3] J. H. Van Vleck, *Theory of Electric and Magnetic Susceptibilities* (Oxford, 1932), p. 288.
[4] J. H. Van Vleck, J. Chem. Phys. **8**, 793 (1940).
[5] Deutschbein, Physik. Zeits. **33**, 874 (1932).

The Migration of Colloids Through the Interface Between Immiscible Liquids under the Influence of an Electric Field, and the Formation of Ultra-Colloids

G. E. Gibson and L. Baldwin
University of California, Berkeley, California
March 16, 1942

It has been shown by Lash Miller and R. H. McPherson that colloidal arsenic sulfide will distribute itself between the two phases of a mixture of water, acetone, and ether provided the mixture is very close to the critical mixing composition (plait point). A very slight excess of ether causes the colloid to go completely into the water-rich phase, when the volumetric ratios are: water : acetone : ether = 1.2 : 1.9 : 1.0.

Placing the two-phase system in a U-tube with electrodes in the upper ether-rich phases we have found that an e.m.f. of 200 volts will cause the arsenic sulfide to go back through the interface into the ether-rich phase, provided the ether is only slightly in excess; otherwise greater voltages are necessary. In similar fashion gold, bentonite clay, and carbon colloids have been made to traverse such an interface.

The phenomenon has been viewed through the ultramicroscope, using gold and bentonite clay. Surprisingly violent motions of the colloid, not visible to the naked eye, became apparent soon after the application of the electric field. Surges back and forth parallel to the interface were observed, always in opposite directions in the two phases, accompanied by vertical wave motions near the interface. After some time a dark band appeared in the ether-rich upper phase immediately above the interface. From time to time particles of greater than average size approaching the interface in an oblique direction would shoot with great velocity through this dark band into the ether-rich phase. This dark band must be a region of high potential gradient, which becomes visible owing to the formation of an extremely fine colloid, not resolvable by the ultramicroscope. The formation of this ultra-colloid has been observed in gold and bentonite and presumably is due to attrition of the larger particles as they shoot through the interface. It probably will occur with other colloids also.

The violence of the surging motion is enhanced by adding small amounts of electrolyte (HCl to bentonite) and much diminished by careful dialyzing to remove electrolytes before use.

We wish to acknowledge the assistance of Messrs. N. L. Ellis and E. Goldberg who took part in the preliminary experiments.

The Absorption Spectrum of Chlorine Fluoride

AUSTIN L. WAHRHAFTIG
Gates and Crellin Laboratories of Chemistry, California Institute of Technology, Pasadena, California
March 16, 1942

THE absorption spectrum of chlorine fluoride has been examined over the region λλ3500–7000 and a band system found at λ4800 has been studied under high dispersion. These bands have single P and R branches and the system appears to be similar in every respect to the $^3\Pi_0{}^+ \leftarrow {}^1\Sigma^+$ system found in iodine chloride[1,2] and iodine bromide.[3] The Deslandres Table I for the band system is given below. The values listed are frequencies in wave numbers for band origins, except those designated by h, which are for band heads. The bands with $v'=11$, 12, and 13 are diffuse, probably because of a perturbing O^+ repulsive state, as in the case of iodine chloride and iodine bromide.

The convergence limit for the progression $v' \leftarrow 0$ is 21508 ± 2 cm^{-1}. The probable dissociation products are $Cl(^2P_{3/2})$ and $F(^2P_{1/2})$. The molecular constants determined by analysis of the bands whose origins are listed are:

Ground state,

$D''_0 = 21101 \pm 2$ cm^{-1}. or 60.31 kcal./mole. $\quad D''_e = 21495 \pm 3$ cm^{-1}.
$B''_e = 0.518 \pm 0.001$ cm^{-1}. $\quad r''_e = 1.625$A.
$\alpha''_e = 0.006 \pm 0.002$ cm^{-1}. $\quad r''_0 = 1.630$A.
$\omega''_e = 793.2$ cm^{-1}. $\quad \omega''_e x''_e = 9.9$ cm^{-1}.

Excited state,

$D'_0 = 2790 \pm 50$ cm^{-1}. $\quad D'_e = 2946 \pm 50$ cm^{-1}.
$B'_e = 0.372$ cm^{-1}. $\quad B'_{14} = 0.132$ cm^{-1}.
$\alpha'_e = 0.014$ cm^{-1}. $\quad B'_{15} = 0.112$ cm^{-1}.
$r'_e = 1.92$A.
$\omega'_e = 313.484$ cm^{-1}. $\quad \omega'_e x'_e = 2.217$ cm^{-1}.
$\omega'_e y'_e = -0.400$ cm^{-1}.

D''_0 and D''_e were calculated assuming the dissociation products to be as given above. B'_e, α'_e, and the excited state vibrational constants represent only the data for $v<11$; that is, below the perturbation region.

TABLE I. Deslandres table for the band system at λ4800

v'	$v''=0$	$v''=1$
6	20395.82	
7	20619.32	
8	20820.37	20047.04
9	20996.94	
10	21145.54	20372.07
11	*h* 21255.5	
12	*h* 21338.3	
13	*h* 21398.4	
14	21445.87	
15	21479.95	
16	*h* 21499.8	
17	*h* 21507.8	
	Isotope bands	
8	20808.6	
9	—	
10	21134.3	

The dissociation energy of chlorine[4] is 57.20 kcal./mole. From this and the dissociation energy of chlorine fluoride listed above, one obtains:

$$Cl_2 + 2F \rightarrow 2ClF \qquad \Delta H = -63.42 \text{ kcal.}$$

or

$$D_0(F_2) + 2Q_f(ClF) = 63.42 \text{ kcal.},$$

in which $D_0(F_2)$ is the dissociation energy of fluorine and $Q_f(ClF)$ is the heat of formation of chlorine fluoride, rigorously at 0°K, but with very little error at room temperature.

The values given in the literature for $D_0(F_2)$, all determined indirectly, range from 62 to 65 kcal./mole.[5] Ruff and Menzel[6] report $Q_f(ClF) = 27.4$ kcal.; Fredenhagen and Krefft[7] state that chlorine and fluorine form an explosive mixture, and that the reaction is more exothermic than that between chlorine and hydrogen, for which $Q_f(HCl) = 22$ kcal. It is apparent from the equation above that at least one of these values is greatly in error. At present it seems most reasonable to assume that $Q_f(ClF)$ is much smaller than 27 kcal., but appreciably greater than zero, and that $D_0(F_2)$ is somewhat smaller than has been generally believed.

A complete report on this research will be published when time permits.

[1] W. G. Brown and G. E. Gibson, Phys. Rev. **40**, 529 (1932).
[2] J. H. Van Vleck, Phys. Rev. **40**, 544 (1932).
[3] W. G. Brown, Phys. Rev. **42**, 355 (1932).
[4] G. Herzberg, *Molecular Spectra and Molecular Structure* (Prentice-Hall, 1939), p. 485.
[5] See, for example, reference 4, p. 486, and W. M. Latimer and J. H. Hildebrand, *Reference Book of Inorganic Chemistry* (Macmillan, 1940), p. 154.
[6] Otto Ruff and Walter Menzel, Zeits. f. anorg. allgem. Chemie **198**, 375 (1931).
[7] K. Fredenhagen and O. T. Krefft, Zeits. f. physik. Chemie **A141**, 221 (1929).